

# Table of Contents

---

<b>Acknowledgements .....</b>	<b>ii</b>
<b>Abstract .....</b>	<b>iii</b>
<b>Research Outputs Arising from this Thesis .....</b>	<b>ix</b>
<b>Table of Contents.....</b>	<b>xi</b>
<b>List of Tables.....</b>	<b>xvii</b>
<b>List of Figures .....</b>	<b>xviii</b>
<b>List of Abbreviations.....</b>	<b>xx</b>
<b>1. Background, Thesis structure, and aims .....</b>	<b>1</b>
1.1 Background .....	2
1.2 Thesis aims and objectives.....	3
1.3 Thesis Structure.....	5
<b>2. Literature Review .....</b>	<b>7</b>
2.1 Abstract .....	8
2.1. Introduction.....	9
2.2 Mechanisms of pH-Responsive Targeted Drug Delivery .....	13
2.2.1 pH triggered protonation to promote extracellular or intracellular release .....	14
2.2.2 Acid labile bond cleavage for extra- or intracellular drug release.....	15
2.2.3 Acid labile bond cleavage for PEG-detachment.....	15
2.3 pH-Responsive Nanocarriers Based on Protonation / Deprotonation Mechanisms .....	17
2.3.1 pH-sensitive polymers .....	19
2.3.1.1 Anionic pH-sensitive polymers .....	19
2.3.1.2 Cationic pH-sensitive polymers .....	21
2.3.2 pH-sensitive lipids .....	28
2.3.3 Polysaccharides.....	29
2.3.4 pH-sensitive peptides.....	30

2.4	pH-Responsive Nanocarriers Based on Acid Labile Bond Cleavage .....	32
2.4.1	Hydrazone bond.....	33
2.4.2	Imine bond .....	38
2.4.3	Oxime bond .....	39
2.4.4	Amide bond .....	40
2.4.5	Polyacetals and ketals .....	41
2.4.6	Ethers .....	43
2.4.7	Orthoesters.....	44
2.5	Conclusion Remarks and Future Prospects.....	47
<b>3.</b>	<b>Characterization of a smart pH-cleavable PEG polymer towards the development of dual pH-sensitive liposomes .....</b>	<b>49</b>
3.1	Abstract .....	50
3.2	Introduction.....	53
3.3	Experimental .....	55
3.3.1	Materials .....	55
3.3.2	Stability-indicating HPLC method development for PEG <sub>B</sub> -Hz-CHEMS .....	55
3.3.2.1	Instrumentation and chromatographic conditions .....	55
3.3.2.2	Synthesis of potential degradation products and preparation of standard solutions.....	56
3.3.2.3	Mobile phase optimisation by multiple linear regression.....	56
3.3.2.4	Validation .....	57
3.3.3	Kinetics of pH-dependent PEG detachment of PEG <sub>B</sub> -Hz-CHEMS .....	58
3.3.4	pH-dependent degradation pathways of PEG <sub>B</sub> -Hz-CHEMS.....	58
3.3.5	Quantification of PEGylation degree towards the development of CL-pPSL.....	58
3.3.6	Size, morphology and stability of the CL-pPSL.....	59
3.3.7	pH-responsive calcein leakage assay.....	60
3.3.8	Statistical analysis.....	61
3.4	Results and Discussion.....	61
3.4.1	Stability-indicating HPLC method for PEG <sub>B</sub> -Hz-CHEMS .....	62

3.4.1.1	Mobile phase optimisation by multiple regression analysis .....	62
3.4.1.2	Validation .....	63
3.4.2	Kinetics of pH-dependent PEG detachment of PEG <sub>B</sub> -Hz-CHEMS .....	65
3.4.3	pH-dependent degradation pathways of PEG <sub>B</sub> -Hz-CHEMS .....	67
3.4.4	Quantification of PEGylation degree of CL-pPSL .....	68
3.4.5	Size, morphology and stability of the CL-pPSL .....	69
3.4.6	pH-responsive calcein leakage kinetics .....	71
3.5	Conclusions .....	73
3.6	Acknowledgements and disclosure .....	73
<b>4.</b>	<b>PEG-Benzaldehyde-Hydrazone-Lipid Based PEG-Sheddable pH-Sensitive Liposomes: Abilities for Endosomal Escape and Long Circulation.....</b>	<b>74</b>
4.1	Abstract .....	75
4.2	Introduction .....	78
4.3	Experimental .....	80
4.3.1	Materials .....	80
4.3.2	Synthesis of PEG <sub>B</sub> -Hz-CHEMS .....	81
4.3.3	Characterization of PEG <sub>B</sub> -Hz-CHEMS micelles .....	83
4.3.3.1	Size and morphology of micelles .....	83
4.3.3.2	Critical micellar concentration (CMC) .....	83
4.3.4	Preparation and characterization of dual pH-sensitive liposomes .....	83
4.3.4.1	Preparation of dual pH-responsive liposomes .....	83
4.3.4.2	Size, zeta potential and morphology of liposomes .....	84
4.3.4.3	Determination of PEGylation Degree and PEG configuration .....	84
4.3.5	Gemcitabine loading and entrapment efficiency (EE) into liposomes .....	86
4.3.6	pH-responsive drug release .....	86
4.3.7	Quantitative determination of cellular drug uptake using HPLC .....	87
4.3.8	Cytotoxicity to Mia PaCa-2 .....	87
4.3.9	Intra-cellular trafficking of CL-pPSL and pPSL .....	88

4.3.10 Pharmacokinetics in rats .....	88
4.3.11 Statistical analysis.....	89
4.4 Results and Discussion.....	90
4.4.1 Synthesis of PEG <sub>B</sub> -Hz-CHEMS .....	90
4.4.2 CMC of PEG <sub>B</sub> -Hz-CHEMS.....	91
4.4.3 Characterization of dual pH-sensitive liposomes .....	92
4.4.3.1 Size, zeta potential and morphology .....	92
4.4.3.2 Quantification of degree of PEGylation .....	93
4.4.3.3 PEG conformation on surface of liposomes .....	94
4.4.4 Drug loading and entrapment efficiency .....	94
4.4.5 pH-sensitive drug release.....	95
4.4.6 Cellular drug uptake determined by HPLC .....	96
4.4.7 Cytotoxicity to Mia PaCa-2 .....	97
4.4.8 Intracellular trafficking of liposomes .....	98
4.4.9 Pharmacokinetics in rats .....	99
4.5 Conclusions.....	101
4.6 Acknowledgements.....	101
<b>5. Dual pH-sensitive liposomes with low pH triggered sheddable-PEG for tumor targeted drug delivery .....</b>	<b>102</b>
5.1 Abstract .....	103
5.2 Introduction.....	106
5.3 Materials and methods .....	108
5.3.1 Materials .....	108
5.3.2 Synthesis of PEG <sub>B</sub> -Hz-DPPE polymer.....	109
5.3.3 Characterization of PEG <sub>B</sub> -Hz-DPPE polymer.....	110
5.3.4 Preparation of the liposomes .....	110
5.3.5 Characterization of liposomes .....	111
5.3.6 pH-responsiveness .....	112

5.3.7	<i>In vitro</i> cellular uptake and endosomal escape .....	113
5.3.8	Subcellular localisation of CL-pPSL and pPSL with live cell imaging .....	113
5.3.9	<i>In vitro</i> cytotoxicity study .....	114
5.3.10	Pharmacokinetics .....	115
5.3.11	Biodistribution Study .....	115
5.3.12	Data and statistical analysis .....	116
5.4	Results .....	116
5.4.1	Synthesis of PEG <sub>B</sub> -Hz-DPPE polymer .....	116
5.4.2	Characterization of PEG <sub>B</sub> -Hz-DPPE polymer .....	117
5.4.3	Characterization of PEGylated liposomes .....	118
5.4.4	pH-responsive drug release .....	119
5.4.5	<i>In vitro</i> cellular uptake and endosome escape studies .....	120
5.4.6	Subcellular localisation of CL-pPSL and pPSL by live cell imaging .....	122
5.4.7	<i>In vitro</i> Cytotoxicity Study .....	125
5.4.8	Pharmacokinetics and Biodistribution study .....	126
5.5	Discussion .....	129
5.6	Conclusion .....	132
5.7	Acknowledgements .....	132
<b>6.</b>	<b>General discussion and future prospects .....</b>	<b>133</b>
6.1	General discussion .....	134
6.1.1	PEG <sub>B</sub> -Hz-CHEMS polymer design and synthesis .....	135
6.1.2	Phospholipid composition .....	136
6.1.3	Formulation development of CL-pPSL <sub>1</sub> .....	137
6.1.4	Characterization of CL-pPSL <sub>1</sub> .....	138
6.1.5	Design and development of PEG <sub>B</sub> -Hz-DPPE modified liposomes, CL-pPSL <sub>2</sub> .....	140
6.1.6	Conclusion .....	142
6.2	Future directions .....	143

6.2.1	Improving the insertion efficiency of PEG <sub>B</sub> -Hz-CHEMS into liposomes .....	143
6.2.2	Quantification of the PEG detachment of PEG <sub>B</sub> -Hz-DPPE .....	144
6.2.3	Formulation Improvement .....	144
6.2.4	Investigating anti-tumor efficacy .....	145
6.2.5	Surface ligand modification for tumor penetration abilities .....	145
<b>7.</b>	<b>Appendices.....</b>	<b>147</b>
	<b>References.....</b>	<b>157</b>

## List of Tables

---

Table 2-1	Examples of pH-sensitive cationic and anionic polymers .....	25
Table 2-2	Examples of acid- labile chemical bonds and their degradation products ..	36
Table 3-1	Intra-day and Inter-day precision and accuracy of PEG <sub>B</sub> .....	64
Table 3-2	Stability of CL-pPSL.....	70
Table 4-1	Insertion efficiency (IE) of PEG <sub>B</sub> -HZ-CHEMS .....	94
Table 4-2	Ratios of intracellular and extracellular concentrations.....	97
Table 4-3	Cytotoxicity of CL-pPSL, pPSL .....	97
Table 4-4	Plasma pharmacokinetic parameters .....	100
Table 5-1	Physio-chemical characterization of gemcitabine-loaded liposomes.....	119
Table 5-2	Summary of plasma pharmacokinetic parameters .....	126

## List of Figures

---

Figure 2-1	Pathways for pH-triggered targeted drug release at the tumor.....	13
Figure 2-2	Schematic representation of pH responsive mechanisms to promote drug release.....	18
Figure 2-3	Schematic representation of applications of acid labile chemical bonds .....	37
Figure 3-1	Graphical abstract for Chapter 3 .....	52
Figure 3-2	Typical chromatograms of .....	63
Figure 3-3	Degradation kinetics of PEG <sub>B</sub> -Hz-CHEMS .....	66
Figure 3-4	Scheme of proposed degradation pathways of PEG <sub>B</sub> -Hz-CHEMS .....	68
Figure 3-5	Cryo-TEM micrographs of unilamellar pH-sensitive liposomes .....	70
Figure 3-6	Fluorescence intensity as a function of calcein concentration, .....	72
Figure 4-1	Graphical abstract.....	77
Figure 4-2	Scheme for synthesis of PEG <sub>B</sub> -Hz-CHEMS with three steps. ....	82
Figure 4-3	A) typical <sup>1</sup> H-NMR spectrum of PEG <sub>B</sub> -Hz-CHEMS in CDCl <sub>3</sub> ; .....	91
Figure 4-4	Physicochemical characterization of PEG <sub>B</sub> -Hz-CHEMS micelles: .....	92
Figure 4-5	A) The influence of PEGylation with PEG <sub>B</sub> -Hz-CHEMS on the particle ...	93
Figure 4-6	pH-sensitive drug release profiles of dual pH-sensitive liposomes .....	95
Figure 4-7	Confocal fluorescence microscopy images of Mia PaCa-2 cells .....	99
Figure 4-8	A) Pharmacokinetic profiles following <i>i.v.</i> injection .....	101

Figure 5-1	Graphical abstract.....	105
Figure 5-2	A) Scheme of synthesis of PEG <sub>B</sub> -Hz-DPPE; .....	117
Figure 5-3	A) Measurement of size, and pH-sensitivity of PEG <sub>B</sub> -Hz-DPPE : .....	118
Figure 5-4	Characterization of PEG <sub>B</sub> -Hz-DPPE modified liposomes for .....	119
Figure 5-5	pH-responsive gemcitabine release profiles.....	120
Figure 5-6	CLSM images showing the cell uptake and endosome escape .....	121
Figure 5-7A	Live cell imaging showing the intracellular trafficking .....	123
Figure 5-7B	Live cell imaging showing the intracellular trafficking .....	124
Figure 5-8	Cytotoxicity profiles.....	125
Figure 5-9	A) Plasma pharmacokinetic profiles .....	128

## List of Abbreviations

---

AUC	Area under the curve
CL-pPSL	Cleavable PEGylated pH-sensitive liposome
CL-pPSL <sub>1</sub>	PEG <sub>B</sub> -Hz-CHEMS modified CL-pPSL
CL-pPSL <sub>2</sub>	PEG <sub>B</sub> -Hz-DPPE modified CL-pPSL
CHEMS	Cholesteryl hemisuccinate
C <sub>e</sub>	Extracellular concentration
C <sub>i</sub>	Intracellular concentration
cryo-TEM	Cryogenic transmission electron microscopy
DOPE	1,2-dioleoyl- <i>sn</i> -glycerol-3-phosphatidylamine
DSPC	1,2-distearoyl- <i>sn</i> -glycero-3-phosphocholine
DPPE	1,2-Dipalmitoyl- <i>sn</i> -glycero-3-phosphoethanolamine
DAPI	4',6-diamidino-2-phenylindole
DL	Drug loading
DLS	Dynamic light scattering
EE	Entrapment efficiency
EPR	Enhanced Permeability and Retention
HPLC	High-performance liquid chromatography

LOD	Limit of detection
LOQ	Limit of quantification
MDR	Multidrug resistance
MRT	Mean residence time
nPSL	Non pH-sensitive liposome
PEG	Poly(ethylene glycol)
PDI	Polydispersibility index
pH <sub>ex</sub>	Extracellular pH
pH <sub>i</sub>	Intracellular pH
pH <sub>en</sub>	endosomal pH
pSL	pH-sensitive liposomes
pPSL	PEGylated pH-sensitive liposome
RES	Reticuloendothelial system
RSD	Relative standard deviation
SD	Standard deviation
V <sub>d</sub>	Volume of distribution

## Co-Authorship Form

This form is to accompany the submission of any PhD that contains published or unpublished co-authored work. **Please include one copy of this form for each co-authored work.** Completed forms should be included in all copies of your thesis submitted for examination and library deposit (including digital deposit), following your thesis Acknowledgements. Co-authored works may be included in a thesis if the candidate has written all or the majority of the text and had their contribution confirmed by all co-authors as not less than 65%.

Please indicate the chapter/section/pages of this thesis that are extracted from a co-authored work and give the title and publication details or details of submission of the co-authored work.

Chapter 1 of the thesis contains a reproduction of the publication below.  
Mechanisms and biomaterials in pH-responsive tumor targeted drug delivery - A review

Nature of contribution by PhD candidate	Conducted experimental design and data interpretation, carried out all the experimental work and prepared the manuscript
Extent of contribution by PhD candidate (%)	75%

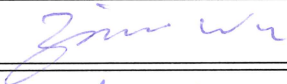
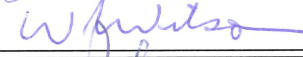
### CO-AUTHORS

Name	Nature of Contribution
A/Prof Zimei Wu	Guided the literature search strategy, edited drafts and overall supervision of the project
Prof William R. Wilson	Provided critical input in relation to intracellular pH regulation in tumours
A/Prof Brian D. Palmer	Reviewed and edited descriptions of chemical matter
Dr Mimi Yang	Assisted with Manuscript preparation

### Certification by Co-Authors

The undersigned hereby certify that:

- ❖ the above statement correctly reflects the nature and extent of the PhD candidate's contribution to this work, and the nature of the contribution of each of the co-authors; and
- ❖ that the candidate wrote all or the majority of the text.

Name	Signature	Date
A/Prof Zimei Wu		22/Feb/2018
Prof William R. Wilson		22/2/2018
A/Prof Brian D. Palmer		22/2/2018
Dr Mimi Yang		28/02/2018

## Co-Authorship Form

This form is to accompany the submission of any PhD that contains published or unpublished co-authored work. **Please include one copy of this form for each co-authored work.** Completed forms should be included in all copies of your thesis submitted for examination and library deposit (including digital deposit), following your thesis Acknowledgements. Co-authored works may be included in a thesis if the candidate has written all or the majority of the text and had their contribution confirmed by all co-authors as not less than 65%.

Please indicate the chapter/section/pages of this thesis that are extracted from a co-authored work and give the title and publication details or details of submission of the co-authored work.

Chapter 2 of the thesis contains a reproduction of the publication below.  
Synthesis and characterization of smart pH-cleavable PEG polymer towards the development of dual pH-responsive liposomes

Nature of contribution by PhD candidate	Conducted experimental design and data interpretation, carried out all the experimental work and prepared the manuscript
Extent of contribution by PhD candidate (%)	80%

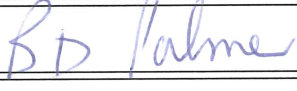
### CO-AUTHORS

Name	Nature of Contribution
A/Prof Zimei Wu	Conceived and directed the research, edited and reviewed the manuscript
Prof William R. Wilson	Assisted with data interpretation and reviewed the manuscript
A/Prof Brian D. Palmer	Reviewed and edited manuscripts of chemical matter

### Certification by Co-Authors

The undersigned hereby certify that:

- ❖ the above statement correctly reflects the nature and extent of the PhD candidate's contribution to this work, and the nature of the contribution of each of the co-authors; and
- ❖ that the candidate wrote all or the majority of the text.

Name	Signature	Date
A/Prof Zimei Wu		22/02/2018
Prof William R. Wilson		22/2/2018
A/Prof Brian D. Palmer		22/2/2018

## Co-Authorship Form

This form is to accompany the submission of any PhD that contains published or unpublished co-authored work. **Please include one copy of this form for each co-authored work.** Completed forms should be included in all copies of your thesis submitted for examination and library deposit (including digital deposit), following your thesis Acknowledgements. Co-authored works may be included in a thesis if the candidate has written all or the majority of the text and had their contribution confirmed by all co-authors as not less than 65%.

Please indicate the chapter/section/pages of this thesis that are extracted from a co-authored work and give the title and publication details or details of submission of the co-authored work.

Chapter 3 of the thesis contains a reproduction of the publication below.  
PEG-benzaldehyde-hydrazone-lipid based PEG-sheddable pH-sensitive liposomes: abilities for endosomal escape and long circulation.

Nature of contribution by PhD candidate	Conducted experimental design and data interpretation, carried out all the experimental work and prepared the manuscript
Extent of contribution by PhD candidate (%)	75%

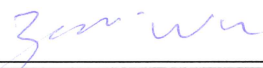
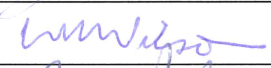
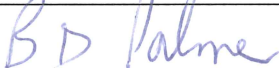
### CO-AUTHORS

Name	Nature of Contribution
A/Prof Zimei Wu	Directed the research, edited and reviewed the manuscript
Prof William R. Wilson	Assisted with data interpretation and reviewed the manuscript
A/Prof Brian D. Palmer	Reviewed and edited manuscripts of chemical aspects

### Certification by Co-Authors

The undersigned hereby certify that:

- ❖ the above statement correctly reflects the nature and extent of the PhD candidate's contribution to this work, and the nature of the contribution of each of the co-authors; and
- ❖ that the candidate wrote all or the majority of the text.

Name	Signature	Date
A/Prof Zimei Wu		22/2/2018
Prof William R. Wilson		22/2/2018
A/Prof Brian D. Palmer		22/2/2018

## Co-Authorship Form

This form is to accompany the submission of any PhD that contains published or unpublished co-authored work. **Please include one copy of this form for each co-authored work.** Completed forms should be included in all copies of your thesis submitted for examination and library deposit (including digital deposit), following your thesis Acknowledgements. Co-authored works may be included in a thesis if the candidate has written all or the majority of the text and had their contribution confirmed by all co-authors as not less than 65%.

Please indicate the chapter/section/pages of this thesis that are extracted from a co-authored work and give the title and publication details or details of submission of the co-authored work.

Chapter 4 of the thesis contains a reproduction of the publication below.  
Low pH triggered PEG-sheddable pH-sensitive liposomes for tumor targeted drug delivery

Nature of contribution by PhD candidate	Conducted experimental design and data interpretation, carried out all the experimental work and prepared the manuscript
Extent of contribution by PhD candidate (%)	75%

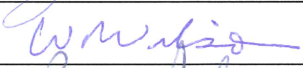
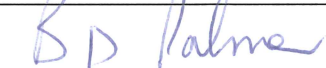
### CO-AUTHORS

Name	Nature of Contribution
A/Prof Zimei Wu	Directed the research, edited and reviewed the manuscript
Prof William R. Wilson	Assisted with data interpretation and reviewed the manuscript
A/Prof Brian D. Palmer	Reviewed and edited manuscripts of chemical aspects

### Certification by Co-Authors

The undersigned hereby certify that:

- ❖ the above statement correctly reflects the nature and extent of the PhD candidate's contribution to this work, and the nature of the contribution of each of the co-authors; and
- ❖ that the candidate wrote all or the majority of the text.

Name	Signature	Date
A/Prof Zimei Wu		22/02/2018
Prof William R. Wilson		22/2/2018
A/Prof Brian D. Palmer		22/2/2018

# **1. Background, Thesis structure, and aims**

---

## 1.1 Background

Cancer is one of the most devastating malignant diseases in the world today. Chemotherapy is a frontline strategy for the treatment of cancer, along with surgery. However, the emergence of side effects due to non-specific drug delivery and low tumor penetration are major impediments to successful chemotherapy. For the last three decades, liposomes have shown tremendous therapeutic potential due to their prolonged circulation time and enhanced tumor accumulation via the enhanced permeation and retention (EPR) effect, leading to several liposomal formulations in clinical use such as Doxil<sup>®</sup> and Marqibo<sup>®</sup>. The intrinsic low pH in tumor microenvironments motivated the development of pH-sensitive phospholipids such as 1,2-dioleoyl-sn-glycero-3-phosphoethanolamine (DOPE), which brought about the concept of pH-sensitive liposomes in the early 1980s. Therefore, developed pH-sensitive liposomes can exploit the low pH of tumors and deliver the payload specifically in selected low extracellular or endosomal regions within the cells. Hence, similar to conventional liposomes, PEGylation is the most commonly employed strategy for the *in vitro* stabilization and *in vivo* long circulation of pH-sensitive liposomes.

However, studies have shown that after reaching the target, PEGylation (which improves the stability and long circulation of DOPE liposomes) will inhibit the interaction of these liposomes with cell membranes, resulting in compromised cellular uptake. Furthermore, PEGylation also results in the poor endosomal escape of liposomes via membrane fusion, and therefore causes the degradation of cargos in lysosomes. Also, in the case of pH-sensitive liposomes such as DOPE liposomes, PEGylation causes a strong steric hindrance to the pH-sensitivity of formulations [1-3] resulting in a significant loss of their therapeutic efficacy, which is known as the PEG dilemma.

## 1.2 Thesis aims and objectives

pH-sensitive liposomes have been widely investigated due to their pH-responsive tumor targeting potential. However, the clinical development of these agents has been constrained due to various limitations associated with pPSL, the major one being the ‘PEG dilemma’. Various strategies [3-5] to overcome this PEG dilemma, such as (i) active targeting with specific ligands [6] and (ii) the ‘stimuli responsive de-PEGylation’ of non pH-sensitive liposomes [4] have been investigated. Recently, the stimuli responsive de-PEGylation of non pH-sensitive liposomes has demonstrated great potential in addressing the poor tumor selectivity and limited intracellular uptake of liposomes. It was found that, post PEG detachment, the non pH-sensitive liposomes were still entrapped in the endosomes, resulting in the lysosomal degradation of cargos. This thesis investigates a combination of strategies that could overcome the PEG dilemma to improve the tumor cellular uptake, endosomal escape and rapid intracellular drug delivery efficiency of pPSL.

The overall aim of this thesis is to develop a combinational strategy, whereby acid labile PEG detachment and the protonation of pH-sensitive liposomes effectively enhances cell uptake, followed by the rapid endosomal escape of pSL, without affecting their long circulation in the blood stream. The thesis discusses how the cleavable PEG polymers were designed, developed and used to fabricate the dual pH-responsive liposomes with cleavable PEGylation, where cleavage was achieved in response to the tumor extracellular or endosomal pH.

The specific objectives are the:

- 1) synthesis and characterization of pH-sensitive cleavable PEG polymers to achieve PEG-detachment at the target, which in turn promotes intracellular drug availability (Chapter 3 for PEG<sub>B</sub>-Hz-CHEMS and Chapter 5 for PEG<sub>B</sub>-Hz-DPPE).

## Chapter 1

- 2) development and characterization of dual pH-sensitive liposomes surface modified with acid-cleavable PEG polymers (Chapter 4 for PEG<sub>B</sub>-Hz-CHEMS and Chapter 5 for PEG<sub>B</sub>-Hz-DPPE).
- 3) evaluation of cell uptake, endosome escape and cytotoxic potentials in pancreatic cell models (Chapter 4 for PEG<sub>B</sub>-Hz-CHEMS and Chapter 5 for PEG<sub>B</sub>-Hz-DPPE).
- 4) evaluation of the effectiveness of these PEG-cleavable systems and non-cleavable liposomal systems, by comparing their pharmacokinetics profiles in SD rats and biodistribution in CD-1 nude mice (Chapter 4 for PEG<sub>B</sub>-Hz-CHEMS and Chapter 5 for PEG<sub>B</sub>-Hz-DPPE).

### 1.3 Thesis structure

This thesis has been prepared in accordance with the University of Auckland 2011 PhD Statute and Guidelines for Including Publications in a Thesis.

The background to this research, and the aims, objectives and structure of the thesis are defined in Chapter 1. A detailed literature review is presented in Chapter 2. Chapter 3 discusses the synthesis and characterization of the pH-cleavable PEG polymer, PEG<sub>B</sub>-Hz-CHEMS, where a stability-indicating HPLC assay was developed and validated using multiple linear regression analysis to characterize the polymer stability and also to facilitate the development of PEG<sub>B</sub>-Hz-CHEMS modified pH-sensitive liposomes, CL-pPSL<sub>1</sub>. The conformation of the PEG<sub>B</sub>-Hz-CHEMS polymer on the liposomal surface and the pH-sensitivity of the resulting liposomes are also discussed in Chapter 3.

Chapter 4 evaluates CL-pPSL<sub>1</sub> for their pH-sensitive drug delivery, cell uptake, endosome escape and cytotoxic abilities compared with pPSL and a free drug solution. The results from investigations of *in vivo* pharmacokinetics in SD rats and biodistribution in CD-1 nude mice highlight the unexpected finding of the shorter half-life and lower AUC of CL-pPSL due to the poor insertion efficiency of PEG<sub>B</sub>-Hz-CHEMS polymer into liposomes. CL-pPSL<sub>1</sub> (PEG<sub>B</sub>-Hz-CHEMS modified liposomes) are referred to as CL-pPSL in Chapters 3 and 4.

Chapter 5 describes how a new pH-cleavable PEG polymer based on the phospholipid lipid anchor DPPE, PEG<sub>B</sub>-Hz-DPPE, is synthesized and fully characterized to overcome the problems encountered with CL-pPSL<sub>1</sub>. Gemcitabine-loaded liposomes are evaluated for their cytotoxicity compared to non-cleavable controls and free drug solutions. The dual fluorescent labelled liposomes are further characterized for their cell uptake and endosome escape abilities in Mia PaCa-2 cells. In addition, the intracellular endosome escape mechanism of these CL-pPSL is investigated by the live cell imaging of lysotracker labelled cells. Results from *in vivo*

## Chapter 1

pharmacokinetics and the biodistribution of CL-pPSL<sub>2</sub> over pPSL and free drug solutions highlighted their abilities of enhanced tumor accumulation without compromise in their circulation half-life. The CL-pPSL<sub>2</sub> (PEG<sub>B</sub>-Hz-DPPE modified liposomes) are referred to as CL-pPSL in Chapter 5.

Chapter 6 discuss the challenges present in current work, and the future studies that are required for the further refining and improvement of both CL-pPSL<sub>1</sub> (PEG<sub>B</sub>-Hz-CHEMS modified liposomes) and CL-pPSL<sub>2</sub> (PEG<sub>B</sub>-Hz-DPPE modified liposomes).

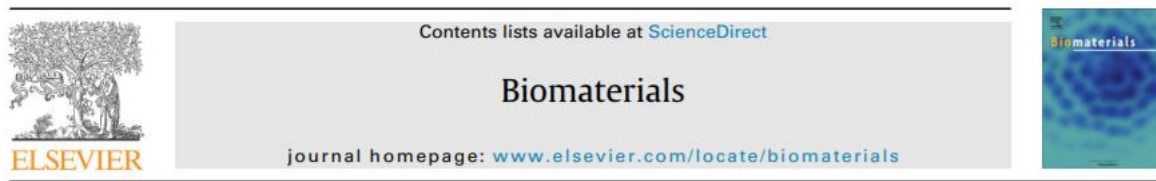
Chapters 2, 3 and 4 are presented in the original manuscript format it was published in, while Chapter 5 is in ready-to-submit form. Each chapter is made up of the following sections:

- 1) an abstract summarising the rationale for the research, followed by the scope, methods and important findings of that Chapter
- 2) a graphical abstract
- 3) an introduction, materials and methods, results, discussion and conclusion in the form of a published, peer-reviewed research article or a manuscript for submission.

These sections are reproduced verbatim from the published manuscript and have been edited solely to harmonise the citation style and numbering of Figures and Tables between Chapters, and for consistency in the terminology used.

## **2. Literature Review**

---



Review

## Mechanisms and biomaterials in pH-responsive tumour targeted drug delivery: A review



Manju Kanamala <sup>a</sup>, William R. Wilson <sup>b</sup>, Mimi Yang <sup>a</sup>, Brian D. Palmer <sup>b</sup>, Zimei Wu <sup>a,\*</sup>

<sup>a</sup> School of Pharmacy, Faculty of Medical and Health Sciences, University of Auckland, Auckland 1142, New Zealand

<sup>b</sup> Auckland Cancer Society Research Centre, Faculty of Medical and Health Sciences, University of Auckland, Auckland 1142, New Zealand

### 2.1 Abstract

As the mainstay in the treatment of various cancers, chemotherapy plays a vital role, but still faces many challenges, such as poor tumor selectivity and multidrug resistance (MDR). Targeted drug delivery using nanotechnology has provided a new strategy for addressing the limitations of conventional chemotherapy. In the last decade, the volume of research published in this area has increased tremendously, especially with functional nano drug delivery systems (nanocarriers). Coupling a specific stimuli-triggered drug release mechanism with these delivery systems is one of the most prevalent approaches for improving therapeutic outcomes. Among the various stimuli, pH triggered delivery is regarded as the most general strategy, targeting the acidic extracellular microenvironment and intracellular organelles of solid tumors.

In this review, we discuss recent advances in the development of pH-sensitive nanocarriers for tumor-targeted drug delivery. The review focuses on the chemical design of pH-sensitive biomaterials, which are used to fabricate nanocarriers for extracellular and/or intracellular tumor site-specific drug release. The pH-responsive biomaterials bring forth conformational changes in these nanocarriers through various mechanisms such as protonation, charge reversal or cleavage of a chemical bond, facilitating tumor specific cell uptake or drug release. A greater understanding of these mechanisms will help to design more efficient drug delivery systems to address the challenges encountered in conventional chemotherapy

**Key words:** pH-sensitive nanocarriers, Tumor targeted drug delivery, pH-sensitive bond, Protonation, Intracellular delivery, PEG detachment

## 2.2 Introduction

Advances in chemotherapy have resulted in the development of many successful cytotoxic drugs such as doxorubicin and paclitaxel, which have significantly improved prognosis and quality of life for cancer patients [7]. However, the lack of selectivity towards neoplastic cells remains a major challenge for chemotherapy, resulting in potentially life-threatening systemic side effects [8]. In addition, the development of multidrug resistance (MDR) due to numerous complex mechanisms is another major impediment for successful chemotherapy [9]. The introduction of molecularly targeted cancer therapeutics such as anti-angiogenic agents, proteasome inhibitors and growth factor receptor inhibitors, have contributed to drug discovery due to their ability to selectively target the physiology of cancer cells [10]. In the last decade, advances in tumor-targeted drug delivery science using nanotechnology have enabled more effective drug design and development, which has revolutionized chemotherapy. There have been more than 4000 academic journal articles in this area, and a total of 1381 nanomedicine formulations for cancer therapy were registered for clinical trials by December 2014 [11]; these include liposomes, micelles, nanoparticles and polymer-drug conjugates [12-14]. Nanocarriers which are able to physically encapsulate or chemically conjugate a drug have the capability to achieve targeted delivery of their payload to solid tumors [15, 16] via the ‘Enhanced Permeability and Retention (EPR) effect’ [17]; the extensive angiogenesis and leaky vasculature in tumors allows the extravasation of nanocarriers, while the relative paucity of functional lymphatics lead to enhanced retention [18].

The exploitation of the EPR effect is arguably the most important strategy for improving the delivery of chemotherapeutic agents to tumors [13, 19]. To utilise the EPR effect, nanocarriers

## Chapter 2

are required to stay in systemic circulation for a prolonged period of time to be extravasated into tumor tissue [20, 21]; therefore long circulation of nanocarriers is essential for maximum tumor targeting [22]. The most common approach in prolonging circulation is achieved by coating the surface of nanocarriers with a hydrophilic polymer, such as polyethylene glycol (PEG), a process known as PEGylation [19, 22, 23]. This hydrophilic coating sterically hinders opsonisation and destruction by the reticuloendothelial system (RES) [21, 24]. This approach is known as ‘stealth technology’. ‘Stealth’ nanocarriers, most notably Doxil<sup>®</sup> or Caelyx<sup>®</sup> (PEGylated liposomal doxorubicin) have been approved for clinical use with notable success. Other polymers poly [N-(2-hydroxypropyl) methacrylamide] (HPMA), poly (vinylpyrrolidone) (PVP), poly(2-methyl-2-oxazoline) (PMOX), (poly(N,N-dimethyl acrylamide) (PDMA), poly(N-acryloyl morpholine) (PACM) [25] and poloxamer 188 [26], have been demonstrated to increase the circulation times of liposomes. Since the approval of Doxil<sup>®</sup>/Caelyx<sup>®</sup> in 1995, the field of targeted delivery by nanocarriers has grown exponentially [27].

However, inefficient drug release at the tumor site and endosomal entrapment of nanocarriers can be barriers that may significantly reduce efficacy. To overcome these barriers, exogenous (externally applied) stimuli to trigger drug release from nanocarriers, such as temperature, ultrasound, light, magnetic and electrochemical triggers, have been investigated. On the other hand, tumor pathophysiology manifests with characteristic changes such as in pH, enzyme activity or redox properties [28], allowing opportunities to exploit these endogenous factors as internal stimuli [20, 21, 29].

Among these stimulus-responsive systems, pH-sensitive nanocarriers have attracted much interest for two quite different reasons. One is that the endosomes into which nanocarriers are incorporated via endocytosis develop markedly acidified lumens ( $\text{pH}_{\text{en}}$  4.5-5.5) primarily through the activity of V-type  $\text{H}^+$  ATPase [30]. Thus the triggering of drug release from

## Chapter 2

nanocarriers at low pH provides a mechanism for drug escape from the endosomal compartment. The second reason is that acidosis in tumor tissue may be exploitable for selective targeting of tumors relative to normal tissues, complementing and extending the selectivity achievable by the EPR effect. It has been known since the pioneering studies of Warburg [31] that tumors have a propensity for glycolytic metabolism of glucose to lactate, which contributes to acidosis. Many studies with pH microelectrodes have demonstrated lower pH values in tumors relative to normal tissues [32, 33]. However, for tumor targeting it is critically important to understand which regions and compartments in tumors have lower pH values than normal tissues – an issue that is often not addressed in nanocarrier literature. In 1986 it was suggested that only the extracellular compartment of tumors is acidic relative to normal tissues [34], based on evidence that pH microelectrode measurements largely reflect extracellular pH ( $\text{pH}_{\text{ex}}$ ) and that  $^{31}\text{P}$  magnetic resonance spectroscopy inorganic phosphate indicates intracellular pH values ( $\text{pH}_{\text{i}}$ ) similar to normal tissues. This interpretation has been confirmed in many subsequent studies [35, 36], and reflects the active extrusion of protons and weak acids by plasma membrane transporters such as the sodium-hydrogen exchanger NHE-1, bicarbonate/chloride exchangers, and the monocarboxylate transporter (MCT) family [37]. It is notable that NHE-1 is activated by oncogenic signalling, driving cytoplasmic alkalinisation which is a trigger for cell proliferation [38]. It is also notable that many of these transporters and coupled enzymes (e.g. carbonic anhydrase IX) are transcriptional targets of HIF-1 and thus are upregulated under hypoxia [39, 40]. This linkage to hypoxia, along with the limited clearance of metabolic acids by the dysfunctional microvasculature in tumors, generates  $\text{pH}_{\text{ex}}$  gradients with maximal acidification in microregions distant from functional blood vessels [41].

To date, a variety of pH-sensitive nanocarriers has been designed to exploit low extracellular  $\text{pH}_{\text{ex}}$  or endosomal  $\text{pH}_{\text{en}}$  [28, 42, 43]. The drugs could be physically encapsulated or chemically conjugated with the carriers, such as liposomes, polymer-drug conjugates, polymeric

nanoparticles, micelles and polymersomes. Two major types of nanocarriers have been widely investigated, pH-sensitive liposomes (pSL), and pH-sensitive polymeric micelles (pSM) [19]. pH-sensitive polymersomes (pPS) are a new type of nanocarriers that are attracting great interest. pPS are mainly composed of amphiphilic block copolymers held together to form vesicles with a bilayer morphology and have recently emerged as combining the advantages of both pSL and pSM in terms of drug loading and stability [22, 44-47]. These pH-sensitive nanocarriers remain stable at physiological pH (7.4), but destabilise or become fusogenic in the acidic environments such as endosomes, releasing their drug content into the cytosol far from the transmembrane efflux pumps. This phenomenon is termed as 'endosomal escape', which enhance cellular bioavailability of the payload by preventing its lysosomal degradation [48]. The increased cytoplasmic drug concentration could exceed the capacity of drug efflux transporters, thus circumventing a major mechanism of drug resistance development in tumor cells. The role and working mechanisms of stimuli-responsive drug delivery systems, including pH-sensitive nanocarriers to overcome MDR have been reviewed [49]. Liu and co-workers [20] have recently classified pH-sensitive nanosystems for potential cancer drug delivery into ionizable, acid-labile and gas-generating types which included organic and inorganic materials. They provided an in-depth insight into the functional properties of different materials and chemical bonds that can be exploited to develop pH-sensitive nanosystems.

In this review, the strategies to design pH-sensitive nanocarriers and their preclinical and clinical findings are discussed. The mechanisms of drug release in response to the low extracellular pH ( $\text{pH}_{\text{ex}}$ ) in tumors and the endosome compartments ( $\text{pH}_{\text{en}}$ ) is fully elucidated. Particular focus is given to novel polymers, various essential chemical bonds and functional groups of the novel biomaterials that are exploited to achieve tumor targeted extra- and intracellular drug delivery. The concept of the 'PEG dilemma', the principles and benefits of pH-responsive 'PEG-detachment' are also discussed.

### 2.3 Mechanisms of pH-Responsive Targeted Drug Delivery

By exploiting the acidic microenvironments in the tumor, pH-responsive delivery systems can be designed for extracellular (pHex) and intracellular (pHen) drug release. These nanocarriers can be designed based on the following three different mechanisms; through the introduction of 1) protonatable groups, or 2) acid labile bonds in the polymers of the carriers; and 3) pH-responsive “PEG detachment”, which may also be achieved at both extracellular or intracellular low pH therefore promoting cell uptake and intracellular drug delivery (Figure 2-1).

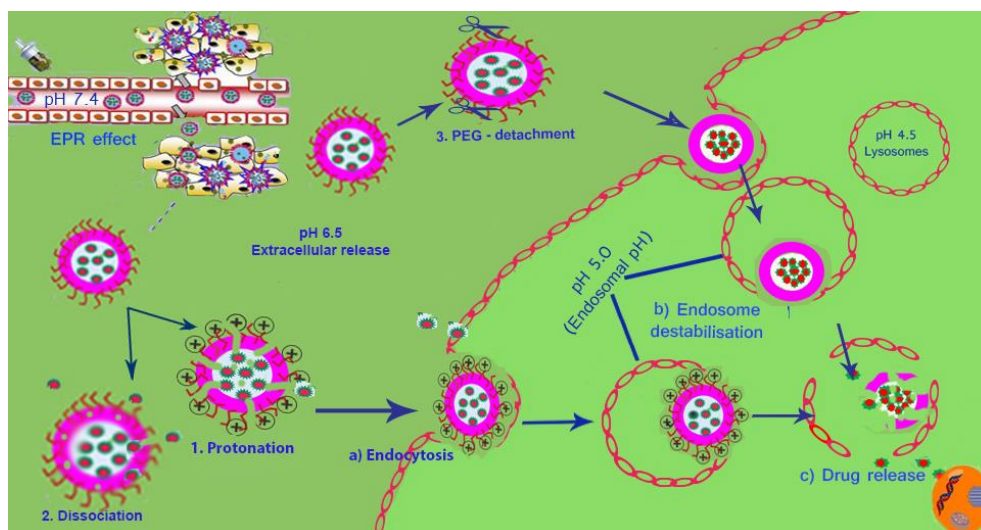


Figure 2-1 Pathways for pH-triggered targeted drug release at the tumor: conformational changes promoting 1) internalization due to protonation or 2) extracellular drug release due to dissociation or; or 3) PEG detachment which facilitates (a) endocytosis of nanocarriers followed by (b) destabilization of endosome membrane, (c) leading to drug release into cytoplasm.

### 2.3.1 pH triggered protonation to promote extracellular or intracellular release

Protonation is one of the most commonly utilised mechanisms to achieve pH-triggered drug delivery. In this strategy, polymers with ionizable chemical groups are utilized as biomaterials to construct the nanocarriers. At physiological pH, they remain deprotonated/deionized, however acidic pH allows protonation or charge reversal of the polymers causing structural transformation or disassembly of the nanocarriers and leads to specific release of the encapsulated payload at either extracellular or intracellular sites [29, 50]. Furthermore, acidic pH induced protonation brings forth hydrophilic-hydrophobic phase transition for the anionic polymers, and hydrophobic-hydrophilic phase transition for cationic polymers. The commonly used ionizable groups include amino, imidazolyl, sulfonates and carboxyl groups. The carboxylic groups of the anionic polymers are deprotonated and hydrophilic at neutral pH, while on reaching acidic conditions they get protonated and become hydrophobic, causing the precipitation of nanocarriers leading to drug release.

Certain anionic polymers, which retain a negative charged surface at physiological pH and change to positive charge with a decrease in pH, are known as charge-reversal polymers. The pH-triggered charge reversal enables very high loading content for positively charged drugs due to electrostatic interaction, and facilitates the cellular uptake by electrostatic absorptive endocytosis [51, 52]. However, they affect the loading of negatively charged drugs due to charge repulsion. The tertiary amine group of cationic polymers remains neutral under basic conditions, whereas under acidic conditions, a positive charge is attained by accepting protons and therefore promotes cell uptake. A summary of the various protonatable pH-sensitive polymers with their  $pK_a$  values and mechanism of drug release at the target is presented in Table 2-1.

### **2.3.2 Acid labile bond cleavage for extra- or intracellular drug release**

Acid labile bond cleavage represents one of the most promising strategies to achieve highly selective tumor targeting, which promotes extracellular drug release or endosomal escape [53, 54] (Figure 2-1). Hydrolysis of the acid-labile bonds between drug and polymer, or within the polymer, represents one of the most promising strategies to achieve the release of drugs at acidic pH. A description of the acid labile bonds that have been investigated, and the preclinical findings, are discussed in section 4.

### **2.3.3 Acid labile bond cleavage for PEG-detachment**

Despite the success of ‘stealth’ systems in achieving stability and long-circulation, the major drawbacks of these nanocarriers are poor cellular uptake and slow drug release from endosomes [55, 56], resulting in low bioavailability in the target and compromised drug efficacy [5, 57], known as the PEG dilemma. To overcome this dilemma, recent efforts have been made in the development of strategies for PEG detachment at target sites. With a pH-responsive PEG detachment mechanism, the PEG shell remains stable at physiological pH facilitating long circulation until reaching the tumor target. At the tumor site, PEG shedding due to the low  $pH_{ex}$  facilitates endocytosis, followed by membrane fusion and endosomal escape (Figure 2-1). Alternatively, PEG detachment can occur in response to the acidic pH following endocytosis of the PEGylated nanocarrier, where it promotes endosomal escape. Taken together, these systems achieve the synergistic benefits of long circulation, enhanced intracellular delivery, and cytoplasmic drug release [58].

Apart from the aforementioned drawbacks, recently researchers identified further concerns with PEGylation. Repeated injection of PEGylated nanocarriers have been reported to induce a significant immune response in some animals through inducing IgM antibodies [59], resulting in a their rapid clearance on repeat injection, a phenomenon known as accelerated blood clearance (ABC) [60-62]. Furthermore, clinical reports showing acute hypersensitivity

## Chapter 2

reactions following infusion of PEGylated liposomes (e.g., Doxil<sup>®</sup>) in certain individuals were recorded. Recently researchers also confirmed that PEGylation could trigger host complement activation [63, 64]. Moghimi's research group has worked extensively in this area [65, 66], and found that complement activation is due to the presence of the anionic phosphate-oxygen moiety of the PEGylated phospholipid, which could be abolished by methylation of the phosphate oxygen [64]. They suggested that structure-activity relationships between conformational states of polymers used for coating and complement activation should be considered for rational design of immunologically safe stealth nanocarriers [67, 68].

It should be pointed out that the strategies for PEG-detachment can promote cell uptake and intracellular delivery but cannot resolve the ABC phenomenon or complement activation. Alternatively water soluble polymers such as HPMA, PDMA, PVP and PMOX [25] have been recently confirmed to confer the liposomes 'stealth' property without causing the ABC phenomenon [25, 69]. Similarly to PEG polymers, however, the hydrophilic polymeric coating causes steric barriers for cellular uptake, and thus the detachment strategy may again be appropriate.

Various PEG-detachable systems achieved via acid labile bonds are discussed in section 4, along with the other pH-cleavable nanocarriers.

## **2.4 pH-Responsive Nanocarriers Based on Protonation / Deprotonation Mechanisms**

Employing this strategy, various pH-sensitive polymers, lipids, polysaccharides and polypeptides have been fabricated by introducing weakly acidic or basic titratable functional groups, such as polyacids or polybases into their structures [70]. These pH-sensitive biomaterials, upon reaching the acidic target, can accept protons and undergo conformational change to their structures via three pathways to achieve targeted drug release: 1) destabilisation, 2) precipitation/aggregation or 3) dissociation (disruption) [28] (Figure 2-2A-C); depending on the  $pK_a$  of the functional group in the biomaterials and the microenvironmental pH. Furthermore, this mechanism can be applied to promote internalization into cells by achieving protonation (ionization) of the functional groups on the surface of nanocarriers at low  $pH_{ex}$  (Figure 2-2D) as the positively charged nanocarriers prefer to contact with negatively charged cell surface via electrostatic interaction [71].

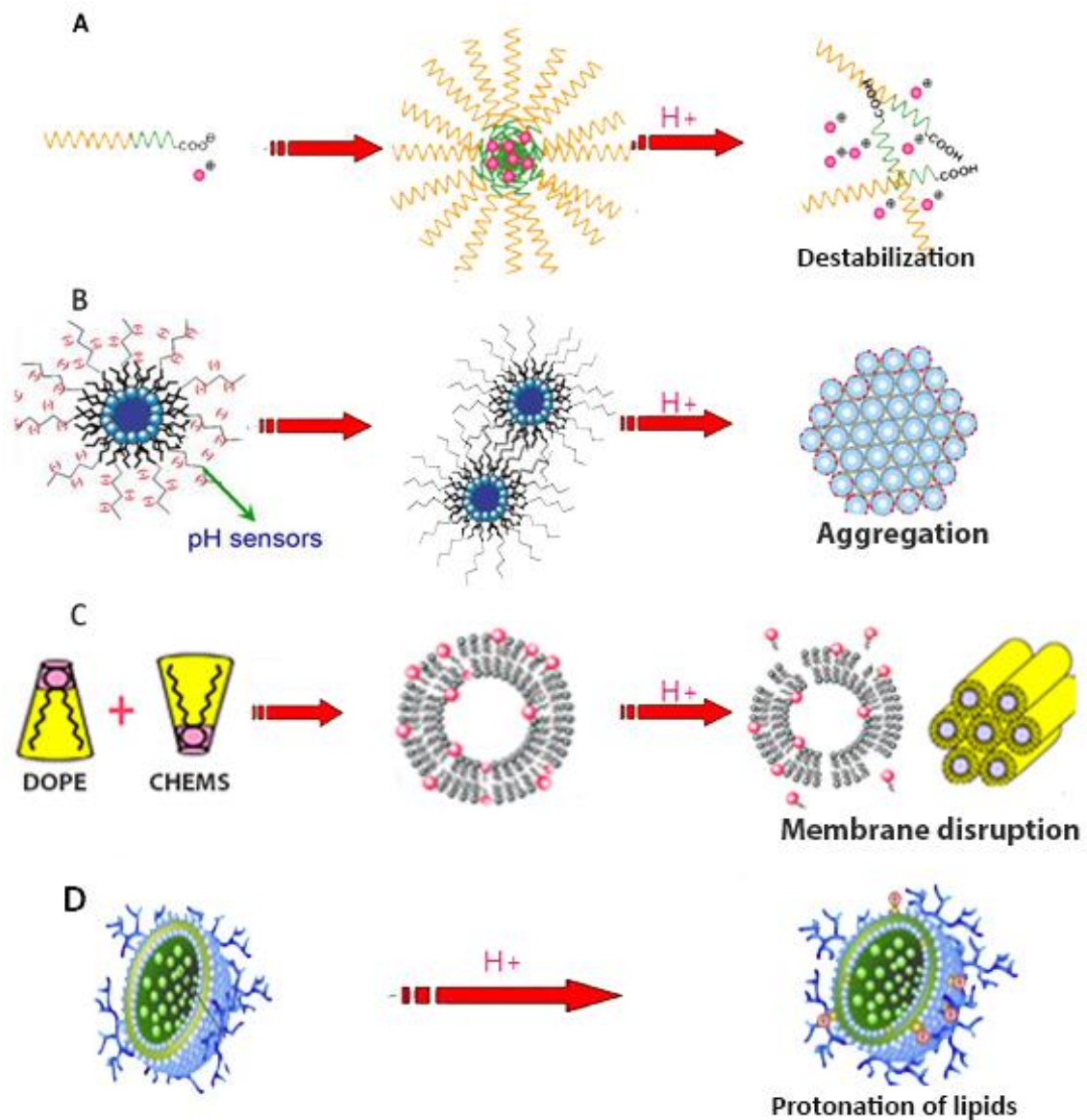


Figure 2-2 Schematic representation of pH responsive mechanisms to promote drug release by (A) destabilization; (B) precipitation; (C) membrane disruption of DOPE-CHEMS liposomes induced by pH-responsive conformational changes of DOPE from bilayer to reverse hexagonal phase (HII); (D) protonation of lipids causing exposure of the positive surface charge which promotes interaction with cell membrane

By selecting a polyacid or polybase containing polymers having  $pK_a$  suitable for the desired pH of target, it is possible to achieve targeted drug release or cellular uptake by the aforementioned mechanisms. These pH-sensitive biomaterials have been used as building blocks for the synthesis of pSL [72], nanoparticles [54], pSM [54], pPS [73], polymer-drug conjugates [74], and dendrimers [75]; while very promising as stimulus-induced drug release systems, efforts are still required to translate proof-of-principle to clinically active products.

### 2.4.1 pH-sensitive polymers

A summary of various pH-sensitive polymers in recent tumor targeted delivery based on the mechanisms of protonation or deprotonation are given in Table 2-1. They are classified as anionic and cationic depending on their charge status at pH 7.4, with some being charge reversible.

#### 2.4.1.1 Anionic pH-sensitive polymers

Anionic polymers with carboxyl pendant groups are commonly used for targeting the acidic pH of tumor tissue. At pH 7.4, the carboxyl groups are deprotonated (ionized) and hydrophilic; conversely at acidic pH, they become protonated (unionized) and hydrophobic. The change from a hydrophobic to hydrophilic molecule leads to the deformation of various nanocarriers, causing drug release (Figure 2-2A). Polyacids, such as poly(acrylic acid) [76, 77], poly(methacrylic acid) (PMAA) [78], poly(2-ethyl acrylic acid) [79], poly(propylacrylic acid) and poly(glycolic acid) are a few examples of this group listed in Table 2-1 [28, 80].

Recently a novel anionic polymer with a bidentate dicarboxylic ligand functionalized polypeptide, methoxy poly(ethylene glycol)-*b*-poly( $\gamma$ -propargyl-L-glutamate-*g*-mercaptosuccinic acid) (mPEG-*b*-(PPLG-*g*-MSA)) was synthesized and self-assembled into polymersomes [46]. Effective drug encapsulation was obtained by electrostatic interaction between anionic mPEG-*b*-(PPLG-*g*-MSA) polymer and cationic DOX (Figure 2-2A). These

## Chapter 2

anionic polymer / DOX complexes were stable at neutral pH but dissociated at endosome/lysosome pH via protonation of carboxylate ligand of polypeptide. The *in vivo* study using a human non-small lung cancer xenograft tumor models demonstrated higher antitumor efficacy of mPEG-*b*-(PPLG-*g*-MSA)-DOX compared with free DOX at an equivalent drug dose.

Polymeric nanoparticles with PMAA-Polysorbate 80 grafted starch (PMAA-PS80-*g*-St) were designed for the pH-triggered delivery of doxorubicin (DOX) and to achieve reversal of MDR [81]. At physiological pH, DOX (basic  $pK_a$  8.2) remains positively charged, therefore it can electrostatically interact with deprotonated carboxyl groups (existing as  $-COO^-$ ) of PMMA in the polymer complex. When the pH is reduced to 6.0, the carboxyl groups become protonated, which triggers drug release from the polymer complex due to the decreased DOX-PMAA electrostatic interaction (Figure 2-2A). *In vitro* studies showed that less than 20% of the drug was released after 90 hours at pH 7.4; this increased to 35% at pH 6.0 and 90% at pH 5.0. These polymeric nanoparticles showed a 20-fold increase in cytotoxicity values in drug resistant cancer cells [81].

NK105, a paclitaxel incorporated micellar formulation, was designed based on a novel amphiphilic block copolymer composed of PEG-poly(aspartic acid) polymers. Half of the carboxylate groups of poly(aspartic acid) were modified with 4-phenyl-1-butanol PEG-poly(asp-phe) to increase core hydrophobicity for encapsulation of paclitaxel, which was loaded by physical entrapment into the micelle system [82]. The free pendant carboxylate groups of poly(aspartate) polymer, which is located in the cores of the micelles, were deprotonated at physiological pH rendering stability to the micelle system. However, on reaching acidic pH they get protonated resulting in accelerated release of the drug due to dissociation of the carrier (Figure 2-2A). Preclinical studies of NK105 showed higher antitumor activity and reduced

neurotoxicity compared with free paclitaxel. The positive results from Phase 1 and 2 clinical trials [83] has led to Phase 3 trial in patients with metastatic breast cancer [84].

Another type of anionic polymer is based on sulfonamide groups [85]. Sulfonamides with  $pK_a$  values  $\sim 7.0$  are most promising due to their ability to shown sharp transition changes around physiological pH [86]. Recently, pSM were developed based on co-polymer stearyl-PEG-poly (sulfadimethoxine) methacrylate for tumor targeting of paclitaxel [87]. Sulfamethoxine, a benzenesulfonamide derivative is a biocompatible polymer with an apparent  $pK_a$  of 6.1 undergoes reversible pH-dependent protonation. At pH 7.4, deprotonated form of sulfamethoxine in the polymeric micelles is negatively charged and hydrophilic, however on reaching tumor acidic pH it converts into a protonated neutral hydrophobic form. The resultant micelles were found to be stable at pH 7.4, while at pH 6.5 (representative of tumor  $pH_{ex}$ ) they rapidly rearranged and aggregated (Figure 2-2B). Confocal microscopy showed that at pH 7.4 the negatively charged polymeric micelles had limited interaction with the cells whereas at pH 6.5, the micelles were readily taken up by the MCF-7 cells and distributed into the cytosol. This was accompanied by increased cytotoxicity relative to the free drug and non pH-sensitive system at pH 6.5.

### **2.4.1.2 Cationic pH-sensitive polymers**

This group of polymers usually comprises polybases (i.e. polyamines, polyethylenimine) which may bear amine groups in their side chains that accept protons at acidic pH and donate protons at basic pH [88]. Poly(*N,N'*-diethylaminoethyl methacrylate) [60] and poly(*N,N'*-dimethylaminoethyl methacrylate) (PDMAEMA) [89] are examples of polybases bearing cationic polymers, Table 2-1. The tertiary nitrogen of amino group plays an important role in the pH sensitivity of cationic polymers. Yang and coauthors synthesized cationic triblock polymers such as poly ( $\epsilon$ -caprolactone) -PDMAEMA-(poly (PEG) methyl-ether-methacrylate),

which self-assembled to form pSM for the intracellular delivery of DOX. The three different polymers arrange themselves into three individual layers with an inner hydrophobic poly ( $\epsilon$ -caprolactone) core to encapsulate the drug, a middle pH-sensitive PDEAEMA layer, then an outside PEG layer. Drug release study showed less than 40% drug released at pH 7.4 in 48 h, which significantly accelerated at pH 6.5 because of the partial protonation of the tertiary amine groups of PDEAEMA. A more rapid release rate was observed at pH 5.0 due to the complete protonation of the amino groups resulting in the formation of channels and cracks on the surface of the micelles [60]. The cytotoxicity of DOX-loaded micelles against HepG2 cells was greater than the free drug solution.

Cationic polymers, poly (vinyl pyridine) (PVP) and in particular, polyhistidine, confer pH-sensitivity of the assembled nanocarriers through the pyridine and imidazole groups, respectively [54]. Polyhistidine has been extensively used in pharmaceutical drug delivery applications due to its biocompatibility and pH-sensitivity [90-98]. The pH-sensitivity of histidine is due to the imidazole moiety ( $pK_b \sim 6.5$ ), which has a lone pair of electrons on the unsaturated nitrogen atom. In slightly acidic conditions the imidazole moiety gets protonated, leading to a lipophilic to hydrophilic phase transition, which causes the destabilization of polymeric nanocarriers, and subsequently the release of encapsulated drugs. Furthermore, polyhistidine was first identified as a pH-sensitive polymer with strong fusogenic and endosmolytic properties [99].

Chiang et al. synthesized HPMA polymer-coated liposomes to target tumor  $pH_{ex}$  [100]. They synthesized a pH-sensitive polymer as methoxy-PEG5000-b- (HPMA-co-histidine)-cholesterol bearing polyhistidine groups and used to coat the surface of the liposomes. These liposomes were then sealed with another polymer, biotin-PEG-biotin, by crosslinking of biotin ( $-C=O$ ) groups with the imidazole ring of histidine via hydrogen bonding to prevent drug leakage. The

## Chapter 2

liposomes were found to be stable at pH 7.4 with a release profile of less than 20% over 24 hours. At pH 6.8 or lower, hydrogen-bond dissociation followed by protonation of histidine triggered destabilization of liposomes and caused drug release. The pH-sensitive liposomes demonstrated a rapid extracellular release profile of DOX, in contrast to the liposomes without polyhistidine. Furthermore, *in vivo* studies demonstrated a relationship between targeting efficiency and anticancer efficacy. Cyanine5.5 NHS ester-labelled liposomes were administered to nude mice bearing HCT116 tumors and their distribution was monitored for 7 days. It was observed that after 1 day the novel liposomes were largely accumulated in the tumor compared to liver and lungs, in contrast to the liposomes coated with the polymer without histidine groups [100]. Further study showed that the liposomes could effectively deliver the encapsulated drug DOX into the cells, and exhibited exceptional anticancer activities *in vivo* and lower hepatic and renal toxicity in nude mice bearing HCT116 colon cancer [101]. Poly ( $\beta$ -amino ester) (PbAE) are biodegradable cationic polymers which are synthesized via conjugation of amines to bis (acrylamides). The ionisable tertiary amine group of the polymer is unprotonated and hydrophobic at physiological pH (7.4). However on reaching the low pH of tumors (6.5), it gets protonated and hydrophilic and triggers drug release. To date PbAE have been extensively used in pH-responsive tumor targeting and have shown pH-responsive degradation, enhanced cell uptake, pH sensitivity and tumor inhibition [102, 103]

Generally speaking, cationic polymers are more toxic than anionic polymers. However, the negative charge of anionic polymers may compromise cell uptake and endosomal escape due to charge repulsion. To address these problems negative-to-positive charge reversal polymers were introduced.

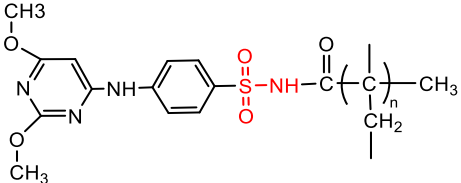
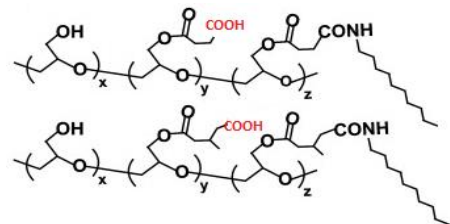
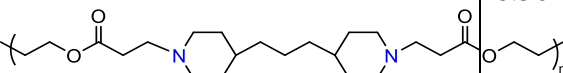
## Chapter 2

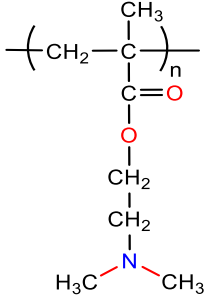
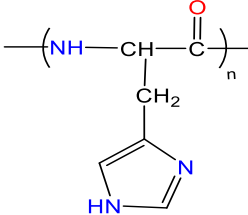
Charge reversal of pH-sensitive polymers at the target can cause the shielding and de-shielding of the outer layer (PEG shell) of the nanocarriers. Based on this effect, histidine-based pPM were designed by Hu and coworkers to target tumor  $pH_{ex}$ , which promoted cellular uptake as a secondary pathway [97]. Paclitaxel-loaded cationic micelles were formed by the self-assembly of two block polymers, poly (L-histidine) and short branched polyethylenimine. Micelles were shielded by coating the surface of cationic polymers with a block polymer composed of  $\alpha$ -methoxy  $\omega$ -hydroxyl PEG and a pH-sensitive anionic polymer, polysulfadimethoxine. Results suggested that micelles were stable at pH 7.4, but when exposed to  $pH_{ex}$  of 6.6, de-shielding of outer PEG layer occurred due to the surface charge conversion of sulfadimethoxine group. This charge reversal combined, with protonation of histidine in  $pH_{en}$ , resulted in enhanced cell uptake and targeted drug delivery. Internalization of micelles into MCF-7 and SKOV-3 cells showed that when shielded micelles were incubated at pH 6.6 de-shielding occurred and a significant increase in cellular uptake was detected (by fluorescence) compared to those incubated at pH 7.4. Furthermore *in vivo* evaluation was carried out in mice bearing MCF-7 xenografts and tumor growth was monitored over 29 days. It was observed that the tumor volume was reduced significantly in pH-sensitive polymer-shielded micelles, compared to unshielded and free drug treated.

Based on the above studies it is evident that pH-sensitive polymers based on the protonation mechanism are able to efficiently enhance the cellular uptake of nanocarriers into cancer cells both *in vitro* and *in vivo*, indicating their potential for applications in cancer treatment.

Table 2-1 Examples of pH-sensitive cationic and anionic polymers and their mechanisms for triggered release.

	pH-sensitive polymer	Chemical structure	pK <sub>a</sub>	pH-sensitive conformation changes of polymer	Examples
Anionic polymers	Poly(aspartic acid) (PASP)	$\left[ \begin{array}{c} \text{O} \\ \parallel \\ \text{CH} - \text{C} - \text{NH} \\   \quad   \\ \text{CH}_2 \quad \text{COOH} \\   \\ \text{COOH} \end{array} \right]_x \left[ \begin{array}{c} \text{O} \\ \parallel \\ \text{CH} - \text{C} - \text{NH} \\   \\ \text{CH}_2 \end{array} \right]_{1-x}$	4.88	Carboxylate groups are deprotonated at pH 7.4 (hydrophilic), but get protonated at pH below 5.0 (hydrophobic), leading to destabilization of nanocarriers.	[104]
	Poly(acrylic acid) (PAA)	$\left( \text{H}_2\text{C} - \underset{\text{COOH}}{\text{CH}} \right)_n$	4.75	An increase in pH causes ionization and swelling of the polymer. At low pH, the carboxylate group of polymer chains becomes protonated and destabilizes the nanocarriers.	[105]
	Poly(ethyl acrylic acid) (PEAA) and Poly(methacrylic acid)(PMAA)	$\left( \text{CH}_2 - \underset{\text{COOH}}{\overset{\text{R}}{\text{C}}} \right)_n$ <p>R=CH<sub>2</sub>CH<sub>3</sub> (PEAA) R=CH<sub>3</sub> (PMAA)</p>	6.30 5.50	Polymer remains stable at pH 7.4 due to its deprotonated state. While at pH < pK <sub>a</sub> carboxyl groups becomes protonated which initiates collapse of the polymer network.	[70, 106, 107]

	Poly-sulfonamides		6.80	pK <sub>a</sub> of sulphonamides ranges from 3-11 depending on the substituents at the SO <sub>2</sub> NH group. These polymers switch their charge in response to pH changes, causing changes of the nanostructure.	[79, 85-87]
	3-Methylglutarylated poly (glycidol)		6.30	Carboxylic groups of methylglutarylated units of polymer chains become protonated/ deprotonated in response to pH changes and act as trigger for destabilization of nanocarriers.	[108] [109]
Cationic polymers	Poly(β-amino ester)		6.50	The ionizable tertiary amine group of the polymer acts a pH trigger for drug release. At pH above 7.4 polymer is deionised and hydrophobic, whereas at pH below 6.5 it becomes ionized and hydrophilic.	[110]

Poly( <i>N,N</i> -dimethylamino) ethyl methacrylate (PDMAEMA)		7.50	This tertiary amine functional group of the polymer is deprotonated at basic pH and become protonated or ionized at acidic pH and, therefore triggering pH dependent drug release.	[111-113]
Poly(L-histidine)		~ 7.0	The lone pair of electrons on the unsaturated nitrogen of the imidazole ring endow pH-dependent amphoteric properties. At neutral pH amine group is deprotonated, while at pH below its pK <sub>a</sub> value, protonation of lone pairs of electrons induces conformational changes in polymers.	[47]

### 2.4.2 pH-sensitive lipids

Liposomes composed of pH-sensitive phospholipids are able to destabilize under acidic conditions of tumors and deliver the encapsulated contents intracellularly [114, 115]. Dioleoylphosphatidylethanolamine (DOPE) is the most commonly used pH-sensitive lipid [116, 117]. The inverted cone shape of the DOPE lipid allows for strong intermolecular interactions between the amine and phosphate groups of the polar head groups, hence these molecules tend to acquire a reverse hexagonal HII shape (non-bilayer phase) at neutral pH [118]. Due to these structural aspects DOPE cannot form lipid bilayers by itself at physiological pH, however incorporation of lipids with a large head group (cone shaped acidic amphiphiles) can stabilize the DOPE vesicles into lipid bilayers (Figure 2-2C). Of the available amphiphiles, cholesteryl hemisuccinate (CHEMS) is considered to be a good candidate due to its cholesterol moiety, which confers higher stability to the DOPE-containing vesicles as compared to other commonly used amphiphilic stabilizers. At acidic pH, the carboxylic group of CHEMS become protonated, which induces change in their conformation from cone shaped to cylindrical resulting in liposomal destabilization, because DOPE molecules revert from a bilayer to an inverted hexagonal II phase [119-121].

A PEGylated pSL system (DOPE:CHEMS:PEG-DSPE) containing gemcitabine has recently demonstrated a high cytotoxicity towards drug-resistant pancreatic cancer (Mia PaCa-2) cells [122]. The studies showed that these liposomes had better endosomal escape compared to non pH-sensitive liposomes. A similar cisplatin-containing PEGylated pSL developed by the Leite group was better tolerated and had higher anti-tumor efficacy than the free drug solution, with 18.2% of the mice showing complete remission of the tumors [123].

### 2.4.3 Polysaccharides

Polysaccharides derived from natural sources such as chitosan, alginate, hyaluronic acid and pullan are used for biomedical purposes to a large extent as they are readily available, biodegradable, non-toxic and can be adapted to different applications by simple chemical modifications. Based on the pH-dependent gelling properties of alginate, glycyrrhetic acid modified alginate nanoparticles were fabricated to selectively target DOX to hepatic tumor cells. Animal studies demonstrated that the concentration of DOX reaching the liver from these nanoparticles was 4.7 times higher than non-alginate modified nanoparticles [124].

Chitosan, a cationic polysaccharide with primary amino groups in its polymeric backbone, is widely used for drug and gene delivery to tumors [125]. In tumor interstitium, following cellular uptake, the positively charged chitosan nanocarriers readily adhere to endosomal surfaces and promote intracellular drug release. To improve the stability of drug delivery systems, cationic chitosan has been used in combination with anionic polymers to form more stable amphiphilic polymers, such as poly (lactic-co-glycolic acid) grafted chitosan oligosaccharide micelles [126] and *N*-octyl-*N*-(2-carboxyl-cyclohexamethenyl) chitosan derivatives [127]. These amphiphilic derivatives undergo self-assembly to form nanocarriers with improved drug loading efficiency and stability. Wang et al synthesized nanocomplexes modified with a folic acid and carboxylated chitosan coating (FA-PEG-CCTS) for pH-sensitive gene delivery. They emphasized that the ability of the carboxylate group to be protonated at the acidic  $\text{pH}_{\text{ex}}$  of tumor promotes intracellular delivery, which augments tumor accumulation, allowing a greater transfection rate [128]. More recently, glycol chitosan-coated liposomes have been demonstrated to have negative-to-positive charge reversion from pH 7.4 to pH 6.5 which mediated cellular uptake [129]. Animal studies showed an enhanced DOX accumulation in tumor cells and higher antitumor efficacy than free drug treated or conventional liposomes. Also various pH-sensitive polysaccharide-based prodrugs have shown their ability to achieve

tumor pH-responsive drug delivery [130]. The pH-sensitiveness of the polysaccharide-based systems is due to the ionization of  $-\text{COOH}$  groups of polysaccharides.

### 2.4.4 pH-sensitive peptides

Since their discovery, cell penetrating peptides (CPP) have been considered promising carriers for overcoming the cellular obstacles in drug delivery [75, 131]. CPPs can be directly conjugated with the drug or with nanoparticles. However, the effectiveness of CPPs as drug delivery systems has been limited due to the lack of *in vivo* site-specificity. To improve tumor selectivity, pH-sensitive CPPs have been designed to exploit the pH gradients of tumors [75, 131]. Histidine has been used to design various pH-sensitive CPPs due to its ability to protonate at mild acidic tumor  $\text{pH}_{\text{ex}}$ , while remaining neutral in physiological condition [131].

Ouahab and coworkers synthesized and compared the effectiveness of two types of pH-sensitive PEG-PLA micelles bearing the CPP, decapeptide arginine-glycine  $(\text{RG})_5$  and a pH-sensitive masking decapeptide histidine-glutamic acid  $(\text{HE})_5$  for docetaxel delivery. The imidazole group of histidine  $(\text{HE})_5$  is neutral at physiological pH 7.4, allowing for the electrostatic interaction between anionic carboxylate groups of glutamic acid ( $\text{p}K_{\text{a}} = 4.25$ ) of  $(\text{HE})_5$  and cationic amino groups of guanidino groups of arginine ( $\text{p}K_{\text{a}} = 13.2$ ). These ionic interactions shielded the decapeptide  $(\text{RG})_5$  at neutral pH and offered a better stability for micelles. The interaction was found to dissociate at slightly acidic pH due to the protonation of imidazole group in histidine, which causes the deshielding of masking decapeptide  $(\text{HE})_5$  and therefore exposes the CPP  $(\text{RG})_5$ . In one set of micelles, the pH-sensitive peptide was conjugated to the outer surface of the PEG layer, resulting in pH-sensitive peptide outside micelles (PHPO); pSM micelles with peptides inside (PHPI) were obtained by conjugating peptides to the PLA block. Results indicated that both formulations exhibited a pH-dependent release profile with 55% of the drug released at pH 7.4, and 70 - 80% drug release at pH 6.8. Cytotoxicity studies showed that

## Chapter 2

compared to PHPI micelles, PHPO micelles had higher toxicity against MCF-7 cells at pH 6.8, due to the enhanced cell internalization [132].

Due to their ability to undergo conformational changes in response to low pH, some peptides were used to design pH-sensitive fusogenic peptides. Subbarao et al. were the first to design the fusogenic peptide GALA, based on the membrane fusion activity of animal viruses. The fusogenic activity of GALA was attributed to the increased helical content at acidic pH [133]. Similarly, introducing fusogenic peptides (such as GALA, KALA [134, 135] and EALA) into nanocarriers such as liposomes, micelles, dendrimers, contributed to cellular uptake and intracellular trafficking (endosomal escape) [136]. A limitation with GALA-modified nanocarriers is their fast elimination from systemic circulation by the RES [137], which can be overcome by PEGylation. However, PEGylation can compromise cellular uptake and endosome escape of the nanocarriers [55, 56]. To overcome this problem and achieve synergistic effects of long circulation without compromise in cell uptake, nanocarriers were incorporated with pH-sensitive tumor-specific PEG-detachable fusogenic peptides such as GALA [55]. GALA-modified liposomes were used for intracellular delivery of small interfering RNA (siRNA) with their PEG layer designed to be cleaved by matrix metalloproteinase-2 (MMP-2) in tumors. *In vivo* studies using nude mice demonstrated the efficient silencing of the target gene and more effective antitumor activity than the non-modified PEGylated liposomes [138].

Amphiphilic polypeptide-based block copolymers can self-assemble into polymersomes, which also known as pepsomes [51]. pH-responsive pepsomes have attracted much attention to achieve tumor targeted drug delivery. In these systems, the protonation of the polypeptides at low pH bring forth conformational changes of polypeptide blocks, which determines the solubility of the copolymer. Recently pH-responsive chimeric pepsomes were developed using

asymmetric PEG-*b*-poly(l-leucine)-*b*-poly(l-glutamic acid) (PEG-pLeu-PGA) triblock copolymers for intracellular delivery of DOX. Pepsomes remain stable at pH 7.4, whereas under the endosomal and lysosomal pH conditions, protonation of block polymer segment induces change from its hydrophilic random coil structure into hydrophobic  $\alpha$ -helical structure, resulting in destabilization and collapse of pepsomes and enhanced release of loaded drug. 3-(4, 5-Dimethylthiazol-2-yl)-2,5-Diphenyltetrazolium Bromide (MTT) assays demonstrated that the DOX-loaded pepsomes were potent toward drug-resistant cancer cells (MCF-7/ADR)[57].

From the above studies, it was evident that pH-sensitive fusogenic peptides and CPPs are promising for tumor-targeted drug and gene delivery.

## 2.5 pH-Responsive Nanocarriers Based on Acid Labile Bond Cleavage

Cleavage of the chemical bond is designed to be initiated at the target [139] by utilizing specific stimulus such as low pH, and enzymes that are over expressed in tumor tissue. Among various stimuli, pH triggered cleavage is regarded as the most general strategy. The bond cleavage causes either drug release (Figures 2-3 A and B) [140-142] or PEG detachment (Figure 2-3C) as mentioned in sections 2.2 and 2.3 [143-145]. Depending on how the drug is loaded, namely chemical conjugation or physical incorporation, the drug release mechanisms include direct dissociation of the drug molecule from the carrier such as gold nanoparticles or dendrimers (Figure 2-3A) or disassembling of the nanostructure (Figure 2-3B). The rate-determining step for pH-triggered bond cleavage is acid catalysed hydrolysis, which can be modulated by choosing appropriate linkers. The most commonly used pH-sensitive linkers for this purpose include hydrazone, imine, oxime, amide, polyacetal and polyketal, ether and orthoester bonds (Table 2-2).

### 2.5.1 Hydrazone bond

Condensation of a hydrazine with aldehydes or ketones results in a class of compounds known as hydrazones, hydroxylamines furnish oximes and primary amines give imines, all with a labile C=N bond. Superior hydrolytic stability of these compounds is due to participation of  $\pi$  electrons in an electron delocalization effect which results in formation of a stable carbocation. The success of use of hydrazone as pH-sensitive linker is due to its acid liability and extended hydrolytic stability at physiological pH [146]. For anthracyclines, the most common method for polymer drug conjugate formation is linking the keto group at the C13 position of the drug with the amino group of polymer hydrazide [147-150].

The hydrazone bond is the most commonly used acid-labile linker and has been successfully utilized to conjugate many anti-cancer drugs such as paclitaxel [151-153], docetaxel [154], cisplatin [155], dexamethasone [156] and mitomycin C [157] to achieve pH-responsive selective targeting to tumors. It has been also employed as a pH-sensitive bond for PEG detachment [158, 159]. Hydrazone bonds linking various nanocarriers with different polymers or macromolecules have been investigated, and some have made their way to the clinical trials [160].

The 6-maleimidocaproyl hydrazone derivative of doxorubicin (INNO-206<sup>®</sup>) provides an example of a pH-sensitive albumin-based macromolecule drug conjugate which has been evaluated clinically; the maleimide moiety reacts covalently with a reactive cysteine on the surface of serum albumin and the resulting conjugate exploits EPR for selective tumor delivery where cleavage of the hydrazone linker releases doxorubicin [160]. However, whether low  $pH_{ex}$  in tumors contributed to that release is unclear.

Hoffman and Stayton initiated and explored the design and development of stimuli responsive HPMA polymer–protein conjugates in early 1980s [161]. They synthesized hydrazone-based

## Chapter 2

dual fluorescent HPMA copolymers, containing a fluorescent dye coupled via a non-cleavable hydrazide bond (polymer label) and a fluorescent model drug bound to a carrier via a pH-cleavable hydrazone [162]. *In vivo* non-invasive optical imaging results confirmed the higher accumulation of the pH-cleavable model drug compared with the non-cleavable polymer. Chytil et al., from the same group, further studied the impact of the acid-labile spacer on the biodistribution of drug and the polymer [163]. Five structurally different spacers were synthesized with pH-sensitive hydrazone bonds and used to link a fluorescent model drug with a polymer backbone, which was conjugated with non-cleavable fluorescent dye. *In vivo* optical imaging demonstrated that the structure of the spacer bearing the hydrazone bond significantly influenced the release rate of the drug and the slow release rate obtained for the spacer with a pyridyl group. They emphasized the importance of careful selection of an appropriate spacer when designing polymer conjugates intended for passive tumor targeting.

Zhou and researchers developed pSM based on the self-assembly of amphiphilic HPMA copolymers with hydrazone bonds. Amphiphilic conjugates were synthesized by conjugating the hydrophobic drug doxorubicin and hydrophobic  $\beta$ -sitosterol to the hydrophilic HPMA polymer backbone via pH-sensitive hydrazone linkages [164]. They further crosslinked HPMA side chains with pH-sensitive hydrazone linkages to ensure their stability in blood circulation. The micelles remained stable at pH 7.4 with less than 20% of the drug released during circulation, whereas at pH 5.0, cleavage of the hydrazone bond lead to an 80% drug release after 8h of incubation. *In vitro* IC<sub>50</sub> values in Hep G2 and A549 cell lines were similar for both crosslinked micelles and non-crosslinked micelles, however *in vivo* studies using a H22 mouse xenocraft model of hepatocarcinoma showed that crosslinked micelles showed a higher tumor accumulation and anti-tumor effect than the non-crosslinked micelles [164]. Results suggested that crosslinked HPMA copolymer micelles with pH-sensitive hydrazone linkages have excellent potential as carriers of anti-cancer drugs.

## Chapter 2

NC-6300, a pSM (40-80 nm) with epirubicin covalently bound to PEG polyaspartate block copolymer via a hydrazone bond, was developed to reduce cardiotoxicity and simultaneously enhance the anti-tumor activity of the drug [165]. The release of epirubicin from NC-6300 accelerated under acidic conditions due to the cleavage of the acid labile hydrazone bond. Pre-clinical tissue distribution studies of NC-6300 showed a 74% drug release in the tumors, which supports the effectiveness of NC-6300 [166]. Only 1.9% of the drug release was observed in the plasma. The AUC of the released drug was 100 times higher in the tumor than in plasma. The animal survival rate increased significantly in the micelle group ( $p = 0.002$ ) and cardiac functions of NC-6300 treated mice were no less well-maintained than in control animals. The results warranted that NC-6300 progressed to clinical trials in patients with hepatocellular carcinoma or other cancers [84].

Table 2-2 Examples of acid-labile chemical bonds and their degradation products

Acid labile bond	Chemical structure	Degradation products
Hydrazone		
Imine		
Oxime		
Cis-acotinyl amide		
Phenyl vinyl ether		
Orthoester		

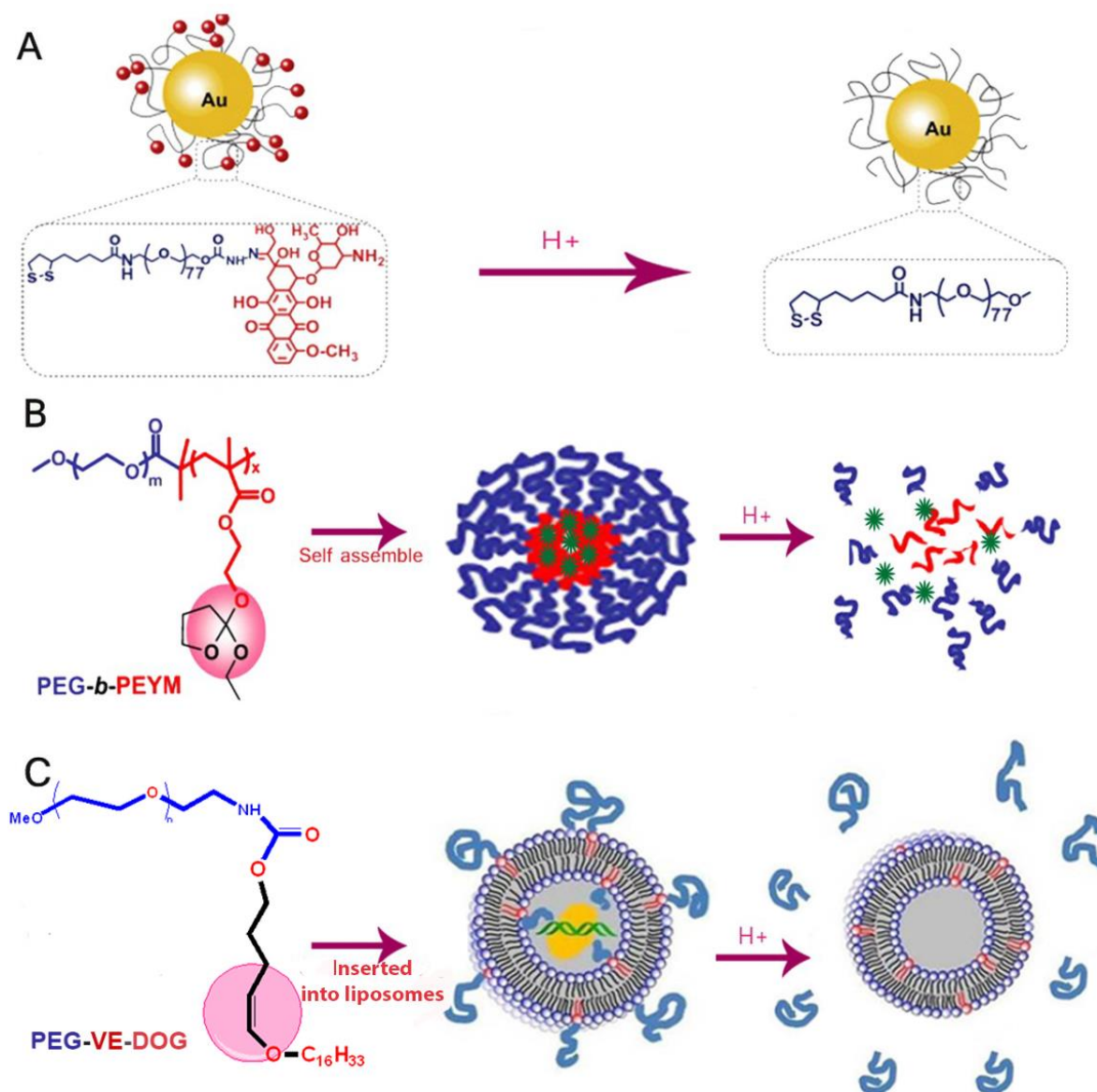


Figure 2-3 Schematic representation of applications of acid labile chemical bonds for the construction of nanocarrier systems for pH-sensitive cleavage such as: A) hydrazone linking drug (i.e. DOX) to the carrier (i.e. a gold (Au) nanoparticle), B) orthoester bonds of polymeric side chain self-assemble micelles with drug incorporated into the core, and C) vinyl ether bond linking PEG to the surface of a nanocarrier (such as a liposome).

## Chapter 2

Pu et al. synthesized poly (L-glutamic acid) dendrimers with polyhedral oligomeric silsesquioxane (POSS) as core. pH-sensitive hydrazone bonds were used to graft doxorubicin and targeting moiety biotin to the surface of the dendrimers. The drug release profile showed pH-dependence with less than 10% of the drug released at pH 7.4, and 90% released at pH 5.0. *In vivo* studies in xenograft breast cancer models demonstrated enhanced tumor inhibition efficiency and reduced systemic toxicity of DOX-dendrimer compared with the free drug solution [167].

Aside from acting as a linker in polymer-drug conjugates, hydrazone has also been utilized to conjugate drugs with inorganic nanomaterials. For example, Sun et.al. synthesized a pH-sensitive nanocarrier system in which DOX was tethered to gold nanoparticles (AuNPs) via hydrazone bonds [141]. *In vivo* studies confirmed that acid labile bond cleavage facilitated the intracellular drug release to cancer stem cells (Figure 2-3A). Pre-clinical studies showed that pH-sensitive AuNPs significantly reduced the tumor formation ability of cancer stem cells by 32-times compared to free Dox. In comparison, the non pH-sensitive system improved only 18-fold.

### 2.5.2 Imine bond

Imine bonds are very sensitive acid-labile linkers that can be hydrolyzed under very slightly acidic conditions (pH ~6.8), near the  $pH_{ex}$  of solid tumors. However, this bond is rarely used to design pH-sensitive systems due to its poor stability at physiological pH. To mitigate this problem, inclusion of  $\pi$ - $\pi$  conjugation into the structure of imine bonds had been employed [58, 168]. Therefore recently investigated imine linkages included  $\pi$ - $\pi$  conjugation in their structure such as benzoic imine [169] and poly(propylene imine)[170].

Based on this strategy, a benzoic imine linker was used to link DOX-loaded amphiphilic poly(l-lysine) micelles with PEG to achieve pH-responsive PEG detachment at target [168]. The

## Chapter 2

resulting pSM showed a neutral zeta potential at physiological pH, but at  $\text{pH}_{\text{ex}}$  ( $\sim 6.8$ ) and  $\text{pH}_{\text{en}}$  ( $\sim 5.0\text{--}6.5$ ) the hydrolysis of the benzoic-imine bond triggered PEG detachment and exposed the positively charged amino groups of the poly (lysine) moiety. The resultant positive charge of micelles promotes electrostatic interaction between the carrier and biological membranes, which significantly promoted cellular uptake and endosomal escape. In another study, pH-dependent polymeric conjugates were formed by covalently bonding 4 $\beta$ -aminopodophyllotoxin (NPOD) with PEG via imine linkage [164]. The mPEG-NPOD conjugates are further used as a carrier for paclitaxel, showing a significantly faster NPOD release at acidic pH values of 5.0 and 4.0 than a physiological pH of 7.4. Cytotoxicity data confirmed the efficient delivery of NPOD to the nucleus of tumor cells and led to increased cytotoxicity to A549, HeLa, and HepG2 cell lines compared to free paclitaxel or the parent NPOD. The loaded PTX also showed pH-triggered fast release behaviour, and a good additive cytotoxic effect was observed for the PEG-NPOD-I/PTX. Preclinical studies showed that NPOD selectively accumulated in tumor tissues and mPEG-NPOD significantly reduced the size of the tumors compared with the untreated control.

### 2.5.3 Oxime bond

A potential advantage of using oxime as the pH-sensitive linker in tumor-targeted nanocarriers is the tunability of its acid lability by facile variation of the substituents. However, the application of oxime bond in bioconjugation is limited to some extent due to its greater thermodynamic stability, which delays the release of drug at acidic targets. Bioconjugates of DOX and daunorubicin were prepared by covalently attaching drug to gonadotropin-releasing hormone-III (GnRh-III) hormone via acid-labile oxime linkage for active targeting of the drug to tumor tissue. GnRh-III is also known as luteinizing hormone-releasing hormone (LHRH), a peptide hormone can be used inhibit the growth of hormone-dependent mammary and prostate cancers. It is also used as targeting moiety to deliver chemotherapeutic agents to tumor cells.

*In vivo* studies showed that treatment of BALB/c mice with drug conjugates resulted in 46% tumor growth inhibition and a 38% increase in median survival times compared to the free drug solution [171]. To achieve tumor-targeted drug delivery, a new pH-responsive tri-block copolymer, PEG-oxime-tethered poly(caprolactone)-PEG (PEG-OPCL-PEG) was synthesized which was assembled into polymeric micelles to incorporate DOX [172]. *In vitro* cellular uptake studies using flow cytometry and confocal laser scanning microscopy on HeLa cells confirm that the DOX-loaded PEG-OPCL-PEG micelles can be efficiently internalised into the cells, which explained their potent anticancer efficacy with a relatively low IC<sub>50</sub> values. The above studies confirm that oxime linkage is a robust tool for the design of pH-sensitive polymeric drug delivery systems.

### 2.5.4 Amide bond

Substituted amide linkages such as  $\beta$ -carboxylic amides are most commonly used for tumor targeting. In one study, methoxy poly(ethylene glycol)-b-poly( $\epsilon$ -caprolactone-co- $\gamma$ -dimethyl maleamic acid - $\epsilon$ -caprolactone) bearing acid-labile  $\beta$ -carboxylic amides on the polyester moiety were designed to form micelles [51]. The  $\beta$ -carboxylic amides are negatively charged and stable in neutral pH allowing a high content of cationic hydrophobic DOX to be encapsulated in the micelles through electrostatic interaction. At pH 6.0, the hydrolysis of  $\beta$ -carboxylic amides led to a negative-to-positive charge reversal due to the regeneration of the cationic primary amines (Table 2-2). This charge reversal not only resulted in rapid drug release, but also enhanced the cellular uptake efficiency by electrostatic absorptive endocytosis.

The cis-aconityl amide linker has a carboxylic acid (C-4) in cis-position to a hydrolytic bond (C-1). This linker undergoes an intramolecular assisted acid-catalysed hydrolysis at the C-1 bond [139, 173]. Among the acid-labile amide linkers, cis-acotinyll amide (Table 2-2) was the first introduced by Shen and Ryser in early 1980s [174]. They demonstrated a longer half-life of the bond at physiological pH ( $T_{1/2}$  = 96 hours) compared to acidic pH (3 hours at pH 4.0).

## Chapter 2

The parent amide was too stable *in vivo* for pH triggered release, while the *cis*-acotinyl form showed suitable properties with enhanced rates of hydrolysis at slight acidic conditions [175]. Further investigation suggested that the *trans* form of the bond reduces acid lability leading to incomplete drug release at target [173, 175]. Therefore, the *cis*-acotinyl bond has been most commonly used to link drug with polymers such as poly-d-lysine [174], HPMA [176], polyvinylalcohol (PVA) [177] and poly(L-lactic acid)-PEG di-block copolymer [178]. For example, pH-sensitive *cis*-aconityl and non pH-sensitive succinic amide linkers (control) were utilized to conjugate DOX to partially PEGylated PAMAM dendrimers [179]. The dendrimers with *cis*-acotinyl bond released DOX in a pH-dependent manner when compared with non pH-sensitive succinic amide linker (control), which released negligible amount in both neutral and acidic pH. The former showed increased cytotoxicity against B16 cells compared to control formulations. *In vivo*, DOX accumulation in tumors was highest for dendrimer with *cis*-acotinyl linker, which was associated with its increased antitumor activity. These results demonstrated the significance of introducing acid-sensitive *cis*-aconityl linkage into nanocarriers for tumor targeting.

### 2.5.5 Polyacetals and ketals

Acetals and ketals are promising candidates for the development of pH-sensitive linkages due to their first-order hydrolysis relative to the hydronium ion, allowing the expected rate of hydrolysis to be 10 times faster with each unit of pH decrease [180-182]. In acidic conditions, oxygen of the acetal group gets protonated and activates the neighbouring carbon, which facilitates the attack of water, resulting in the cleavage of the acetal to the appropriate aldehyde and alcohol.

Heller and co-authors first reported the synthesis of linear and cross-linked polyacetals by the condensation of polyols with divinyl ethers [183]. Later on Tomlinson et al. synthesized amino

functionalized linear pH-sensitive polyacetals to form water soluble polyacetal-DOX conjugates [184]. *In vivo* biodistribution studies in mice bearing subcutaneous B16F10 tumors confirmed that polyacetal-DOX conjugates had a 2-fold increase in half-life compared to the control (HPMA-DOX conjugates). These pH-sensitive conjugates not only exhibited a 1.4-fold increase in tumor accumulation of DOX, but also led to significantly less deposition of DOX in the liver and spleen. pH-sensitive core cross-linked degradable micelles were synthesized based on a diblock copolymer, PEG-*b*-poly(mono-2,4,6-trimethoxy benzylidene-pentaerythritol carbonate-co-acryloyl carbonate) (PEG-*b*-P(TMBPEC-co-AC)) [185]. This polycarbonate block diblock polymer was linked with acid-labile acetal bond and cross-linkable acryloyl groups for pH<sub>en</sub> triggered release of paclitaxel. *In vitro* drug release showed that the cross-linking of micelles inhibited drug release at pH 7.4, but at pH<sub>en</sub> 5.0, 78% of the drug was released in 23h due to the breakage of acetal linkages. An MTT assay showed that pH-sensitive cross-linked micelles retained anti-tumor activity with a cell viability of 9.2% observed for RAW 264.7 cells following 72h incubation, which was comparable to PTX-loaded non-crosslinked counterparts (cell viability 7.5%) under the same conditions, supporting efficient drug release from PTX-loaded crosslinked micelles inside the tumor cells.

Yinfeng and group developed pH-sensitive degradable chimaeric polymersomes based on poly(ethylene glycol)-*b*-poly(trimethoxybenzylidene tris(hydroxymethyl)ethane methacrylate)-*b*-poly(acrylic acid) (PEG-PTTMA-PAA) triblock copolymers for the targeted delivery of DOX [22]. The pH-sensitive degradation of trimethoxybenzylidene acetals in PTTMA block triggered DOX release in the endo/lysosomal compartments of cancer cells. Confocal imaging demonstrated that these polymersomes efficiently delivered DOX into the nuclei of HeLa cells. Anti-tumor activity by MTT assays in HeLa cells demonstrated that DOX-loaded polymersomes exhibited high anti-tumor activity compared to the free drug solution.

## Chapter 2

Polyketals are hydrophobic polymers with biodegradable ketal linkages in polymeric backbones [186]. Polyketal polymers were assembled into nanoparticles that can encapsulate either hydrophobic drugs or proteins. They undergo acid-catalyzed hydrolysis into low molecular weight compounds, releasing their payload at conditions of low pH [187]. Recently Chen et al., reviewed the recent developments on novel pH-sensitive ketal-based biodegradable polymeric drug delivery systems [188]. Murthy et al. prepared polyketals from acyclic diene ketal monomers to form different hydrogels and microgels for the pH-triggered delivery of proteins and protein-based vaccines to the targets [187].

One advantage of polyketals compared to other biodegradable polymers, such as polyesters, is that upon hydrolysis, polyketals do not release acidic by-products (Table 2-2) which causes inflammation. The hydrolytic half-life of polyketals is shorter than polyesters, but longer than poly(orthoesters) or poly( $\beta$ -aminoesters).

### 2.5.6 Ethers

Phenyl vinyl ether linkers were explored for pH-triggered tumor targeting by Thompson's group [143-145, 189]. Hydrolysis of the vinyl ether (VE) bond proceeds through the acidic pH induced protonation of the  $\beta$  carbon of the vinyl ether, which forms a rapidly degradable hemiacetal intermediate. [143, 144]. Protonation and formation of the intermediate is the rate-determining step for vinyl ether hydrolysis. The rate of hydrolysis, however, can be varied by the rational selection of phenyl ring substituents [139, 143, 144, 190]. VE linkers have been used to design acid-cleavable lipopolymers by conjugating PEG with 1, 3-dioctadecyl-rac-glycerol (DOG) lipids to stabilize DOPE liposomes and to promote tumor endosomal escape through PEG-detachment (Figure 2-3C) [144]. The PEG-DOG was inserted in the liposomes membrane. Drug release studies showed that single VE linkages produced faster drug release at pH conditions below 5.0, depending on PEG-lipid molar ratio and PEG molecular weight

[144]. They further investigated the effect of various substituents on pH-sensitivity of ten mPEG-VE-DOG conjugates with varying substituents on VE linkage [143]. It was found that  $\alpha$ -acyl substituted VEs were particularly insensitive to mildly acidic conditions, but an intermediate rate of hydrolysis was noted for  $\alpha$ -methylene-substituted and  $\beta$ -alkyl-substituted VEs. *In vivo* studies showed that  $\alpha$ -methylene-substituted VE stabilized DOPE liposomes showed good differential selectivity of pH 7.5 and pH 4.5 over 24 hours. In contrast,  $\beta$ -alkyl-vinyl-substituted conjugates exhibited long circulation, but moderate selectivity to acidic pH. Studies suggested that phenyl VE linkers were readily and reliably incorporated into a variety of compounds to enable more control of acid-triggered intracellular drug delivery [144, 145]. Cytoplasmic delivery has also been mediated by an acid-labile cholesterol-VE-PEG modified DOPE liposomes via dePEGylation of the latent fusogenic DOPE liposomes [189]

### 2.5.7 Orthoesters

Since their introduction in the early 1970s, this acid labile group was thoroughly reviewed and investigated by Heller and co-workers [191]. The favourable characteristics of poly(orthoesters) for pH-triggered targeting include: 1) the ability to modulate the pH-sensitivity by the alteration of the structure and nature of substituents such as a 6-membered ring structure or methyl substitution, enhances the rate of hydrolysis by several tens or hundreds of times, respectively [192], and 2) the highly hydrophobic nature of poly(orthoesters), which improves the entrapment efficiency of lipophilic drugs [193].

Guo et al. developed the pH-sensitive di-orthoester modified phospholipids (PEG)-diorthoester-lipid conjugate (POD) [194] and orthoester phosphocholine (OEPC) [195] to improve the stability of the DOPE liposomes in blood circulation from opsonisation without compromising their pH-sensitivity. pH-triggered collapse and content release from POD/DOPE liposomes occurs in two phases, a lag phase at physiological pH 7.4 and a burst release phase at acidic pH 5.0 [196]. Drug release studies demonstrated that at pH 7.5, the POD/DOPE

## Chapter 2

liposomes were relatively stable, and the aggregation did not occur after more than 10 h of incubation at 37 °C. POD had remarkably fast degradation even at mildly acidic pH (5-6). At pH 6.2, liposomal size increased within an hour, and when pH was decreased to 5.0 (pH<sub>en</sub>), extensive aggregation was observed within 10 minutes due to the aggregation of the lipids. OEPC was similar to POD with a more biocompatible phosphocholine head group [195]. The pH-dependent content leakage of OEPC liposomes was found to be similar to POD liposomes, but with a shorter lag phase due to its accelerated hydrolysis at acidic pH. The hydrolysis of orthoester bonds in OEPC liposomes leads to leaky vesicles with pores formed on the surface of the vesicles, resulting in rapid content release. *In vitro* studies in CV-1 cells (monkey kidney fibroblasts) for gene delivery showed that pH-sensitive OEPC liposomes significantly enhanced the *in vitro* transfection efficiency compared with the pH-insensitive phosphocholine liposomes.

Paclitaxel-loaded pH-sensitive amphiphilic micelles composed of block copolymers, PEG-PMAA-2-methoxy-5-methyl-[1,3]dioxin-5-ylmethyl ester) (PEG-b-PMME) with acid-labile 6-membered orthoester rings in side chains were synthesized [197]. Cytotoxicity studies showed that paclitaxel-loaded micelles retained potency in killing lung cancer cells (A549), compared with the free paclitaxel. *In vivo* acute toxicity studies on female BABL/c mice showed that pSM did not affect the blood chemistry, liver function, and renal function of mice. The above studies demonstrated that these orthoesters possess unique acid-labile characteristics and have potential for drug delivery. In another study, Tang et al. designed micelles by the self-assembly of an amphiphilic diblock copolymer consisting of a hydrophilic PEG block and a hydrophobic polymethacrylate block (PEYM) bearing acid-labile ortho ester side-chains (Figure 2-3B) [140]. These micelles were then loaded with DOX. Acid-induced hydrolysis of orthoester bonds in sidechains resulted in disruption of the micelles, thereby releasing the drug from the cores. The IC<sub>50</sub> values of the DOX-loaded micelles were approximately 10-times (by 24h) lower than

## Chapter 2

the free drug solution. This enhanced cytotoxicity against the drug-resistant human glioma cells was attributed to a high intracellular drug concentration and the subsequent endosomal escape of the pH-responsive micelles. Similarly Thambi et al., developed pSL based on amphiphilic block copolymers composed of hydrophilic poly(ethylene glycol) (PEG) and hydrophobic poly( $\gamma$ -benzyl L-glutamate) (PBLG) bearing an acid-sensitive orthoester linkage for the targeted delivery of DOX [198].

Lin and co-workers developed pH-sensitive polyplexes by linking poly(ethylene glycol) and poly(2-(dimethylamino)ethyl methacrylate) (PEG-*a*-PDMAEMA) block copolymers via acid labile cyclic orthoester bonds to achieve PEG-detachment at  $\text{pH}_{\text{ex}}$ , which exposes the surface charge of polyplexes, enhancing cell uptake [187]. However, cytotoxicity studies on 293T cells showed the lower transfection efficacy of pH-responsive (PEG-*a*-PDMAEMA) polyplexes at  $\text{pH}_{\text{ex}}$  (6.5) compared to  $\text{pH}_{\text{en}}$  5.0. This is attributed to the ineffective PEG-detachment at  $\text{pH}_{\text{ex}}$  (6.5), due to the low acid lability of cyclic orthoesters. In another comparative study by Chen et al., they found that linear orthoesters were more acid-responsive than cyclic orthoesters. This is due to the steric hindrance in the structure of cyclic orthoesters [199], which could be greatly enhanced by some structural alterations, such as altering substituents on the orthoester rings. For instance the amide group might affect cyclic conformation of the orthoesters via intramolecular hydrogen bonding, which would influence the hydrolysis [22, 200].

Poly (orthoesters) are significantly more responsive to acidic pH than acetals, ketals and vinyl ethers [140, 201, 202]. This is due to the formation of a dialkoxy carbocation intermediate with four lone pairs of electrons, which readily gets protonated and hydrolysed in mild aqueous acid, whereas acetals and vinyl ethers form a monoalkoxy carbocation intermediate with only two lone pairs of electrons.

## 2.6 Conclusion Remarks and Future Prospects

Cancer remains one of the leading causes of death worldwide. Targeted drug delivery has marked a new dimension addressing the limitations of conventional chemotherapy. An example of this success is the invention of Doxil<sup>®</sup>/Caelyx<sup>®</sup>. The pH-sensitive nanocarriers, particularly after PEGylation are capable of exploiting the EPR effect and releasing the payload in response to the acidic pH<sub>ex</sub> of the solid tumors. Various new biomaterials have been designed to allow the development of these ‘smart’ drug delivery systems. The efficient intracellular delivery of the encapsulated drug(s) is pertinent in overcoming multidrug resistance due to efflux mechanisms. The design could be simultaneously utilized to increase drug loading through drug-polymer interactions (electrostatic or hydrophobic). Due to safety concerns about PEG, and to overcome the ABC phenomenon, various non-PEG hydrophilic polymers were utilized to achieve long-circulation. A pH-responsive detachment strategy may be used in combination with both PEG and other polymers, such as HPMA, to reduce steric barriers to overcome the PEG dilemma and to promote cell uptake. Synergistic effects could be achieved by combining both the strategies of protonation and bond cleavage. After the detachment of the outer shell by bond cleavage, nanocarriers are readily taken up if they possess the ability to protonate or ionize into systems with positive charged surfaces.

Recent attention has been given to the development of multifunctional pH-sensitive nanocarriers, for example by the introduction of ligands that can specifically recognize tumor cells and/or cell penetrating peptides. Such systems could further improve selectivity, enhancing tumor accumulation and the cellular uptake of the anticancer drug, thus improving efficacy and reducing systemic side effects [57, 203]. In the future, there is no doubt that these multifunctional nanocarriers will alleviate many of the challenges in cancer therapy as one of the main components of the therapeutic arsenal.

## Chapter 2

Despite the obvious potential of pH-sensitive nanocarriers, the heterogeneity of  $\text{pH}_{\text{ex}}$  both within and between tumors [204] represents a significant challenge for this tumor targeting strategy, particularly given that low  $\text{pH}_{\text{ex}}$  regions are likely to be the least accessible to nanoparticles that do not distribute readily within the tumor interstitium. This factor, and the lower pH values for  $\text{pH}_{\text{en}}$  than  $\text{pH}_{\text{ex}}$ , suggests that enhancing endosomal escape is the more realistic objective for pH-sensitive nanocarriers in the short term. However, if sufficient sensitivity to mild acidification can be achieved, then selective tumor targeting via  $\text{pH}_{\text{ex}}$  certainly warrants exploring given recent evidence that extracellular acidification is an important contributor to tumor invasion and metastasis [205, 206]. Other strategies that may further suppress  $\text{pH}_{\text{ex}}$  in tumors include an i.v. bolus of 25% glucose which can be used to lower tumor  $\text{pH}_{\text{ex}}$  transiently [207]. In addition to these considerations, the entry of pH-sensitive tumor-targeted nanocarriers into clinical use will require the addressing of broader challenges including: i) a lack of collaboration in innovative research between academia and the pharmaceutical industry, which is essential for the ‘benchtop-to-clinic’ success of a formulation and ii) issues with reproducibility and scale up of manufacture.

### **3. Characterization of a smart pH-cleavable PEG polymer towards the development of dual pH-sensitive liposomes**

---



## Characterization of a smart pH-cleavable PEG polymer towards the development of dual pH-sensitive liposomes

Manju Kanamala <sup>a</sup>, Brian D. Palmer <sup>b</sup>, William R. Wilson <sup>b</sup>, Zimei Wu <sup>a</sup>  

### 3.1 Abstract

To facilitate the development of PEG-cleavable pH-sensitive liposomes (CL-pPSL), this study aimed to fully characterize a new pH-sensitive polymer, PEG<sub>B</sub>-Hz-CHEMS. Polyethylene glycol (PEG) functionalised with 4-carboxybenzaldehyde (PEG<sub>B</sub>) was linked to cholesteryl hemisuccinate (CHEMS) via an acid labile hydrazide–hydrazone hybrid bond (–CO–NH–N=CH–) to form PEG<sub>B</sub>-Hz-CHEMS. The polymer was post-inserted into DOPE/CHEMS liposomes to form CL-pPSL. A fully validated stability-indicating HPLC-UV method was developed with the aid of multiple linear regression for the mobile phase. The assay was used to evaluate the pH-sensitivity, pathways of cleavage of the polymer and the PEGylation degree of CL-pPSL. The pH-sensitivity of CL-pPSL was compared with conventional PEGylated pH-sensitive (pPSL) using a calcein leakage assay. At 37 °C, PEG<sub>B</sub>-Hz-CHEMS was relatively stable at pH 7.4 with a half-life of 24 h. In comparison, at pH 5.5 and pH 6.5 PEG detachment within 1 h was determined as 80%, and 50%, respectively. PEG detachment of the polymer was through simultaneous cleavage of the hydrazide (CO–N) and hydrazone (N=C) bonds, depending on pH, thus the polymer is more pH-sensitive than those with a hydrazine bond only. The grafting densities of PEG<sub>B</sub>-Hz-CHEMS on CL-pPSL were optimised to achieve a PEG density of 1.7% (mol). The unilamellar CL-pPSL (123 nm) were shown to be stable at least for 3 months at 4°C and have enhanced pH-sensitivity compared with pPSL in the calcein leakage

### Chapter 3

assay. Therefore, the smart cleavable PEG polymer is promising in liposome formulation to overcome the PEG dilemma.

**Key words:** Cleavable PEG, Stability-indicating HPLC method, Hydrazide-hydazone, Multiple linear regression model, PEG detachment pathway, Dual pH-sensitive liposomes

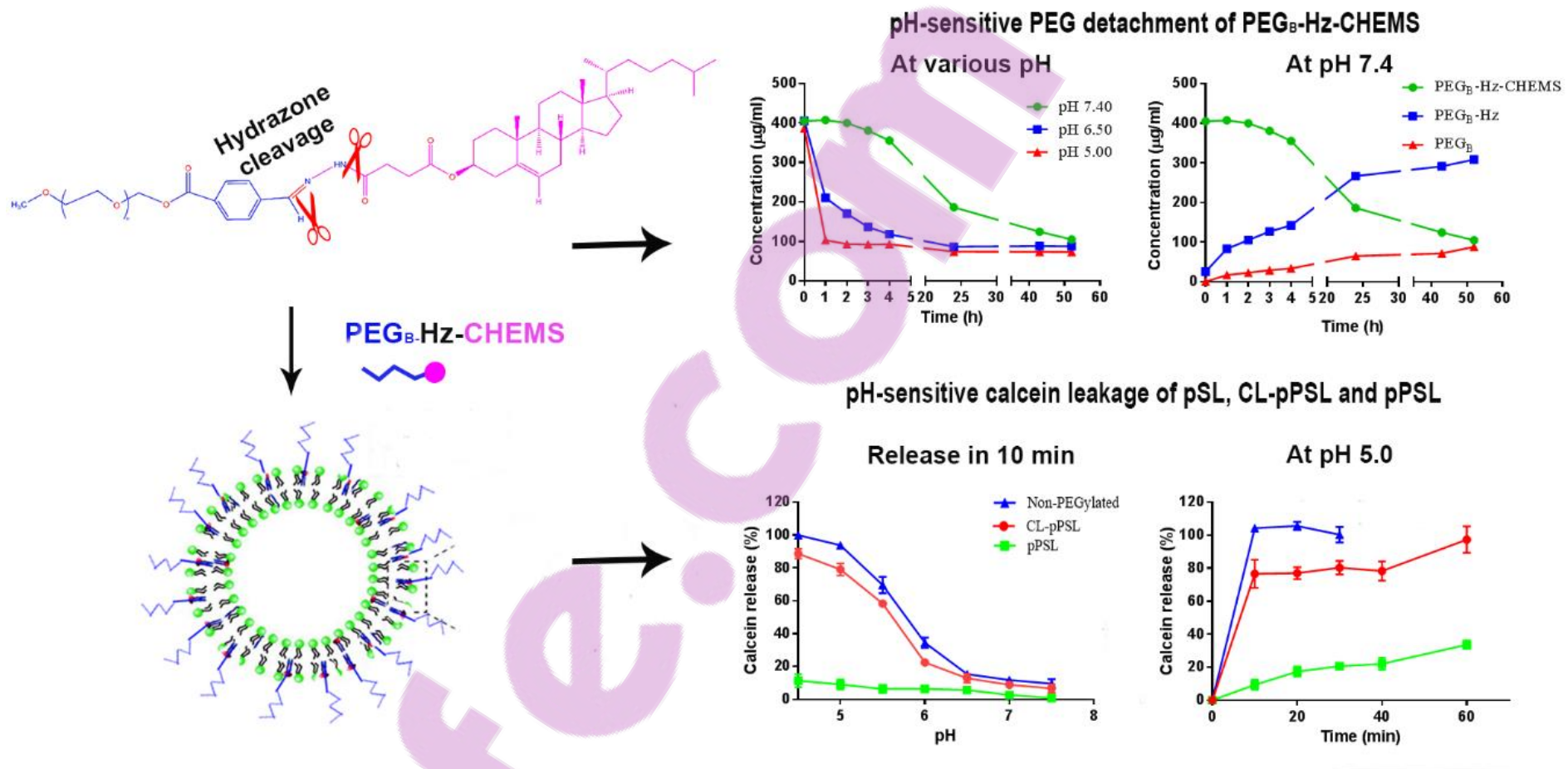


Figure 3-1 Graphical abstract for Chapter 3

## 3.2 Introduction

Liposomes have been extensively investigated as versatile carrier systems for drug and gene delivery with a number of FDA approved clinical products. Covalently linking liposomes with hydrophilic polymers, such as polyethylene glycol (PEG), has been demonstrated to stabilize liposomes *in vitro* and extend their circulation times *in vivo* [208]. The gold standard for stealth coating is still PEG, typically using PEG-conjugated phospholipids [209]. However, PEG coating hinders the cellular uptake of liposomes by target cells [122], and further prevent their rapid escape from endosomes, thus compromising their efficacy. To overcome this limitation, known as the ‘PEG dilemma’ [5], PEG-cleavable liposomes are designed to be triggered by various tumor-specific stimuli such as low pH [210], enzymes [211], or reduction [2, 197] to detach PEG at tumor microenvironment, while retaining steric stabilisation by PEG in the systemic circulation. The low pH cleavable PEG polymers are typically constructed by linking PEG via a pH-sensitive bond such as hydrazone [48, 141, 160], to the lipid anchor, that is subsequently inserted into the bilayers [212]. At the tumor site, low extracellular pH triggers bond cleavage, and initiates PEG shedding to facilitate endocytosis, followed by membrane fusion and endosomal escape of liposomes [213]. The chemical bond, length and density of PEG chains used for polymer synthesis are important factors for determining the kinetics of PEG detachment which in turn are required for better *in vivo* performance of the liposomes.

Despite the great efforts in development of tumor targeted PEG-cleavable liposomes [22, 143-145, 159, 192], there is a lack of an accurate and simple method for the quantitative analysis of surface PEG density of liposomes, which is key to estimate their *in vivo* performance. To date, PEGylation is quantified utilizing direct methods such as colorimetric [214], radiolabelled [215], <sup>1</sup>H nuclear magnetic resonance (<sup>1</sup>H NMR) spectroscopic [216] or some indirect methods as enzyme-linked immunosorbent (ELISA) [217] and high performance liquid chromatography (HPLC) [218-220] that require <sup>13</sup>C-labeling [221]. Compared with HPLC, other methods

### Chapter 3

involve considerable sample treatment, which makes the process time consuming. HPLC is the most convenient technique, yet quantification of these condensation polymers of ethylene oxide and water, using ultraviolet (UV) detection is challenging as PEG polymers do not contain active UV chromophore. Therefore, alternative detectors such as refractive index detectors [218], mass spectrometry [220] and evaporative light scattering detectors [219] are used. Another challenge with HPLC is to achieve adequate resolution between the free PEG and the PEG-conjugate [218, 219]. Thus, a simple and convenient HPLC method to quantify PEG and its conjugate is required to assist the development of smart dual pH-responsive liposomes.

To develop a pH-responsive PEG-cleavable liposomal formulation (CL-pPSL), a PEG-lipid polymer, PEG2000-4-carboxybenzaldehyde-hydrazone-cholesteryl hemisuccinate (PEGB-Hz-CHEMS) has been synthesized in which PEG is conjugated with cholesteryl hemisuccinate (CHEMS) via a hydrazide-hydrazone bond ( $-\text{CO}-\text{NH}-\text{N}=\text{CH}-$ ) [222]. The hydrazide-hydrazone bond was expected to undergo cleavage at acidic pH while remaining relatively stable at physiological pH. In this paper, we report the characterization of the pH-sensitivity of PEGB-Hz-CHEMS, including the degradation kinetics at different pH, the pathways for PEG detachment, and the preliminary work towards formulation of dual pH-sensitive liposomes, CL-pPSL, using the PEG polymer.

To achieve this goal, firstly a simple and reliable stability-indicating HPLC method was developed using ultraviolet visible (UV) detection due to the presence of carboxybenzaldehyde moiety in PEGB-Hz-CHEMS. A multiple linear regression analysis was performed to predict the optimal mobile phase compositions [223] and thus achieve desirable resolution and satisfactory run times for PEGB-Hz-CHEMS and the main degradation products. The HPLC assay was further used in the development of CL-pPSL for the quantification of the insertion efficiencies (IE) of the PEG polymer into liposomes.

### 3.3 Experimental

#### 3.3.1 Materials

Phospholipids, 1,2-dioleoyl-sn-glycero-3-phosphoethanolamine (DOPE), and 1,2-distearoyl-sn-glycero-3-phosphocholine (DSPC), cholesteryl hemisuccinate (CHEMS), 1,2-distearoyl-sn-glycero-3-phosphoethanolamine-N-[amino(polyethylene glycol)-2000] (DSPE-PEG2000) were purchased from Avanti Polar Lipids (Alabama, USA). Polyethylene glycol methyl ether (mPEG2000), dicyclohexyl carboimide (DCC), 4-(dimethyl amino) pyridine (DMAP), and Sephadex G-25 were obtained from Sigma Chemical Co. (MO, USA). HPLC grade acetonitrile and methanol were obtained from Merck. All other chemicals and solvents were reagent grade. Milli Q water (HPLC grade) was obtained from a Millipak filter unit (Millipore, pore size 0.22  $\mu\text{m}$ ).

PEG<sub>B</sub>-Hz-CHEMS was synthesised as described previously [222], and newly prepared polymer was utilized to develop stability-indicating HPLC method and for further characterization studies.

#### 3.3.2 Stability-indicating HPLC method development for PEG<sub>B</sub>-Hz-CHEMS

##### 3.3.2.1 Instrumentation and chromatographic conditions

To characterize the pH-sensitivity of PEG<sub>B</sub>-Hz-CHEMS and the resulted liposomes, a stability-indicating method was developed and validated on an Agilent 1260 series HPLC system comprising a quaternary pump equipped with an auto-sampler injector and a diode array detector (DAD). Data acquisition was performed using Agilent 1260 software. Separation was carried out on a Luna C18, 5  $\mu\text{m}$ , 4.6 mm  $\times$  250 mm column connected with a 4.6 mm  $\times$  30 mm pre-column of the same type (Phenomenex<sup>®</sup>, New Zealand) maintained at 30 °C and flow rate was 1 mL/min. The injection volume was 20  $\mu\text{l}$ . Dual UV wavelengths were set at 300 nm and 254 nm for detection of PEG<sub>B</sub>-Hz-CHEMS and its degradation products, respectively. Finally,

the optimal HPLC mobile phase (water: acetonitrile: methanol, 50:5:45, v/v/v) were applied for the simultaneous determination of PEG<sub>B</sub>-Hz-CHEMS and main degradation products.

### ***3.3.2.2 Synthesis of potential degradation products and preparation of standard solutions***

To confirm the stability-indicating nature of the assay, first, the potential degradation products, PEG<sub>2000</sub>-4-carboxybenzaldehyde (PEG<sub>B</sub>) and PEG<sub>2000</sub>-4-carboxybenzaldehyde-hydrazone (PEG<sub>B</sub>-Hz) were synthesised. PEG<sub>B</sub> was synthesised as described previously [222]. PEG<sub>B</sub>-Hz was obtained by reacting PEG<sub>B</sub> with hydrazine-hydrate in 2 mL of chloroform at 25 °C in a tightly closed reaction vessel. This was followed by purification of the obtained PEG<sub>B</sub>-Hz on Sephadex G-25 using Milli Q water, and its chemical structure was confirmed by NMR spectrometry.

A mixed stock solution containing PEG<sub>B</sub> and PEG<sub>B</sub>-Hz-CHEMS both at 1 mg/ml was prepared in acetonitrile and stored at -20 °C. Working standards were freshly prepared by serial dilutions of the stock solution to obtain concentrations of 8 to 125 µg/mL. Quality control (QC) samples were prepared at low (20 µg/ml), medium (40, 80 µg/ml) and high (100 µg/ml) concentrations in the same way as described above from the working standard solutions.

### ***3.3.2.3 Mobile phase optimisation by multiple linear regression***

A multiple linear regression model using Minitab version 12.1 (Minitab Inc., PA, USA) was utilized as a chemometric tool to determine the mobile phase composition that achieves desirable retention times (R<sub>t</sub>) of multiple analytes [223]. The mobile phase composition consisting of water, acetonitrile (A) and methanol (M) was employed. The volume percentage of water (X<sub>1</sub>) and solvent ratio A/M (X<sub>2</sub>) was chosen as the variable factors to achieve suitable R<sub>t</sub> for two analytes, PEG<sub>B</sub>-Hz-CHEMS and PEG<sub>B</sub>. The levels of X<sub>1</sub> was set from 40-50%, and

## Chapter 3

the X2 was set from 3-9%, respectively. A total of six experiments with various mobile phase compositions were carried out and chromatographic responses were collected.

A multiple linear regression of the  $R_t$  of each analyte as a function of the variables (X1 and X2) was performed using Minitab version 12.1 and a regression equation was generated (equation 3.1) to predict the mobile phase composition required to achieve appropriate  $R_t$  for the analytes.

$$R_t = \beta_0 + \beta_1 X_1 + \beta_2 X_2 + e \quad \text{Equation 3.1}$$

Where,  $\beta_0$ ,  $\beta_1$  and  $\beta_2$  are model coefficients determined by regression analysis, and  $e$  is the experimental residual error.

### **3.3.2.4 Validation**

The specificity of the assay was determined by comparing the chromatograms of analyte-free blank samples with the samples spiked with standard solutions [224]. The linearity of the assay was determined for both the analytes PEG<sub>B</sub>-Hz-CHEMS and PEG<sub>B</sub> by analyzing three replicates of seven standards at a concentration range of 8 to 125  $\mu\text{g/mL}$ . Intra-day variability was determined by three replicate analyses of QC samples for both the analytes. Similarly, inter-day variability was determined by repeated analysis of all the QC samples on three different days. A new calibration curve was prepared on each day. Assay precision was assessed by the percent relative standard deviation (%R.S.D.) Accuracy was determined by comparing the experimental concentrations of the control samples against their respective theoretical concentrations. Limit of detection (LOD) and quantification (LOQ) were calculated as 3 and 10 times residual standard deviation of a calibration curve over slope of the regression lines respectively.

### **3.3.3 Kinetics of pH-dependent PEG detachment of PEG<sub>B</sub>-Hz-CHEMS**

The kinetics of pH-dependent PEG detachment of the hydrazine-hydrazone-based PEG<sub>B</sub>-Hz-CHEMS was investigated at physiological pH 7.4, in acidic tumor extracellular, pH 6.5 and endosomal pH 5.0 maintained at 37°C using the above developed stability-indicating HPLC method. PEG<sub>B</sub>-Hz-CHEMS polymer was dissolved in 10 mM PBS buffer with various pH (5.0, 6.5 and 7.4) to yield a final concentration of 1 mg/mL and incubated at 37 °C for different times. Samples were collected at intervals and the withdrawn samples were diluted to levels in the calibration range and subjected to HPLC analysis to monitor the decrease in the peak area of PEG<sub>B</sub>-Hz-CHEMS, and the presence of degradation products over time.

### **3.3.4 pH-dependent degradation pathways of PEG<sub>B</sub>-Hz-CHEMS**

The degradation products were further identified by comparing their retention times and the UV spectra obtained using DAD with the synthesized starting materials of PEG<sub>B</sub> and PEG<sub>B</sub>-Hz. After confirmation, the degradation scheme was plotted. The half-life of the PEG<sub>B</sub>-Hz-CHEMS at different pH was estimated based on the changes in the HPLC peak areas over time. The degradation pathways, through the cleavage of hydrazone and hydrazide bonds were analysed.

### **3.3.5 Quantification of PEGylation degree towards the development of CL-pPSL**

CL-pPSL was prepared by the thin film hydration method. In brief, DOPE, DSPC, CHEMS and cholesterol at the molar ratio of 4:2:2:2 were dissolved in chloroform, and then solvent was removed on a rotary evaporator at 30 °C under vacuum to form thin lipid films, which was kept under vacuum overnight. The resulting films were hydrated with phosphate-buffered saline (PBS; 0.1 M, pH 7.4) at 30 °C to produce multilamellar vesicles, which were later subjected to 7 cycles of freeze and thaw [225]. The size was controlled by extrusion of the lipid vesicles

## Chapter 3

through a 100 nm pore sized polycarbonate membrane filters (Whatman, UK) for 10 times with a pressure of ~500 psi [226] using a LIPEX™ Extruder (Northern Lipids Inc., Burnaby, Canada).

The naked liposomes were PEGylated by the post insertion technique [122] with 5 mol% of PEG<sub>B</sub>-Hz-CHEMS to form a dual pH-responsive liposomes, CL-pPSL. Briefly, after ultracentrifugation (186,000×g) of the naked liposomes for 2 h at 4 °C, the pellet was re-suspended in a 3.5 mg/mL of PEG<sub>B</sub>-Hz-CHEMS solution in PBS (0.05M, pH 7.4), and incubated at 4 °C for 8 or 24 h for PEGylation, respectively. The resulting liposome suspensions were subjected to ultracentrifugation at 4 °C for 2 h, to completely pelletize the liposomes and to separate the free polymer. It was found that 1-hour ultracentrifugation, which is usually used [122], could not completely pelletize either the naked liposomes or CL-pPSL, possibly due the low density of the liposomes.

Following 8 h or 24 h of PEGylation, the IE of PEG<sub>B</sub>-Hz-CHEMS into the pH-sensitive liposomes was immediately determined by quantifying the PEG<sub>B</sub>-Hz-CHEMS in the liposomes pellet. The pellet was destroyed with 1 mL of 10% triton X-100 solution [122] and further diluted with PBS (pH 7.4, 0.01 M) to achieve a concentration within the range of calibration curve. Meanwhile, the supernatant was also collected and diluted with PBS (pH 7.4, 0.01M) for HPLC analysis of the free polymer. The IE (%) was calculated as the percentage of the inserted versus the amount used for PEGylation. During HPLC analysis the presence of the degradation products, PEG<sub>B</sub> and PEG-Hz, in the chromatograms was closely monitored to assess the stability of PEG<sub>B</sub>-Hz-CHEMS during PEGylation.

### **3.3.6 Size, morphology and stability of the CL-pPSL**

The physical stability of the CL-pPSL was assessed by determining the particle size, polydispersity index (PDI), and zeta potential of the liposomes stored either as liposomal pellets

or suspension in PBS (0.01M, pH 7.4) at 4 °C using dynamic light scattering (DLS) technique with a Nano ZS (Malvern Instruments, UK). Samples were diluted with PBS (0.01 M, pH 7.4) prior to characterization. Morphology of the liposomes before and after PEGylation was analyzed by cryo-transmission electron microscopy (cryo-TEM, FEI, Hillsboro, Oregon). Stability over 3 months was assessed by monitoring the particle size and distribution.

### 3.3.7 pH-responsive calcein leakage assay

To determine the pH-sensitivity of CL-pPSL in comparison to pPSL, the non-cleavable PEGylated pH-sensitive, with a similar PEGylation degree (1.7 mol%) and pSL (the non-PEGylated), calcein was passively loaded into these liposomes. Briefly, an 80 mM calcein solution dissolved in PBS (pH 7.4, adjusted to 320 mOsm with NaCl) was prepared and diluted to concentrations ranging from 0.01 mM to 100 mM and evaluated for its self-quench property by measuring the fluorescence using plate reader  $\lambda_{\text{ex}}$  470 nm;  $\lambda_{\text{em}}$  509 nm. Thus, prepared 80 mM calcein solution was used to hydrate the lipid thin film at 30 °C for 1 h. The liposomes were subjected to freeze and thaw for 7 cycles, followed by extrusion and spin down to remove the untrapped calcein. The liposomes pellet was reconstituted with PBS, 0.01M, pH 7.4 (total lipids concentration 10 mg/ml) before the calcein leakage assay. The concentration was determined with a NanoSight (Malvern, Herrenberg, Germany) to be approximately  $10^8$  liposomes/ml.

The pH-responsive calcein leakage of liposomes was tested by incubating 100  $\mu\text{L}$  of the above obtained liposomal suspension with 900  $\mu\text{L}$  of various pre-warmed PBS buffers (pH 4.5, 5.0, 5.5, 6.0, 6.5, 7.0 and 7.4) for 10 min in water bath at 37°C with shaking at 250 rpm. Based on the volume of liposomal core  $9 \times 10^{-13}$   $\mu\text{L}$  (for a liposome of 120 nm) and the total liposome concentration ( $10^7$  liposomes /mL), the maximal calcein concentration was calculated to be 0.72 mM. After incubation, calcein release was quantified by measuring its fluorescence intensity

## Chapter 3

using a plate reader (excitation, 470 nm and emission, 509 nm). In another experiment, the kinetics of calcein leakage from CL-pPSL was measured over a time period of 1 h at pH 5.0 whereas pPSL and freshly prepared non-PEGylated pH-sensitive liposomes were used as references. The total fluorescence intensity was measured by destroying the liposome with 10% of Triton-X<sub>100</sub>, followed by dilution with PBS (pH 7.4, 100 mM). To quantify the amount of calcein, linear calibration curves at various pH were established. The pH-sensitivity of the liposomes was calculated using the following equation 3.2.

$$\text{Calcein Release (\%)} = \frac{M_{pH} - M_{7.4}}{M_t - M_{7.4}} * 100 \quad \text{Equation 3.2}$$

Where  $M_{7.4}$  is the mass of calcein released to medium at pH 7.4 at the initial time,  $M_{pH}$  is the mass released at different pH buffers, and  $M_t$  is the total mass of calcein entrapped in the liposomes.

### 3.3.8 Statistical analysis

The level of significance for all statistical analysis was set at 0.05. Data was analyzed by one-way analysis of variance (ANOVA) using GraphPad Prism 6.01 (GraphPad Software Inc., La Jolla, U.S.A).

## 3.4 Results and Discussion

PEG<sub>B</sub>-Hz-CHEMS was synthesized and characterised as reported [222]. PEG<sub>B</sub>-Hz formation was confirmed by NMR spectrum, which showed the disappearance of aldehyde proton at  $\delta$  10.5 ppm and appearance of new peak at  $\delta$  8.32 ppm indicating C=N (hydrazone) bond formation. The polymer and the intermediate products such as, PEG<sub>B</sub>-Hz were freshly prepared and utilized for the development of stability indicating HPLC method and further characterisation studies in this work.

### 3.4.1 Stability-indicating HPLC method for PEG<sub>B</sub>-Hz-CHEMS

#### 3.4.1.1 Mobile phase optimisation by multiple regression analysis

To determine the pH-sensitive PEG detachment of the polymer, a novel HPLC method was developed for the determination of the PEG<sub>B</sub>-Hz-CHEMS and its degradation products. The multiple linear regression method was used for ternary mobile phase optimisation, which was particularly useful for the resolution of co-eluting peaks [223]. In the regression analysis, only six chromatographic experiments were performed by varying aqueous phase (X<sub>1</sub>) and A/M (X<sub>2</sub>) ratios simultaneously and the resulting data of retention times of PEG<sub>B</sub> and PEG<sub>B</sub>-Hz-CHEMS obtained for the various mobile phase compositions were recorded. From the obtained data, linear regression equations 3.3 and 3.4 were generated, which defines the optimised mobile phase composition required to achieve the desired retention times for each analyte.

$$R_t(\text{PEG}_B) = 16.37 - 0.19X_1 - 0.26 X_2 \quad \text{Equation 3.3}$$

$$R_t(\text{PEG}_B\text{-Hz-CHEMS}) = 26.63 - 0.21 X_1 - 0.36 X_2 \quad \text{Equation 3.4}$$

In all cases, the regression coefficients were good ( $r \geq 0.995$ ). The probability (p-value) of the model was less than 0.05, indicating that the fitted model could describe the relationship between the variables and responses. Furthermore, the regression equations suggest that both X<sub>1</sub> and X<sub>2</sub> had different elution strength for each analyte and the A/M ratio (X<sub>2</sub>) had higher influence on their elution strength and resolution.

Finally using the regression model, an optimized mobile phase composition of X<sub>1</sub>, and X<sub>2</sub> as 50% and 9%, respectively was predicted (water:acetonitrile:methanol at 50:5:45, v/v/v) and used to yield R<sub>t</sub> of 5.0 min for PEG<sub>B</sub>, as well as 12.6 min for PEG<sub>B</sub>-Hz-CHEMS respectively (Figure 3-2). This would allow sufficient time for elution of other potential product(s) from the

pH-dependent degradation of PEG<sub>B</sub>-Hz-CHEMS. This multiple component mobile phase enabled efficient optimisation of mobile phase for better separation efficiency for PEG and PEG-conjugate than the previously reported methods [218, 219, 227].

### 3.4.1.2 Validation

a) Specificity: The chromatograms from the analysis of the standard solution (nominal concentration), and extracts of non-polymer inserted liposomes (blank) and polymer-inserted liposome pellets were used to justify the specificity of the analytical method. As shown in Figure 3-2A, the blank chromatogram showed no interference peaks at the retention times of either PEG<sub>B</sub> or PEG<sub>B</sub>-Hz-CHEMS. The other degradation product peaks were found at 5.01 min for PEG<sub>B</sub>, and at 4.36 min for PEG<sub>B</sub>-Hz as confirmed by comparing with the retention time and spectra of synthesized starting materials.

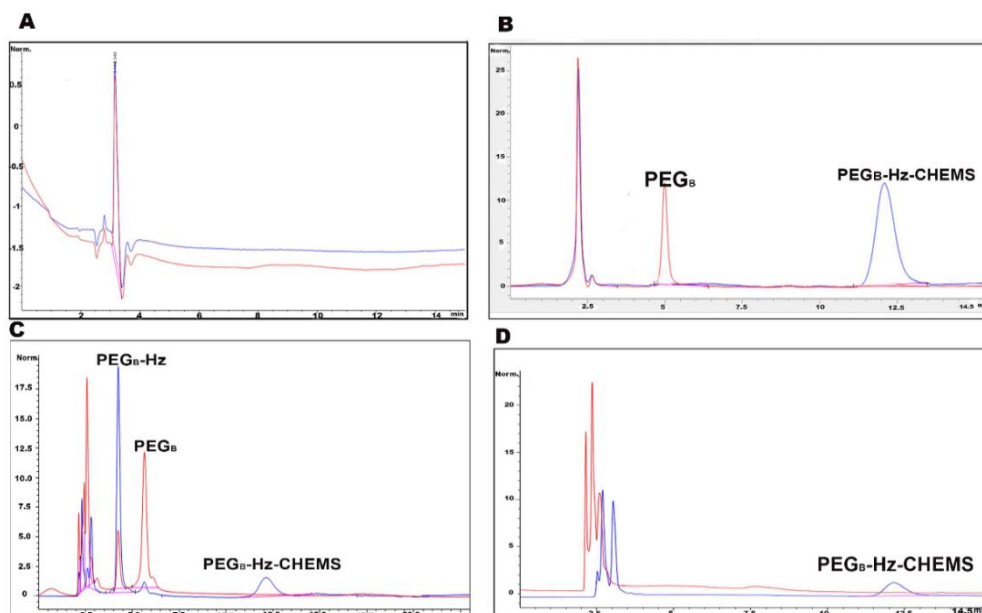


Figure 3-2 Typical chromatograms of : (A) Blank liposomes extracted with 10% Triton X-100 solution; (B) A standard containing 80  $\mu\text{g/ml}$  (each) of PEG<sub>B</sub> and PEG<sub>B</sub>-Hz-CHEMS; (C) Degradation products, PEG<sub>B</sub> and PEG<sub>B</sub>-Hz formed from PEG<sub>B</sub>-Hz-CHEMS after its incubation at pH 5.0, for 1 h; (D) PEG<sub>B</sub>-Hz-CHEMS extracted by destroying pellet of polymer-coated liposomes with Triton X-100.

- b) Linearity:** A relationship between chromatographic response and concentration was established on three different days over the range 8 to 125 µg/mL. The calibration curves obtained by analysing PEG<sub>B</sub> and PEG<sub>B</sub>-Hz-CHEMS were linear in the observed range with a correlation coefficient R<sup>2</sup> of 0.9999. In addition, RSD at each concentration level over three days did not exceed 8% in all cases.
- c) Accuracy and precision:** Table 3-1 summarises the precision and accuracy results of the simultaneous assay of PEG<sub>B</sub> and PEG<sub>B</sub>-Hz-CHEMS. The results suggest satisfactory intra-day and inter-day precision (% R.S.D. between 0.1 and 6.0) and accuracy (96.6–107.0 %) for both PEG<sub>B</sub>-Hz-CHEMS and PEG<sub>B</sub>.
- d) Limit of detection and quantification:** The LOD and LOQ were estimated as 0.58 and 0.91 µg/mL for PEG<sub>B</sub>, and 1.50 and 5.58 µg/mL for PEG<sub>B</sub>-Hz-CHEMS, respectively.

Table 3-1 Intra-day and Inter-day precision and accuracy of PEG<sub>B</sub> and PEG<sub>B</sub>-Hz-CHEMS (Data are mean ± SD; n=3)

Compound	Nominal Conc (µg/mL)	Conc found (µg/mL)	Precision (% RSD)	Accuracy (% Nominal)
PEG <sub>B</sub>	Intra-day			
	20	20.7 ± 0.3	1.3	103.6 ± 1.4
	40	42.5 ± 1.2	2.8	106.2 ± 2.9
	80	79.4 ± 0.6	0.7	99.3 ± 0.7
	100	99.8 ± 0.4	0.3	99.8 ± 0.3
	Inter-day			
	20	18.9 ± 1.1	6.0	94.3 ± 6.9
	40	41.0 ± 0.8	2.0	102.5 ± 2.0
	80	85.6 ± 0.6	0.7	107.0 ± 0.7
	100	99.1 ± 3.1	3.6	99.1 ± 3.6
PEG <sub>B</sub> -Hz-CHEMS	Intra-day			
	20	19.4 ± 0.8	4.3	97.0 ± 4.2
	40	39.5 ± 0.5	1.3	98.6 ± 1.3
	80	83.3 ± 1.9	2.2	104.1 ± 2.3
	100	96.6 ± 4.8	5.0	96.6 ± 4.8
	Inter-day			
	20	20.1 ± 0.5	2.5	100.5 ± 2.5
	40	41.2 ± 0.8	1.8	103.1 ± 1.9
	80	84.5 ± 0.1	0.1	105.6 ± 0.1
	100	99.9 ± 0.9	0.9	99.9 ± 0.9

### 3.4.2 Kinetics of pH-dependent PEG detachment of PEG<sub>B</sub>-Hz-CHEMS

PEG<sub>B</sub>-Hz-CHEMS was found to be more stable at pH 7.4, 37 °C compared to acidic pH, with a half-life of about 24 h (Figure 3-3A). However, at lower pH, it showed a half-life of 1 h at pH 6.5 (Figure 3-3B), and 0.5 h at pH 5.0 (Figure 3-3C). About 80% of PEG was detached within 1 h at pH 5, the lysosomal pH.

The polymer PEG<sub>B</sub>-Hz-CHEMS showed a higher pH-responsiveness compared to the one synthesized by Chen et al, which was more stable at pH 5.0 (half-life of 6.5 h) [159, 228] and to those synthesized by Torchillin et al., which showed a half-life of > 48 h at pH 5.5 [146]. The reason for the stability of PEG<sub>B</sub>-Hz-CHEMS at pH 7.4 could be due to the resonance stabilization obtained from the conjugation of the  $\pi$  bonds of -C=N- bond of the hydrazone with the  $\pi$  bonds of its electron withdrawing substituent, or phenyl ring. In addition, its higher pH-responsiveness may be due to its structural configuration, which has only one aromatic ring, therefore H<sup>+</sup> from the acid medium easily protonate the C=N bond and facilitates the formation of a tetrahedral intermediate, which undergoes rapid decomposition due to the cleavage of the hydrazone bond.

In general, pH-dependent reactions accelerate by a factor of 10 for each unit drop in pH. However, in this case, as pH dropped from pH 7.4 to 6.5, the degradation of PEG<sub>B</sub>-Hz-CHEMS occurred at an acceleration factor of 24, and another factor of 3 with a further reduction in pH from 6.5 to 5.0. As shown in Figure 3-3B, this faster degradation rate factor of the polymer at pH 6.5 could also be due to the simultaneous cleavages of hydrazide-hydrazone via two different pathways, as discussed below.

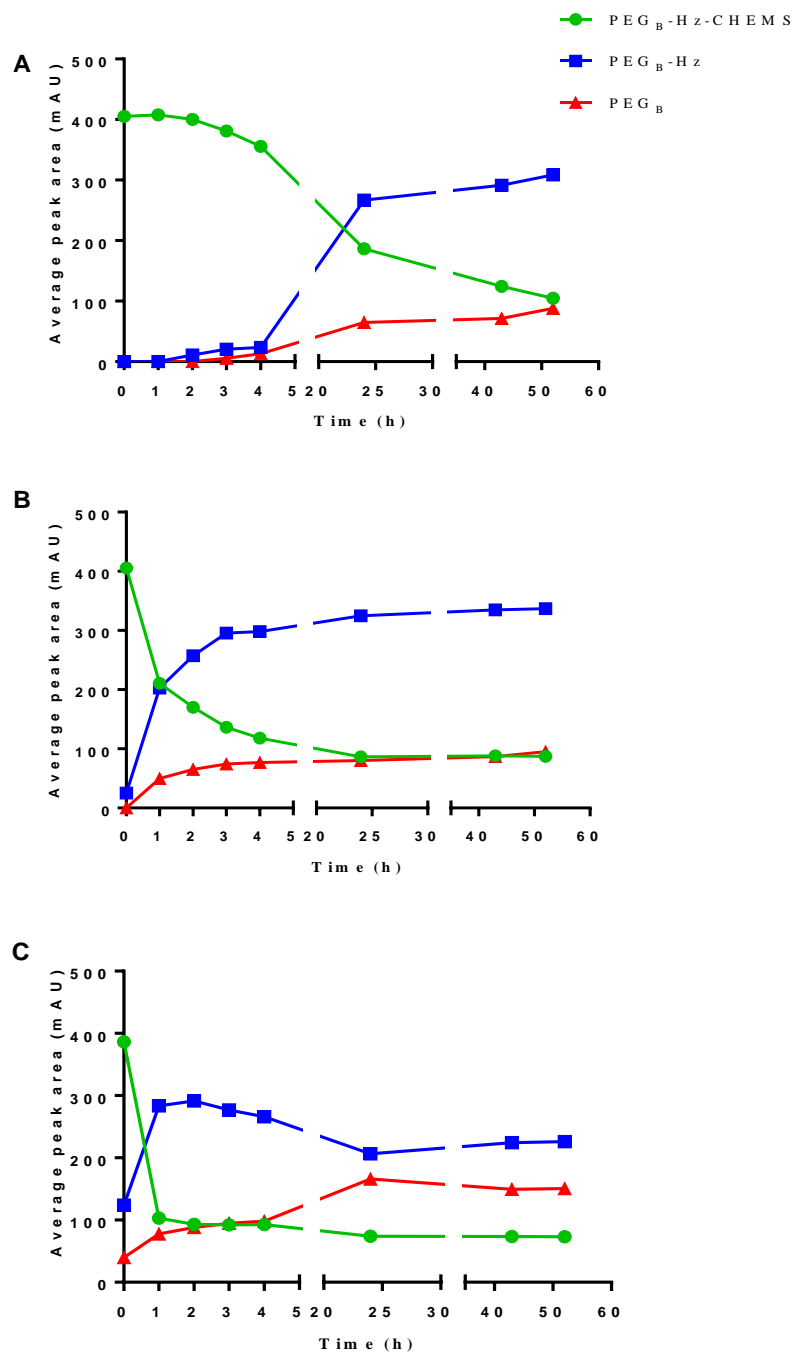


Figure 3-3 Degradation kinetics of PEG<sub>B</sub>-Hz-CHEMS (initial concentration was 200 μg/mL) and formation of main degradation products, PEG<sub>B</sub> and PEG<sub>B</sub>-Hz at (A) pH 7.40, (B) 6.50, and (C) 5.0. (Data are mean ± SD; n=3)

### 3.4.3 pH-dependent degradation pathways of PEG<sub>B</sub>-Hz-CHEMS

While monitoring for the degradation products, interestingly two degradation peaks were observed at retention times 5.01 and 4.36, which were identified as PEG<sub>B</sub> and PEG<sub>B</sub>-Hz after comparison with the UV spectrum of their synthesized starting materials. As predicted, PEG<sub>B</sub>-Hz-CHEMS underwent two hydrolytic pathways (Figure 3-4), the cleavage of the hydrazide-hydrazone hybrid,  $-\text{CO}-\text{NH}-\text{N}=\text{C}-$ , resulted in two different PEG products in the chromatograms, PEG<sub>B</sub> and PEG<sub>B</sub>-Hz (Figure 3-2C), with different retention time 5.01 min and 4.36 min (detectable at 254 nm), respectively. Specifically, hydrazide (CO-N) cleavage resulted in the formation of PEG<sub>B</sub>-Hz, and acid catalysed hydrolysis of the hydrazone bond (N=C) led to the formation of PEG<sub>B</sub>. Interestingly, as shown in Figure 3-3(A-C), the formation of PEG<sub>B</sub>-Hz was much faster compared to PEG<sub>B</sub> at all pH 5-7.4, suggesting that the hydrazide (CO-N) bond is more susceptible to hydrolysis under mild acidic conditions than the hydrazone bond. The rapid hydrolysis of hydrazide-hydrazone may be suppressed to some extent after incorporation of the polymer into liposomes as the bonds may remain protected within the lipid bilayers.

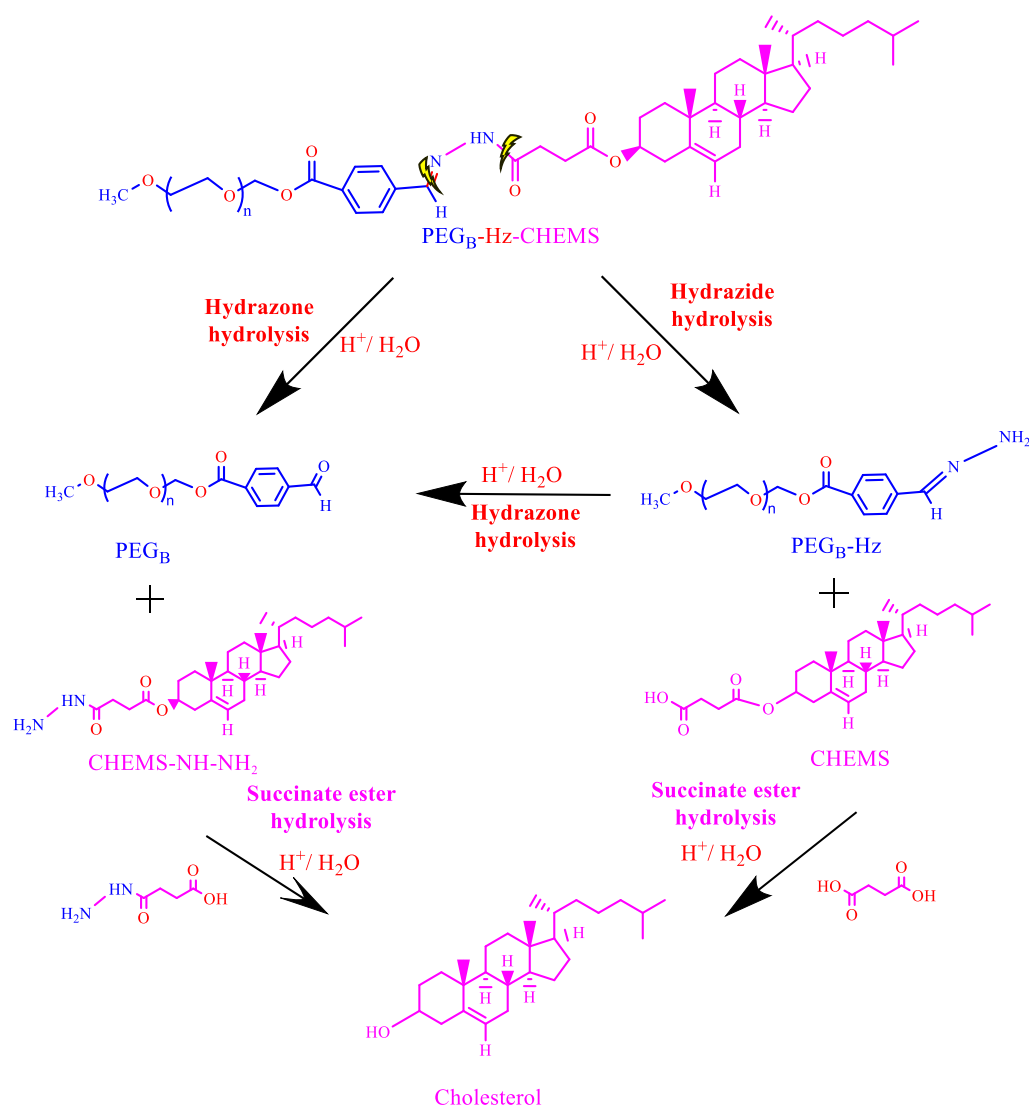


Figure 3-4 Scheme of proposed degradation pathways of PEG<sub>B</sub>-Hz-CHEMS in acidic conditions, showing the structures of PEG<sub>B</sub>-Hz-CHEMS and its major degradation products, found with the stability-indicating HPLC assay.

### 3.4.4 Quantification of PEGylation degree of CL-pPSL

The amount of PEG<sub>B</sub>-Hz-CHEMS inserted into pH-sensitive liposomes was quantified by analysing pellet and supernatant using the validated HPLC-UV method. It was found that post-insertion of PEG<sub>B</sub>-Hz-CHEMS to liposomal surface bilayers (5 mol% of the total lipids) at 4°C for 8 h resulted in an IE of 18%, and thus a low PEG degree (0.5 mol% of the total lipids). Increasing the incubation time to 24 h resulted in an increase in its IE to 33.6%, which is equivalent to a PEGylation degree of 1.7%. No degradation peaks were detected either in the

supernatant or the liposome pellet with a mass balance of PEG<sub>B</sub>-HZ-CHEMS close to 100%, indicating minimal degradation occurred during PEGylation at 4 °C.

### **3.4.5 Size, morphology and stability of the CL-pPSL**

Freshly prepared naked pH-sensitive liposomes showed an average size of  $100.5 \pm 1.4$  nm and a surface charge of  $-25.2 \pm 0.6$  mV. PEGylation was performed by incubating the non-PEGylated liposomes with the polymer solutions at 4°C to minimize degradation. CL-pPSL had an average size of 123 nm with unimodal distribution (PDI <0.05) and a zeta potential of -7.6 mV (Table 3-2). The reduction of zeta potential is most likely an indication of PEGylation as the PEG layer had a shielding effect [229]. The increase in size post-PEGylation is larger than the thickness of PEG<sub>2000</sub> which is reported to be up to 3.7 nm [230], indicating some fusion occurred between liposomes before or during the PEGylation process. This was consistent with the cryo-TEM observations. The naked liposomes were unilamellar and had a size ranging from 50-100 nm (Figure 3-5A). Some of the naked liposomes were observed about to fuse with each other. Fusion of these liposomes is highly possible due to the lack of PEG layer and particularly when they were pelletized which facilitated the aggregation of liposomes. However, most of the CL-pPSL appeared to be discrete, and spherical unilamellar vesicles (Figure 3-5B).

The CL-pPSL containing PBS (0.01M, pH 7.4) in the cores were found to be stable over a 3 month period with no remarkable change in particle size or zeta potential, although the changes were statistically significant (Table 3-2). However, 3 months saw small increases in particle size and zeta potential, indicating the potential for aggregation and possibly de-shielding of PEG.

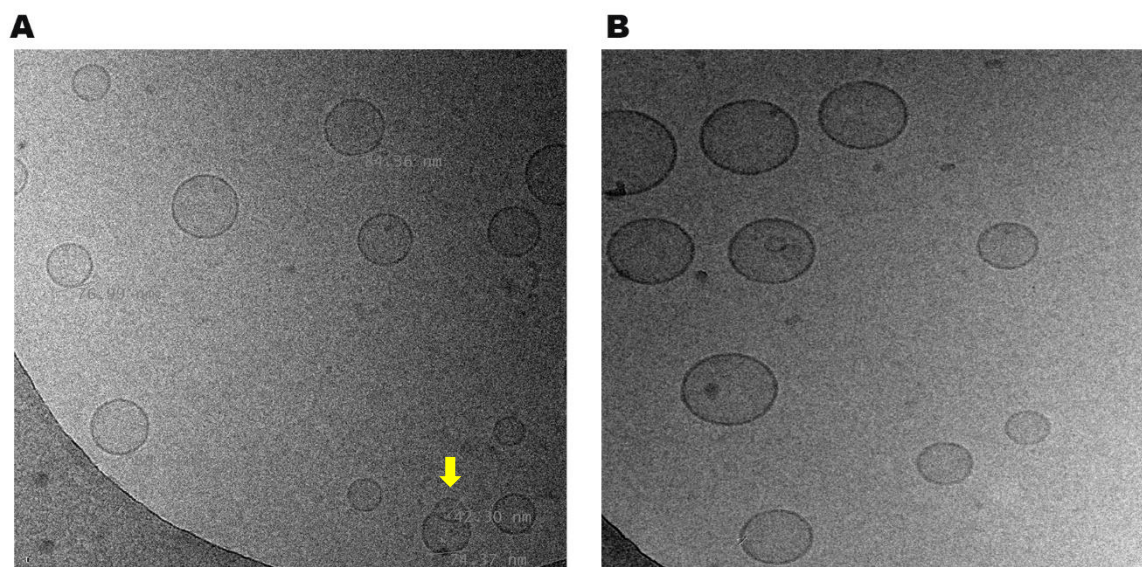


Figure 3-5 Cryo-TEM micrographs of unilamellar pH-sensitive liposomes before PEGylation, showing a sign for fusion (arrow) (A), and after PEGylation (CL-pPSL) (B).

Table 3-2 Stability of CL-pPSL (containing PBS, pH 7.4 in the cores) stored at 4 °C (mean  $\pm$  SD, n = 3).

Formulation	Time (month)	Particle size (nm)	PDI	Zeta potential (mV)
<b>CL-pPSL (as pellets)</b>	0	123.3 $\pm$ 0.2	0.03 $\pm$ 0.01	- 7.54 $\pm$ 0.01
	1	120.6 $\pm$ 0.1	0.05 $\pm$ 0.02	- 7.42 $\pm$ 0.04
	2	125.2 $\pm$ 0.2*	0.03 $\pm$ 0.01	- 7.39 $\pm$ 0.02
	3	135.4 $\pm$ 0.5**	0.14 $\pm$ 0.04	- 9.39 $\pm$ 0.02
<b>CL-pPSL suspended in PBS (pH 7.4)</b>	0	122.6 $\pm$ 0.1	0.02 $\pm$ 0.01	- 7.64 $\pm$ 0.02
	1	123.4 $\pm$ 0.3	0.05 $\pm$ 0.02	- 7.55 $\pm$ 0.01
	2	124.9 $\pm$ 0.2*	0.03 $\pm$ 0.01	- 7.52 $\pm$ 0.04
	3	128.4 $\pm$ 0.3*	0.14 $\pm$ 0.05	- 11.34 $\pm$ 0.11

\*denotes  $P < 0.05$ , and \*\*  $P < 0.01$  in comparison to the respective freshly made formulations.

### 3.4.6 pH-responsive calcein leakage kinetics

A linear relationship between the concentration and fluorescence intensity of calcein was demonstrated at concentrations below 1 mM (Figure 3-6A). At a concentration of 80 mM, the intensity of fluorescence was equivalent to 0.01 mM, confirming the fluorescence was self-quenched. Therefore, 80 mM of calcein solution was chosen to be incorporated into various liposomes for the determination of pH-dependent calcein leakage. The maximal concentration of calcein released to the medium was estimated to be < 1 mM (0.72 mM) and all samples after dilution were within the linear range of the calibration curve. The CL-pPSL gave a rapid release of calcein at pH 5.0 with about 80% released within 10 min (Figure 3-6B), which is only slightly slower than the non-PEGylated pH-sensitive liposomes (Figure 3-6C), indicating their abilities to undergo rapid escape from endo/lysosomes. In comparison, pPSL showed a significantly slower calcein leakage at various media, indicating the compromised pH-sensitivity of these liposomes due to the steric hindrance by non-cleavable DSPE-mPEG<sub>2000</sub> coating. Our previous research [122] demonstrated that exposing the DOPE / CHEMS (6:4) pH-sensitive liposomes to pH 5.0 led to a nearly 100% calcein release in 10 min. Post-insertion of DSPE-PEG<sub>2000</sub> of even at 0.5% reduced the calcein release to 15%. The non-pH sensitive liposomes coated with pH-cleavable PEG polymer using the hydrazone bond only achieved drug release of 65.8% at pH 5.5 after 24 h, [228], most likely due to the insufficiency of using a ketone derivatized hydrazone bond as well as the non pH-sensitive lipid bilayers.

It is assumed that the rapid release from CL-pPSL at pH 5.0 could be attributed to two reasons. First, the detachment of PEG from PEG<sub>B</sub>-Hz-CHEMS, due to the cleavage of hydrazone bonds by either of the two proposed pathways, resulting in 'naked' pH-sensitive liposomes. Figure 3-3C shows that approximately 75% of PEG<sub>B</sub>-Hz-CHEMS cleaved after 1 h at pH 5.0. Therefore, more than 20% of the PEG<sub>B</sub>-Hz-CHEMS can be broken down in 10 min at this pH, assuming it followed a first-order kinetics. This PEG-detachment facilitates the aggregation of liposomes,

thus causing pores to form on the surface of the vesicle, resulting in rapid content release. A similar phenomenon was also observed in a study on the liposomes modified with an acid-cleavable PEG-lipid polymer containing an orthoester linker [192, 195]. Second, the liposome membrane was mainly composed of DOPE:CHEMS lipids. At acidic pH, the carboxylic group of CHEMS becomes protonated, which induces conformational changes of DOPE molecules from cone shaped to cylindrical shape resulting in liposomal destabilization from a bilayer to an inverted hexagonal II phase [42]. Therefore, the dual pH-responsiveness of the CL-pPSL contributed to their rapid acid triggered release.

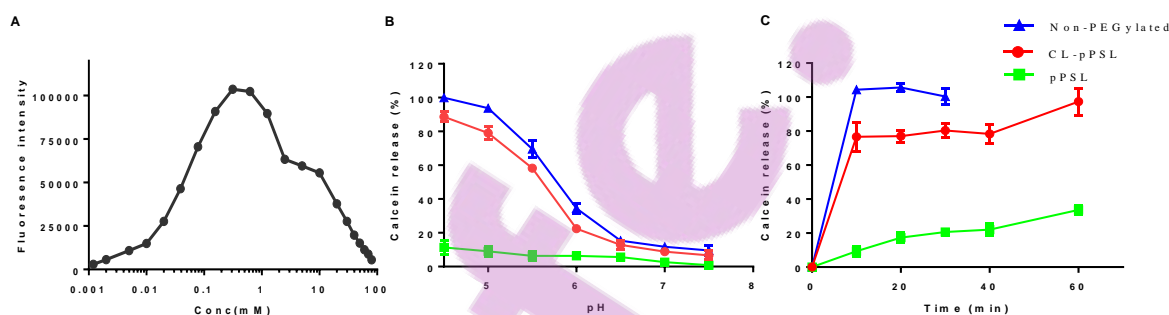


Figure 3-6 Fluorescence intensity as a function of calcein concentration, showing the self-quench property of calcein (A), and pH-sensitive calcein leakage from various liposomes at various pH after 10 min (B), and the release profiles over 60 min at pH 5.0 (triangle symbols: non PEGylated liposomes, square symbols: pPSL, and circle symbols: CL-pPSL). Data are mean  $\pm$  SD,  $n = 6$ .

### **3.5 Conclusions**

The pH-sensitive PEG detachment is an important strategy to enhance the blood circulation time of liposomes without compromising their intracellular delivery abilities. In this study, a smart PEG<sub>B</sub>-Hz-CHEMS polymer was fully characterized and utilized for the development of dual pH-responsive liposomes (CL-pPSL). The stability-indicating HPLC assay, established with the aid of multiple linear regression for the mobile phase development, provided insight into the degradation pathways of PEG<sub>B</sub>-Hz-CHEMS. The simultaneous cleavage of both hydrazide-hydrazone bonds resulting in rapid PEG detachment at low pH with a favourable short half-life of 0.5 h at pH 5. The calcein leakage assay showed that the CL-pPSL was capable of achieving rapid acid labile content release while remained stable at pH 7.4. Overall, this study demonstrated that the PEG<sub>B</sub>-Hz-CHEMS could be a promising polymer to overcome the PEG dilemma. Further study to increase the IE is of our interest.

### **3.6 Acknowledgements and disclosure**

The financial support for this study was provided by the Marsden Fund by the Royal Society of New Zealand (grant number UOA1201), and Performance Based Research Fund from the School of Pharmacy, University of Auckland. The authors declare that they have no conflicts of interest to disclose.

## **4. PEG-Benzaldehyde-Hydrazone-Lipid Based PEG-Sheddable pH-Sensitive Liposomes: Abilities for Endosomal Escape and Long Circulation**

---



[Pharmaceutical Research](#)

August 2018, 35:154 | [Cite as](#)

## PEG-Benzaldehyde-Hydrazone-Lipid Based PEG-Sheddable pH-Sensitive Liposomes: Abilities for Endosomal Escape and Long Circulation

Authors

[Authors and affiliations](#)

Manju Kanamala, Brian D. Palmer, Hamidreza Ghandehari, William R. Wilson, Zimei Wu 

### 4.1 Abstract

**Purpose:** To fabricate an acid-cleavable PEG polymer for the development of PEG-cleavable pH-sensitive liposomes (CL-pPSL), and to investigate their ability for endosomal escape and long circulation.

**Methods:** PEG-benzaldehyde-hydrazone-cholesteryl hemisuccinate (PEG<sub>B</sub>-HZ-CHEMS) containing hydrazone and hydrazide bonds was synthesised and used to fabricate a dual pH-sensitive CL-pPSL. Non-cleavable PEGylated pH-sensitive liposome (pPSL) was used as a reference and gemcitabine as the model drug. The cell uptake and endosomal escape were investigated in pancreatic cancer Mia PaCa-2 cells and pharmacokinetics were studied in rats.

**Results:** The CL-pPSL showed accelerated drug release at endosomal pH 5.0 compared to pPSL. Compared to pPSL, CL-pPSL released their fluorescent payload to cytosol more efficiently and showed a 1.4-fold increase in intracellular gemcitabine concentration and higher cytotoxicity. In rats, the injection of gemcitabine-loaded CL-pPSL resulted in a slightly smaller V<sub>d</sub> (149 ± 27 ml/kg; 170 ± 30 ml/kg) and shorter terminal T<sub>1/2</sub> (5.4 ± 0.3 h; 5.8 ± 0.6 h) (both  $p > 0.05$ ) but a significantly lower AUC ( $p < 0.01$ ), than pPSL, due to the lower PEGylation degree (1.7 mol%) which means a ‘mushroom’ configuration of PEG. A 5-times increase in the dose with CL-pPSL resulted in a 11-fold increase in AUC and a longer T<sub>1/2</sub> (8.2 ± 0.5 h).

## Chapter 4

**Conclusion:** The PEG-detachment from the CL-pPSL enhanced endosome escape efficiency compared with pPSL, without significantly compromising their stealth abilities.

**Key words:** Dual pH-sensitive liposomes, Endosome escape, Hydrazone, PEG detachment

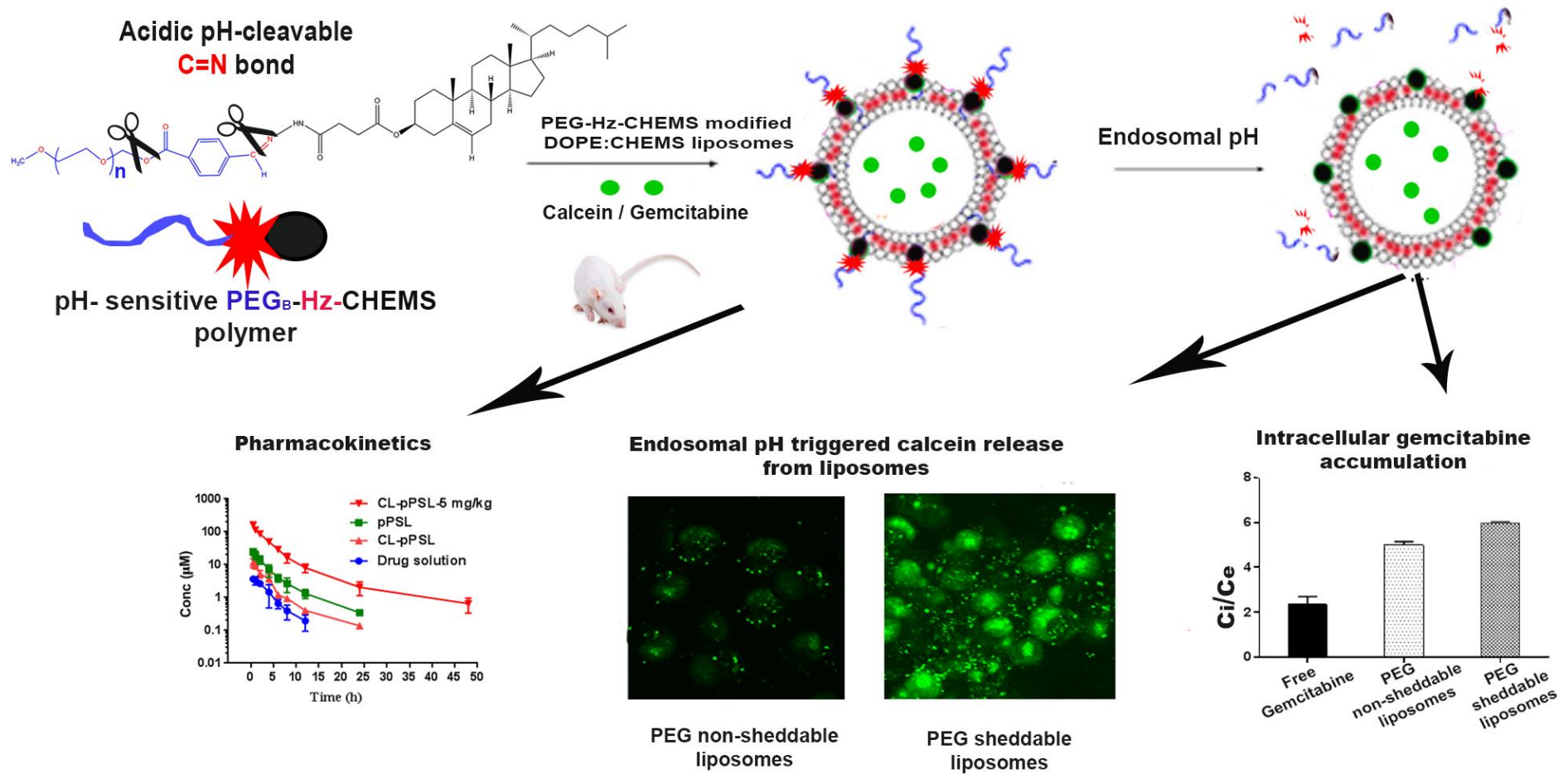


Figure 4-1 Graphical abstract

## 4.2 Introduction

Since their discovery by Bangham in the early 1960s, liposomes have attracted unprecedented attention as drug delivery systems which resulted in numerous publications, however, this has resulted in few FDA approved clinical products [231]. To date, 15 liposomal products have been approved for clinical use and nearly twice as many are in clinical trials [232]. However there is still room for improvement in these numbers by rational formulation design. Two critical factors needing attention in the development of liposomal anticancer drug delivery systems are their long circulation time in the blood stream which facilitates drug accumulation at tumors, and their ability to release cargos at the target cells [233]. Surface modification of liposomes with hydrophilic polymers, such as poly(ethylene glycol) (PEG), poly(vinyl pyrrolidone) (PVP) [234], and Poloxamer 188 [26], have been demonstrated to extend liposome circulation times. The hydrophilic polymers sterically prevent adsorption of opsonins, thus allowing liposomes to bypass the recognition of the host mononuclear phagocyte system, a major clearance pathway for liposomes. This technique is known as ‘steric stabilization’ or ‘stealth coating’. To date, the gold standard for stealth coating is still PEG [209]. However, from the first PEGylated liposome, Doxil<sup>®</sup> (containing doxorubicin) approved in 1995, to the latest Onivyde<sup>®</sup> (irinotecan liposome injection) for metastatic pancreatic adenocarcinoma in 2015, although the side effects in patients have been minimized, the improvement in efficacy is marginal [235]. This could partially be attributed to the poor cellular uptake and slow intracellular drug release due to PEGylation, known as the ‘PEG dilemma’ [4].

pH-sensitive liposomes (PSL) have been developed to refine the conventional liposomes to promote extra- and intra-cellular drug release to cancer cells [236]. PSL, conceptualized by Yatvin et al. in 1980 [237], are designed to maintain stability in physiological pH, but release the payloads at a threshold of low pH [237], such as the endosomal lumen (pH 5-5.5), i.e. ‘endosome escape’ allowing the drug to be released into the cytosol. In contrast, conventional

liposomes can be entrapped in the endosome and transported to lysosomes where the drug may be degraded [238]. Similar to conventional liposomes, PEGylation is required to stabilise PSL *in vitro* and *in vivo*. However, PEGylation hinders the cellular uptake of liposomes by cancer cells [122], reduces the pH sensitivity of PSL and their ability of endosomal escape [56], compromising the efficacy.

To overcome the PEG dilemma [5], PEG-detachable liposomes are designed using various tumor specific features as stimuli: low pH [210], enzymes [211], and reduction [239]. Low-pH triggered PEG-detachable liposomes are typically constructed by conjugating PEG to the liposomes surface via a pH-sensitive bond [212]. The bond cleavage at low pH initiates PEG shedding that facilitates endocytosis, followed by membrane fusion and endosomal escape [213]. The chemical bonds used are important in determining the PEG detachment efficiency, as well as the stability at physiological pH, thus the circulation half-life. Various pH-sensitive bonds have been investigated, such as hydrazone (Hz), ester and vinyl ether [210], and hydrazone [146] is commonly used due to its greater stability at pH 7.4. Chen et al., reported on PEG-detachable liposomes (non-pH sensitive bilayers) using mPEG-Hz-CHEMS based on ketone-derived hydrazone. The study revealed that the PEG-detachable liposomes might overcome another PEG dilemma, the accelerated blood clearance (ABC) phenomenon induced by repeated injection in animal models. However, an increased accumulation in the liver and spleen was found with these novel liposomes compared with the conventional liposomes [159].

In this paper, we aimed to develop a PEG-cleavable pH-sensitive liposome system (CL-pPSL) and investigate the effects of PEG detachment on cellular uptake, endosome escape, and the stealth property of the dual pH-sensitive liposomes. A novel PEG-lipid, PEG-benzaldehyde-hydrazone-cholesteryl hemisuccinate (PEG<sub>B</sub>-Hz-CHEMS) was synthesized and subsequently used to fabricate CL-pPSL with backbone bilayers composed of CHEMS and 1, 2-distearoyl-

## Chapter 4

sn-glycero-3-phosphocholine (DOPE). The proposed mechanism was that the cleavage of pH-labile bonds, the hydrazide bond of CHEMS, but mainly hydrozone (Hz), enables PEG detachment from CHEMS at extracellular or endosomal pH, which generates naked CHEMS/DOPE PSL. Gemcitabine, a first line chemotherapeutic agent for pancreatic cancer was chosen as the model drug. Gemcitabine is a prodrug which is activated in the cells after its phosphorylation which inhibits the synthesis of DNA. Additionally, the cellular uptake of gemcitabine relies on active influx transporters, and may be limited by the low expression of human equilibrative nucleoside transporter-1 (hENT1) [240], one of the mechanisms associated with pancreatic cancer resistance [240-242]. The PEGylation degree of CL-pPSL was determined by HPLC analysis of PEG<sub>B</sub>-Hz-CHEMS. The cell uptake and endosome escape of CL-pPSL was investigated on Mia PaCa-2 pancreatic cancer cell line using confocal imaging, and cytotoxicity by MTT assay. The liposomal stealth property was investigated in Sprague Dawley rats.

### 4.3 Experimental

#### 4.3.1 Materials

Phospholipids, 1, 2-dioleoyl-sn-glycero-3-phosphoethanolamine (DOPE), and 1, 2-distearoyl-sn-glycero-3-phosphocholine (DSPC), cholesteryl hemisuccinate (CHEMS), 1,2-distearoyl-sn-glycero-3-phosphoethanolamine-N-[amino(polyethylene glycol)-2000] (DSPE-PEG2000) were purchased from Avanti Polar Lipids (Alabama, USA). Poly(ethylene glycol) methyl ether (mPEG2000), dicyclohexyl carbodiimide (DCC), 4-(dimethylamino)pyridine (DMAP), and Sephadex G-25 were obtained from Sigma Chemical Co. (MO, USA). HPLC grade acetonitrile and methanol were obtained from Merck. All other chemicals and solvents were reagent grade. Gemcitabine HCL (99.95 % purity) was obtained from Selleckchem (Houston, USA). Calcein, Nile Red and 3-(4,5-dimethylthiazol-2-yl)-2,5-diphenyl-tetrazolium bromide (MTT, for cytotoxicity studies) were from Sigma (Auckland, New Zealand). Gibco™ Dulbecco's

## Chapter 4

Modified Eagle's Medium (DMEM) cell culture media were purchased from ThermoFisher Scientific (Auckland, New Zealand).

Sprague-Dawley (SD) rats were obtained from the Vernon Jansen Unit (The University of Auckland) and used for the pharmacokinetic study. All procedures were approved by the Committee on Animal Experiments of The University of Auckland (ethics approval number 001228).

### 4.3.2 Synthesis of PEG<sub>B</sub>-Hz-CHEMS

The synthesis of PEG<sub>B</sub>-Hz-CHEMS was carried out in three steps.

**Step 1:** CHEMS (1 mM) in 20 mL of dichloromethane was reacted with 0.5 mL of thionyl chloride at room temperature for 2 h. The solvent was evaporated under vacuum to leave a sticky, oily product, to which was then added benzene (50 mL). The benzene was removed under reduced pressure, and the residue was dissolved in dichloromethane (20 mL). The above solution was placed on ice bath and added with hydrazine hydrate (0.3 mL) with stirring for 1 h and concentrated to dryness under reduced pressure. The residue was dissolved with dichloromethane, filtered and the filtrate was concentrated under reduced pressure to obtain CHEMS with a yield of 50%. The structure of the final product was confirmed by <sup>1</sup>H NMR spectroscopy using a Bruker Avance-400 spectrometer.

**Step 2:** A solution of mPEG<sub>2000</sub> (1 mmol) in 20 mL of dichloromethane was added to 4-carboxybenzaldehyde (10 mmol), DCC (10 mmol), and DMAP (2.5 mmol) and stirred for 24 h. The resulting reaction mixture was filtered, and the solid product obtained was collected, washed with isopropanol and diethyl ether and dried under vacuum. A light-yellow powder was obtained with 80% yield. The final product, PEG<sub>B</sub> was confirmed by <sup>1</sup>H NMR spectroscopy.

**Step 3:** PEG<sub>B</sub> (0.06 mmol) was reacted with hydrazine activated CHEMS (0.09 mmol) in 2 mL of chloroform at 25 °C in a tightly closed reaction vessel. After overnight stirring, the solvent was removed under reduced pressure, and the residue was purified by dissolving in Milli Q water (pH adjusted to 7.4) and applied to a Sephadex G-25 column. The turbid fractions containing the component were pooled and freeze dried overnight at -80 °C. The structure and molecular weight of PEG<sub>B</sub>-Hz-CHEMS were confirmed by <sup>1</sup>H NMR and mass spectrometry.

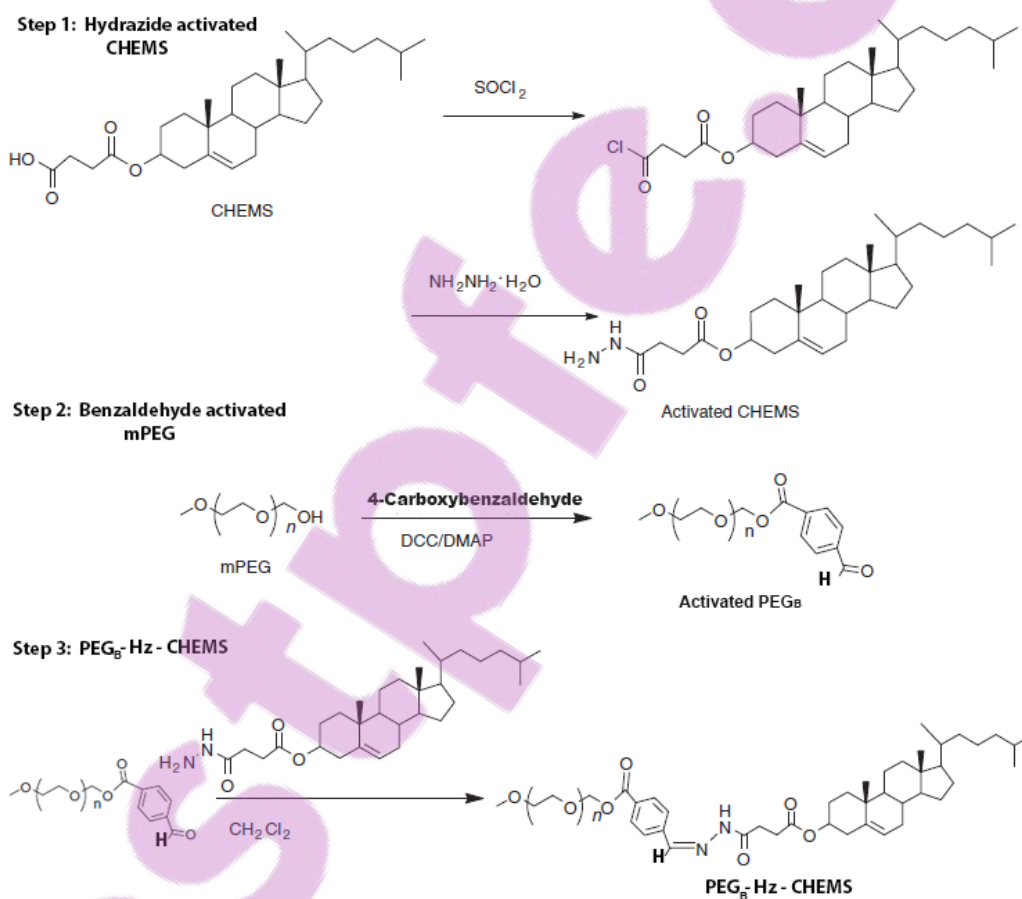


Figure 4-2 Scheme for synthesis of PEG<sub>B</sub>-Hz-CHEMS with three steps.

### **4.3.3 Characterization of PEG<sub>B</sub>-Hz-CHEMS micelles**

#### ***4.3.3.1 Size and morphology of micelles***

The size of the polymeric micelles of PEG<sub>B</sub>-Hz-CHEMS was determined by dynamic light scattering (DLS, ZS90, Malvern, U.K.). The polymeric micelles diluted in 10 mM PBS, pH 7.4, was filtered through 0.45 μm pore size filters and the measurements were conducted in a 1.0 mL quartz cuvette, using a diode laser of 800 nm at 25 °C, and the scattering angle was fixed at 90°. The morphology of the micelles was observed by Transmission Electron Microscopy (TEM, JSM5600LV, Japan).

#### ***4.3.3.2 Critical micellar concentration (CMC)***

The CMC of the micelles was determined by a modified fluorescence technique using Nile Red as a fluorescent probe [243]. To prepare micelles loaded with Nile Red, 30 mg PEG<sub>B</sub>-Hz-CHEMS and 0.2 mg Nile Red were first dissolved in 2 mL methanol, followed by the addition of 10 mL PBS, 0.01 M, pH 7.4 dropwise into the solution. After stirring for 8 h at 37 °C, excess Nile Red was removed from the polymeric micelles by filtration through a 0.45 μm membrane. For CMC determination, Nile Red-loaded micelles were diluted to a concentration of the polymer range from  $2 \times 10^{-7}$  mol L<sup>-1</sup> to  $2 \times 10^{-4}$  mol L<sup>-1</sup>. Fluorescence measurements were taken at an excitation wavelength of 550 nm and the emission from 580 to 720 nm using a Fluoro Max-4 Spectrofluorometer. Excitation and emission slit widths were maintained at 5.0 nm and spectra were accumulated with a scan speed of 200 nm/min. The CMC of the polymer was determined by plotting the fluorescence intensity against log polymer concentration (mol L<sup>-1</sup>).

### **4.3.4 Preparation and characterization of dual pH-sensitive liposomes**

#### ***4.3.4.1 Preparation of dual pH-responsive liposomes***

Two kinds of liposomes were prepared by the thin film hydration method. Conventional pPSL were prepared by DOPE, CHEMS, DSPC, cholesterol, and DSPE-PEG<sub>2000</sub> at the molar ratio of

## Chapter 4

4:2:2:2:0.5. Our previous study [244] showed this pPSL membrane had superior pH-sensitivity using a non-PSL as control. CL-pPSL were prepared using the same lipids at the same ratios but by replacement of DSPE-PEG with PEG<sub>B</sub>-Hz-CHEMS. All lipids apart from the PEG polymers were dissolved in chloroform, and the solvent was removed on a rotary evaporator at 30 °C under vacuum to form thin lipid films, which was kept under vacuum overnight. The resulting lipid films were hydrated with phosphate buffered saline (PBS, 0.1 M, pH 7.4) at 30 °C. The hydrated suspension was subjected to 7 cycles of freeze and thaw before extrusion through a 100 nm membrane. The liposomes were then subjected to ultracentrifugation to obtain pellets. PEG<sub>B</sub>-Hz-CHEMS was coated on liposomes by post-insertion, i.e., incubation of the polymer solution with the liposomes. Optimal time and polymer concentrations (equivalent to 3, 5, and 10 mol % to lipids) were determined.

### ***4.3.4.2 Size, zeta potential and morphology of liposomes***

The selected liposome formulations with better IE of PEG<sub>B</sub>-Hz-CHEMS were characterized. Hydrodynamic particle diameter (Z-average) and polydispersity (PDI) were determined by photon correlation spectroscopy (PCS) on a Zetasizer Nano ZS (Malvern Instruments, Germany) at a temperature of 22 °C and a scattering angle of 173 °. Liposome pellets were resuspended in 1 mL PBS, pH 7.4, 0.01 M and further diluted as required. Particle size and zeta potentials before and after PEGylation were compared to evaluate the surface modification of liposomes with PEG.

### ***4.3.4.3 Determination of PEGylation degree and PEG configuration***

The degree of PEGylation was determined by measuring the insertion efficiency of PEG<sub>B</sub>-Hz-CHEMS using an Agilent 1260 series HPLC system with a diode array detector (DAD) on a Luna C18, 5 µm, 4.6 mm × 250 mm column connected with a 4.6 mm × 30 mm pre-column of same type (Phenomenex<sup>®</sup>, New Zealand). The mobile phase consisted of methanol–

## Chapter 4

acetonitrile–Milli Q water (5:45:50, v/v) and the flow rate was set at 1 ml/min. Dual UV wavelength was set at 300 nm for the detection of PEG<sub>B</sub>-Hz-CHEMS and at 254 nm for its degradation product PEG<sub>B</sub>. The method was validated to be linear in the concentration range of 8 to 125 µg/mL ( $r^2=0.9999$ ,  $n=3$ )

The insertion efficiency (IE) of PEG<sub>B</sub>-Hz-CHEMS into the liposomes was determined by analysing both the supernatant and the pellet. In brief, the liposome suspensions were subjected to ultracentrifugation (186,000×g) for 2 h which was proved to have complete separation of unbound PEG<sub>B</sub>-Hz-CHEMS from the liposomes. The supernatants were collected and diluted with 0.01M PBS (pH 7.4) to the concentration levels within the calibration range and analysed by HPLC immediately. In parallel, the liposome pellet was destroyed with 10% triton X-100 solution and diluted with PBS before quantification of PEG<sub>B</sub>-Hz-CHEMS. The IE (%) was calculated as a percentage of the polymer inserted in liposomes to the total amount of polymer used in preparation.

The mean distances  $D$  between the grafting sites of the PEG-chains and  $R_F$  (Flory radius) will determine the conformation of the polymer on the liposome surface [245]. Distance  $D$  can be calculated using equation 4.1

$$D = \left( \frac{A}{\text{Mole ratio of PEG attached}} \right)^{1/2} \quad \text{Equation 4.1}$$

$A$  is the area per lipid molecule in the liposome, which is reported in literature as 50 Å [246].

$R_F$  (Flory radius), can be determined using equation 4.2 [245].

$$R_F = \alpha N^{3/5} \quad \text{Equation 4.2}$$

Where,  $\alpha$  is monomer size;  $N$  is the degree of polymerization.

### 4.3.5 Gemcitabine loading and entrapment efficiency (EE) into liposomes

Gemcitabine was loaded into the selected CL-pPSL and pPSL using small volume incubation (SV1) method [247]. In brief, 20  $\mu$ L of gemcitabine suspension (1.5mg/ml), pH 7.4 was added to the liposomal pellet, vortexed for 3 minutes and incubated at 60  $^{\circ}$ C for 3 h for drug loading. Free drug was removed by eluting the liposomal suspension through a gel filtration column, Sephadex G-75 column (100  $\times$  20 mm), using 20 mM PBS containing 0.15 M NaCl at pH 7.4. Collected liposomal fractions were dissolved using Triton X-100 and subjected to HPLC analysis. Drug concentration was measured to determine the entrapment efficiency (EE) and drug loading (DL) using the following equations.

$$EE (\%) = \frac{\text{mass of the drug liposomes}}{\text{mass of the drug used for loading}} \times 100 \quad \text{Equation 4.3}$$

$$DL (\%) = \frac{\text{mass of the drug in liposomes}}{\text{mass of drug-loaded liposomes}} \times 100 \quad \text{Equation 4.4}$$

### 4.3.6 pH-responsive drug release

The pH-responsiveness of drug release from PSL and CL-pPSL was compared using a dialysis method. A cellulose acetate dialysis bag (MWCO 12–14 kDa) containing 1 ml of the liposome suspension was placed in 50 ml of release medium (PBS 50 mM, pH 7.4, 6.5 and 5.0, adjusted with NaCl to 320 mOsm) at 37 $^{\circ}$ C with stirring throughout the experiment. At different time intervals, samples (0.1 ml each) were taken and analysed by HPLC to obtain the percentage of the drug released [247].

The *in vitro* drug release-time profiles were compared using the similarity factor ( $f_2$ ) approach [247]. The  $f_2$  value is a logarithmic transformation of the sum-squared error of the differences in % release between two formulations ( $T_j$  and  $R_j$ ) through all the time points, as described in equation 4.5:

$$f_2 = 50 \log \left\{ \left[ 1 + \left( \frac{1}{m} \right) \sum_{j=1}^m w_j |R_j - T_j|^2 \right]^{-0.5} \times 100 \right\} \quad \text{Equation 4.5}$$

Where,  $m$  represents the total time points, and  $w_j$  is an optional weight factor. An  $f_2$  value between 50 and 100 indicates the release profiles are similar.

#### 4.3.7 Quantitative determination of cellular drug uptake using HPLC

To determine the cellular uptake, Mia PaCa-2 pancreatic cancer cells were seeded in 6-well plates ( $2 \times 10^6$  cells/well in 2 ml) and cultured in DMEM with 10% FBS for 24 h at 37 °C, 5% CO<sub>2</sub> to form cell monolayers. The cells were further incubated with free drug, pPSL or CL-pPSL at 37 °C with the final drug concentration fixed at 120 μM, which was shown to cause minimal cell death. After drug exposure for 4 h, the medium was aspirated and the plate was placed on ice and washed with ice-cold PBS three times before the cells were lysed with 80 μl methanol. The sample was dried and reconstituted with mobile phase and the drug concentration was determined by a validated HPLC method [247]. Intracellular drug concentration ( $C_i$ ) was calculated based on the drug amount and cell size, measured by microscope. The ratio of  $C_i/C_e$  (extracellular drug concentration) was determined to evaluate the cellular uptake of each formulation.

#### 4.3.8 Cytotoxicity to Mia PaCa-2

MTT assay was used to evaluate the cytotoxicity of gemcitabine formulations on the Mia PaCa-2 pancreatic cell line. Briefly, cells were seeded into a 96-well plate (800 cells/well) with 100 μL/well cultured at 37 °C, 5% CO<sub>2</sub> for 24 h. Various concentrations of free gemcitabine or drug-loaded CL-pPSL and pPSL dispersed in PBS (pH 7.4) were separately added into the wells and cultured for 4 and 24 h. After drug exposure, cells were washed, 100 μL of fresh medium was added, and cells were allowed to grow for 72 h. After this, MTT cell viability was measured with untreated cells in the culture medium used as controls (100%). Blank liposomes were also tested for cytotoxicity. The drug concentration causing 50% inhibition of viable cell density

(IC<sub>50</sub>) with the 95% confident intervals was calculated using a non-linear fitting model in a GraphPad Prism (GraphPad Software, USA).

### **4.3.9 Intra-cellular trafficking of CL-pPSL and pPSL**

To investigate their intra-cellular trafficking or endosomal escape, liposomes were dual labelled with fluorescent dyes: lipophilic Nile Red (0.2 µg/ml) was incorporated into the lipid membrane to probe the intracellular fate of liposomes whereas hydrophilic calcein at its self-quenched concentration (80 mM) was loaded into the core, which acts as an indicator of lipid vesicle leakage, to study their endosome escape properties [248]. Mia Paca-2 cells were seeded at  $1 \times 10^5$  cells/well in four-well chambered slides and cultured for 24 h. The dual-labelled liposomes were added to the plates with a total lipid concentration of 0.4 mmol/L.

After incubation at 37 °C for 1 and 2 h respectively, the cells were washed three times with cold PBS (pH 7.4) and fixed using 4% paraformaldehyde for 10 min. Then, nuclei was stained by incubation with DAPI for 5 min, followed by positioning the coverslips with mounting agent. The cellular uptake and endosomal escape of various liposomes was observed using a confocal laser scanning microscope (Olympus Fluroview FV1000, Olympus Corporation, Japan) with an excitation wavelength of 366 nm for DAPI, 488 nm for calcein and 546 nm for Nile Red.

### **4.3.10 Pharmacokinetics in rats**

Sprague-Dawley rats (195 - 205 g) were randomly divided into three groups, namely gemcitabine solution (n=4), pPSL (n = 4) and CL-pPSL (n=6). Each formulation (0.2 mg/ml) was injected via the tail vein at 1 mg/kg equivalent gemcitabine. Blood samples (100–200 µl) were collected from the tail vein at various time points. Furthermore, a high dose of 5 mg/kg was injected to test the dose dependence of pharmacokinetic parameters of CL-pPSL. Blood samples were treated with a 2-step protein precipitation method by acetonitrile and analysed using the method previously reported [249]. Gemcitabine concentration was calculated using a

## Chapter 4

freshly prepared external standard curve ranging from 0.1 to 10  $\mu\text{M}$ . The assay was linear with  $r^2 = 0.9992$ . No interference was observed from plasma components and the recovery was  $> 94\%$  at low and high concentrations.

The gemcitabine pharmacokinetic profiles were fitted to a non-compartmental model using a Kinetica 5 program and the pharmacokinetic parameters such as the area under the concentration-time profile curve (AUC), mean residence time (MRT) and elimination half-life ( $T_{1/2}$ ), were obtained.

### **4.3.11 Statistical analysis**

The level of significance for all statistical analysis was set at 0.05. Data was analysed by one-way analysis of variance (ANOVA) with Tukey's multiple comparisons test using a GraphPad Prism 6.01 (GraphPad Software Inc., La Jolla, U.S.A).

## 4.4 Results and Discussion

### 4.4.1 Synthesis of PEG<sub>B</sub>-Hz-CHEMS

As shown in Figure 4-2, PEG<sub>B</sub>-Hz-CHEMS was successfully synthesized via three steps: 1) activated CHEMS was synthesized based on the literature [228] in which CHEMS was reacted with thionyl chloride to form the acyl chloride, which readily reacted with hydrazine hydrate to form hydrazine-activated CHEMS; 2) benzaldehyde-derivatized PEG (PEG<sub>B</sub>) was obtained by introducing 4-carboxybenzaldehyde into mPEG 2000 under catalysis of DCC and DMAP; and 3) PEG<sub>B</sub> was then reacted with a 1.5 M excess of hydrazine-activated CHEMS to form PEG<sub>B</sub>-Hz-CHEMS. The yield of the final product was 90%.

The structure of PEG<sub>B</sub>-Hz-CHEMS was confirmed by <sup>1</sup>H NMR spectroscopy. As shown in Figure 4-3A, the proton signals attributed to the (-OCH<sub>2</sub>CH<sub>2</sub>)<sub>n</sub> cluster of PEG<sub>B</sub> (peak a) at δ 3.09 – 4.00 ppm, the adjacent methyl cluster group (peak b) at δ 0.8–1.2 ppm and peaks at δ 7.9-8.0 ppm for protons of the aromatic ring of benzaldehyde, demonstrated the successful conjugation of the aldehyde group of PEG with hydrazide. Of particular significance was the disappearance of the peak representing the aldehyde group at chemical shift δ 10.50 ppm and the appearance of new peaks (c and c<sup>1</sup>) for Ph-HC=N bond formation at δ 8.32 ppm and δ 8.60 ppm, indicating the successful formation of the hydrazone bond. Furthermore, mass spectrometry of the final compound using a Q-Exactive Hybrid Quadrupole mass spectrometer showed an average molecular mass of 2600, indicating the successful addition of CHEMS (MW: 501) to PEG<sub>B</sub> (average MW: 2100; Figure 4-3B).

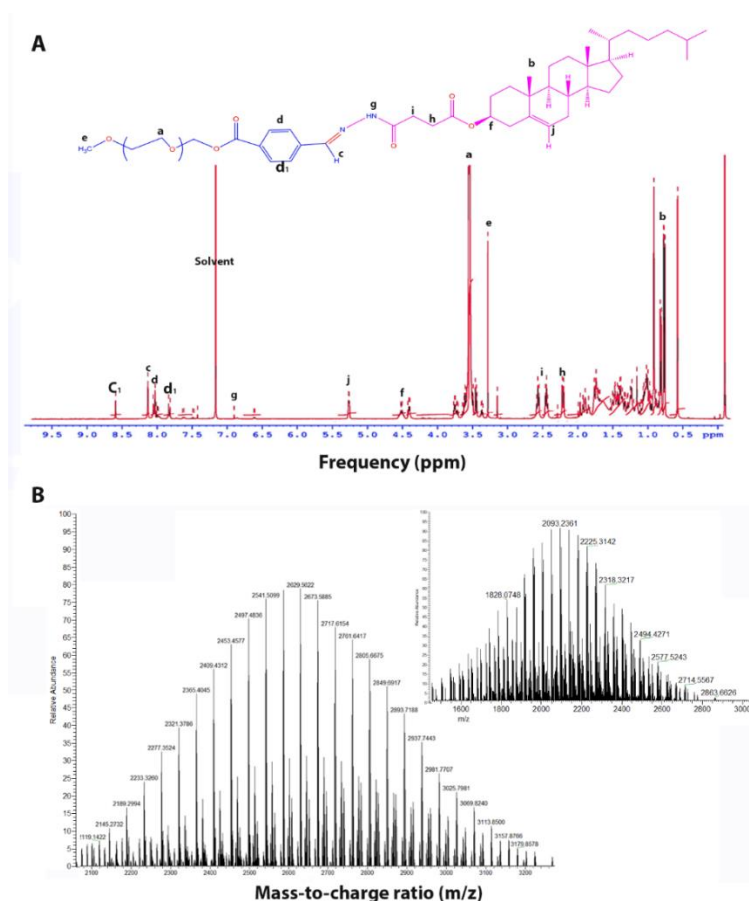


Figure 4-3 A) typical  $^1\text{H-NMR}$  spectrum of  $\text{PEG}_B\text{-Hz-CHEMS}$  in  $\text{CDCl}_3$ ; B) mass spectrum showing an average molecular mass of 2600, indicating the successful addition of CHEMS (MW: 501) to  $\text{PEG}_B$  (average molecular mass of 2100, as shown in the insert) thereby confirming the molecular structure of  $\text{PEG}_B\text{-Hz-CHEMS}$ .

#### 4.4.2 CMC of $\text{PEG}_B\text{-Hz-CHEMS}$

As expected,  $\text{PEG}_B\text{-Hz-CHEMS}$  could self-assemble into micelles in an aqueous medium due to its amphiphilic property. The average particle size of micelles was 30 nm (Figure 4-4A). Cryo-TEM showed that the micelles appeared as discrete particles with a spherical shape (Figure 4-4B). The CMC value determined was  $14.4 \mu\text{M}$  (Figure 4-4C), equivalent to 0.04 mg/mL.

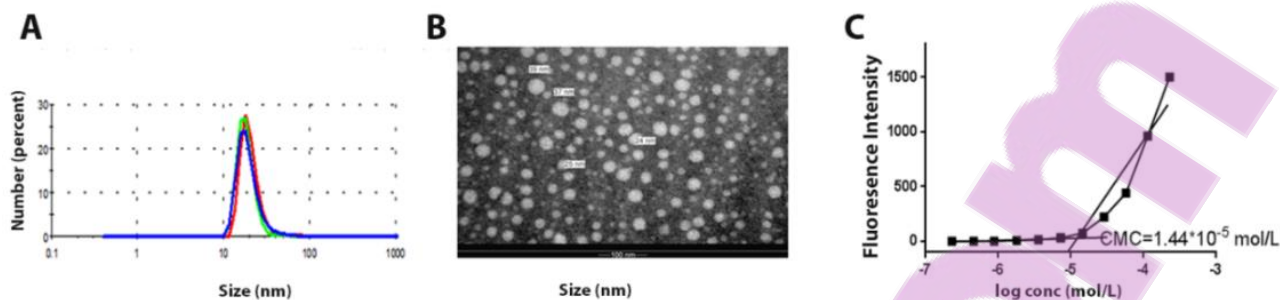


Figure 4-4 Physicochemical characterization of PEG<sub>B</sub>-Hz-CHEMS micelles: A) particle size by DLS, B) morphology by TEM; C) CMC determination by a Nile Red method.

### 4.4.3 Characterization of dual pH-sensitive liposomes

#### 4.4.3.1 Size, zeta potential and morphology

Blank liposomes before PEG modification showed an average size of  $100.5 \pm 1.4$  nm for CL-pPSL (Figure 4-5A), which increased to  $124.2 \pm 0.9$  nm after incubation with 5% PEG<sub>B</sub>-Hz-CHEMS (molar ratio to other lipids). PEG coordinates about three water molecules per monomeric unit resulting in a large hydrodynamic volume, thus an increase particle diameter was observed post PEG modification. However, a further increase in polymer concentration to 10% (mol to lipids) during post-insertion resulted in a reduction in pellet size, possibly because excessive PEG caused the micellization of lipids, as previously reported [250].

Along with the size change, the zeta potential of liposomes ( $-25.4$  mV before PEGylation) was neutralized after PEGylation due to the shielding effect of PEG chains. Similarly, the reference formulation, pPSL with 5% mol DSPE-PEG2000 had a particle size of  $128.8 \pm 1.3$  nm and zeta potential of  $-8.0 \pm 0.3$  mV.

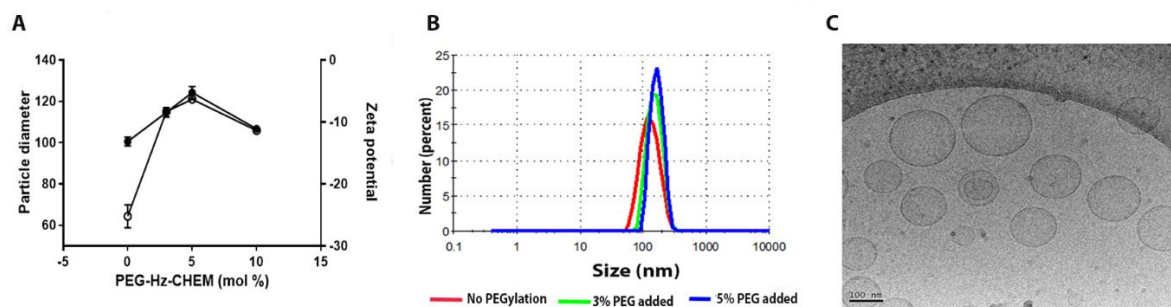


Figure 4-5 A) The influence of PEGylation with PEG<sub>B</sub>-Hz-CHEMS on the particle size (closed symbols) and zeta potential (open symbols) (mean  $\pm$  S.D, n = 3). The concentrations of PEG<sub>B</sub>-Hz-CHEMS represent the molar ratio to total lipids of the added PEG. B) DLS showing shift in average particle size with PEGylation extent, C) Cryo-TEM showing morphology of CL-pPSL with 5% PEG<sub>B</sub>-Hz-CHEMS.

#### 4.4.3.2 Quantification of degree of PEGylation

Degree of PEGylation for CL-pPSL with 3, 5 and 10 mol% PEG<sub>B</sub>-Hz-CHEMS to other lipids as shown in Figure 4-5B was determined by HPLC analysis. Surprisingly, only < 20% of the PEG was found to be inserted into liposomes after incubation for 8 h (Table 4-1). An increase in the insertion time to 24 h resulted in an increased IE, but only to about 34%. Incubation with 10% of PEG<sub>B</sub>-Hz-CHEMS destabilized the liposomes, as seen from the liposomal pellet size. Therefore, the CL-pPSL with 5% PEG<sub>B</sub>-Hz-CHEMS with resulted in a PEGylation degree of 1.7% mol was selected for further studies.

The formation of micelles reduces IE as the thermodynamic barrier to insertion into the liposome bilayers is lower in the case of monomeric PEG-lipids compared to the micellar PEG-lipids, as reported [251].

Table 4-1 Insertion efficiency (IE) of PEG<sub>B</sub>-Hz-CHEMS estimated by analysing pellet and supernatant after incubation at 4 °C at different concentrations of polymer (Data are mean ± SD; n=3)

Polymer added (%)	Incubation time (hours)	PEG <sub>B</sub> -Hz-CHEMS in supernatant (%)	PEG <sub>B</sub> -Hz-CHEMS in pellet (%)	IE (%)	Mole ratio in liposomes %
3	8	81.1±0.05	18.4±0.04	18.4	0.6
	24	71.4±0.08	34.3±0.01	34.2	1.0
5	8	82.7±0.03	17.9±0.02	18.0	0.9
	24	68.4±0.06	33.7±0.07	33.6	1.7*

\*Liposome selected for further studies. Incubation with 10% of PEG<sub>B</sub>-Hz-CHEMS reduced liposomal pellet size.

#### 4.4.3.3 PEG conformation on the surface of liposomes

Once IE was determined, the conformation of PEG chains on the surface of liposomes depends on the Flory radius  $R_F$  and the distance  $D$  between the grafting sites. If  $D < R_F$ , PEG, coils start to repel each other and extend outward from the liposome surface resulting in a ‘brush’ conformation [252]. When  $D > R_F$ , individual polymer chains remain widely separated and do not interact with each other, resulting in a ‘mushroom’ conformation.

With a molecular weight of 2000, the PEG<sub>2000</sub> derivatives used in this synthesis was estimated to have a  $R_F$  of 3.7 nm (37 Å) [230]. The distance ‘ $D$ ’ in the selected CL-pPSL (PEGylation 1.7% mol) and pPSL (PEGylation 5% mol) was calculated to be 54 Å and 32 Å, respectively. Therefore  $D > R_F$  for CL-pPSL but  $D < R_F$  for pPSL which predicts ‘mushroom’ and ‘brush’ configurations on the liposomal surface, respectively

#### 4.4.4 Drug loading and entrapment efficiency

With the SVI method, the optimized incubation time on the EE of gemcitabine was determined to be 3 h to give an EE of  $37.0 \pm 1\%$ , and DL 4% (w/w), similar to the previous report [247]. The mechanism for drug loading was passive diffusion of the drug into liposomes, which is

driven by a high concentration gradient established using a drug suspension. After drug loading, the size of liposomes was increased to about 145 nm for both liposomes.

#### 4.4.5 pH-sensitive drug release

Release of gemcitabine from CL-pPSL after 24 h was 41.9% at pH 7.4, 52.1% at pH 6.5 and increased to 95.5% at pH 5.0. The faster release profile at pH 5.0 demonstrated that the endosomal acidic environment could expedite the gemcitabine release from CL-pPSL. Similarly, gemcitabine also showed pH responsive release from the pPSL, but to a lesser extent than CL-pPSL with 47.4% at pH 7.4, 54.1% at pH 6.5 and 72.7% at pH 5.0 after 24 h.

Between CL-pPSL and pPSL, the overall release profiles of (Figure 4-6) are similar at pH 7.4 ( $f_2 = 61.6$ ). Whereas, at pH 6.5 and 5.0, an  $f_2$  value of 41.6 and 38.6 was obtained, which indicates that the release profiles from the two liposomes were not similar, with CL-pPSL producing a faster release than pPSL. This could be due to the presence of the non-cleavable DSPE-PEG-2000 coating on the outer surface, which hindered the release of the drug. At pH 5, PEG detachment from CL-pPSL may have contributed to the rapid drug release.

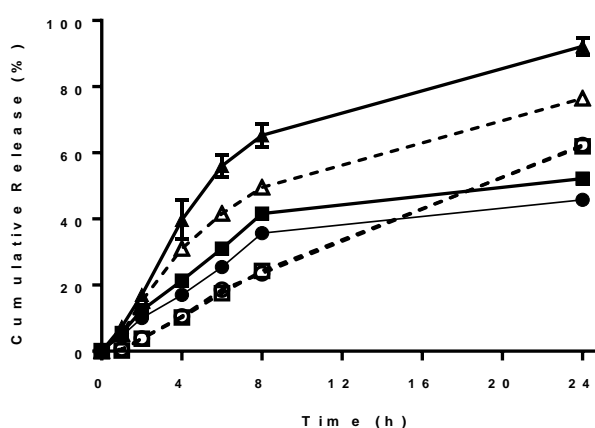


Figure 4-6 pH-sensitive drug release profiles of dual pH-sensitive liposomes (CL-pPSL, close symbols) and pPSL (open symbols), at pH 5 (triangles), pH 6.5 (diamonds) and pH 7.4 (circles). Data are mean  $\pm$  S.D, n=3.

#### 4.4.6 Cellular drug uptake determination by HPLC

The Mia PaCa-2 cells had an average diameter of  $28.8 \pm 2.54 \mu\text{m}$  and based on that the total intracellular volume was calculated to be  $1.25 \pm 0.21 \mu\text{l}$  in each well. Following drug exposure to cells for 4 h at  $37^\circ\text{C}$ , all  $C_i$  values were significantly lower than  $C_e$  (Table 4-2), indicating gemcitabine had limitations in entering cells, or had been converted to its metabolites. However,  $C_i/C_e$  was 2.0 and 3.0-fold higher for pPSL ( $P < 0.01$ ) and CL-pPSL ( $P < 0.001$ ), respectively compared with the free drug solution. Notably, cells treated with CL-pPSL showed a 2.3-fold higher intracellular drug concentration compared with those treated with pPSL ( $P < 0.01$ ).

In general, cell uptake of both liposomes should be similar at neutral pH given that their size and surface charge are similar. The higher intracellular concentrations found in CL-pPSL treated cells could be due to their more rapid endosomal escape than pPSL. Studies emphasize that the lysis of lysosomes is only achieved by extraction using hypotonic solutions such as concentrated glucose [253]. Otherwise endosomes-lysosomes stay intact and retain the contents. In this study methanol was used as the extraction solvent to lyse the cells, which is the most commonly used solvent for extracting intracellular drugs, but endosome-lysosomes might not be completely lysed and therefore the entrapped drug was not measured by HPLC. Therefore, we concluded that the rapid endosomal escape of CL-pPSL, rather than the cellular uptake, lead to their higher cytoplasmic concentration compared to pPSL.

Table 4-2 Ratios of intracellular and extracellular concentrations ( $C_i/C_e$ ) of gemcitabine in Mia PaCa-2 cells after incubation with free drug solution, pPSL, CL-pPSL for 4 h (Data are mean  $\pm$  SD, n=3 experiments).

<b>Formulation</b>	<b><math>C_i</math> (<math>\mu\text{M}</math>)</b>	<b><math>C_e</math> (<math>\mu\text{M}</math>)</b>	<b><math>C_i/C_e</math> (*<math>10^{-2}</math>)</b>
<b>Free drug</b>	2.41 $\pm$ 0.31	102.80 $\pm$ 0.46	2.34 $\pm$ 0.25
<b>pPSL</b>	4.31 $\pm$ 0.20	100.12 $\pm$ 0.20	4.30 $\pm$ 0.20
<b>CL-pPSL</b>	6.05 $\pm$ 0.27	100.22 $\pm$ 1.82	6.04 $\pm$ 0.15

#### 4.4.7 Cytotoxicity to Mia PaCa-2

Blank liposomes with lipid concentrations equivalent to the gemcitabine-loaded liposomes caused negligible toxicity in the Mia PaCa-2 cells over 24 h exposure (>85% cell viability). As shown in Table 4-3, after 4 h exposure, no significant difference in cytotoxicity was observed between free drug, CL-pPSL and pPSL treated cells. Interestingly, with an increase in treatment periods as 24 h, CL-pPSL was significantly more cytotoxic ( $P < 0.05$ ) than pPSL. This could be attributed to the PEG-detachment (with the hydrazide bonds but more effectively the hydrazone bond) and their ability to undergo accelerated destabilisation in endosome-lysosome, and therefore facilitate rapid drug release into the cytoplasm.

Gemcitabine is a nucleoside analogue and works by replacing one of the building blocks of nucleic acids during DNA replication. Therefore, in this study the cells were allowed to grow for 72 h after treatment before the MTT assay.

Table 4-3 Cytotoxicity of CL-pPSL, pPSL and free gemcitabine following 4 h or 24 h exposure, and after growth for 72 h of Mia PaCa-2 cells, measured with MTT cell viability assay. Data are mean  $\pm$  SD, n = 3.

<b>Formulation</b>	<b>4 h</b>	<b>24 h</b>
	<b><math>IC_{50}</math> (<math>\mu\text{M}</math>)</b>	<b><math>IC_{50}</math> (nM)</b>
<b>Free gemcitabine</b>	570.6 $\pm$ 52.5	45.1 $\pm$ 2.4
<b>Ppsl</b>	663.4 $\pm$ 76.1	79.5 $\pm$ 3.2
<b>CL-pPSL</b>	585.2 $\pm$ 31.2	52.4 $\pm$ 2.1

#### 4.4.8 Intracellular trafficking of liposomes

As shown in Figure 4-7, a strong red fluorescence intensity produced by the Nile Red in liposome membrane was observed for both liposomes, particularly CL-pPSL at 1 h, indicating that both the liposomes were internalized through endocytosis. It was found that clathrin-mediated endocytosis accounted for about 50% [244]. The Nile Red signal increased at 2 h with more red 'dots' presented.

The kinetics of endosome escape was shown with the second fluorescence marker, calcein (80 mM) which was loaded into the liposomal cores. The fluorescence of calcein is quenched at a concentration of 80 mM [254] and thus liposomes are less visible if sequestered in endosomes, but would produce strong fluorescence if content was released from endosomes into the cytoplasm. Our previous study [236] showed that the fluorescence of calcein peaked at 10 mM. After 1 h treatment with CL-pPSL or pPSL, intracellular calcein fluorescence was observed but mostly as 'dots' (punctate), which indicates the sequestration of liposomes in endosomes. After 2 h, the calcein fluorescence in both cases was enhanced, however the fluorescence in CL-pPSL treated cells was seen more homogeneously distributed in the cytosol (Figure 4-7), providing evidence that CL-pPSL had a more rapid endosome escape than pPSL. Interestingly, some strong calcein 'dots' with a larger size were collocated with the Nile Red 'dots' at 2 h, indicating endosomal escape was still in process, and possibly by the fusion of liposomes with endosomes. Using a EPC/EPE/Chol (40:20:30 mol%) liposomes as an endosome membrane model, Vanic et al [255] reported that half of the non PEGylated DOPE/CHEMS liposomes fused with endosome membrane at pH 5.5 within 30 min. Any PEGylation ( $\geq 0.6\%$  mol) would reduce the fusion unless the pH was lower than 4.5.

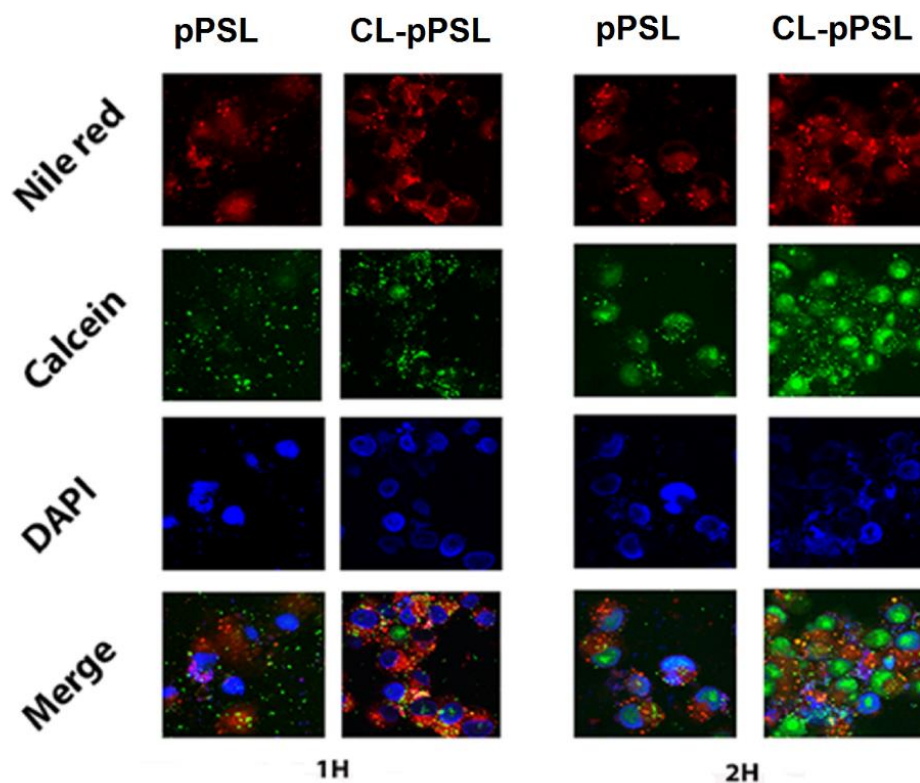


Figure 4-7 Confocal fluorescence microscopy images of Mia PaCa-2 cells excited with a laser at 360 nm (blue), 488 nm (green) and red (546 nm) visualizing the cell uptake and endosome escape after 1 and 2 h incubation with CL-pPSL or pPSL both dual labelled with Nile Red and 80 mM of calcein.

#### 4.4.9 Pharmacokinetics in rats

Figure 4-8 presents the gemcitabine plasma concentration-time profiles in SD rats after i.v. administration of various gemcitabine formulations at a dose of 1 mg/kg. Compared with the gemcitabine solution, an approximate 4 to 6-fold increase in the  $AUC_{0-\infty}$  along with 1.5 to 2-fold increases in  $T_{1/2}$  and MRT were observed for both liposomes. Furthermore, the volume of distribution ( $V_d$ ) and the clearances (CL) were both significantly reduced (Table 4-4). Between the liposomal formulations, the CL-pPSL had a 2-times lower AUC and slightly shorter  $T_{1/2}$  ( $p>0.05$ ) than pPSL, suggesting the PEGylation of CL-pPSL was not as efficient as for pPSL.

Differences in half-life and AUC between the two liposome systems could be explained by the difference in PEG density on their surface, which was predicted from the results of quantification of surface PEGylation. Even though an equivalent amount of PEG<sub>B</sub>-HZ-CHEMS

and PEG<sub>2000</sub>-DSPE was used to prepare the liposomes (Table 4-1), only 34% of the added polymer was found to be successfully inserted in CL-pPSL, resulting in differences in the PEG density and conformation. IE with PEG<sub>2000</sub>-DSPE to a pPSL similar to the one in this study was found to be nearly 100% [122]. As determined earlier, PEG<sub>B</sub>-Hz-CHEMS acquires a dense ‘mushroom’ conformation compared to pPSL,  $D > R_F$ , in ‘brush’ conformation, which has a stronger stealth ability.

Further study with an increased dose of CL-pPSL to 5 mg/kg showed a 3-h longer  $T_{1/2}$  and an 11-fold, rather than 5-fold, increase in AUC. This again supports the insufficient PEGylation which resulted in initial rapid entrapment of liposomes by the liver or spleen. As the major clearance of liposomes is by these organs, the increase in liposomes dose could lead to a saturation of liver/spleen uptake [256], resulting in a longer half-life of these liposomes in the bloodstream. Overall, the pharmacokinetics study confirms that the pH-sensitive PEG-detachment from PEG<sub>B</sub>-Hz-CHEMS in CL-pPSL may compromise their stealth abilities, but not significantly.

Table 4-4 Plasma pharmacokinetic parameters in SD rats after a single i.v. administration of drug solution or liposome formulations with dose of 1 mg/kg unless stated otherwise. Data are mean  $\pm$  SD, n = 6 for CL-pPSL formulations and n=4 for the rest.

Formulation	AUC ( $\mu\text{g/ml}\cdot\text{h}$ )	$V_d$ (ml/kg)	Clearance (ml/h/kg)	$T_{1/2}$ (h)	MRT (h)
Drug solution	17.0 $\pm$ 1.7	742 $\pm$ 4	202.3 $\pm$ 18.4	3.2 $\pm$ 0.4	3.5 $\pm$ 0.2
pPSL	103.1 $\pm$ 12.8	170 $\pm$ 30	29.3 $\pm$ 4.4	5.8 $\pm$ 0.6	5.0 $\pm$ 0.3
CL-pPSL	63.0 $\pm$ 2.8**	149 $\pm$ 27 <sup>ns</sup>	33.3 $\pm$ 1.2*	5.4 $\pm$ 0.3 <sup>ns</sup>	4.5 $\pm$ 0.1
CL-pPSL- 5 mg/kg	682.1 $\pm$ 37.1	141 $\pm$ 11	24.7 $\pm$ 1.3	8.2 $\pm$ 0.5	5.8 $\pm$ 0.8 <sup>ns</sup>

\*  $p < 0.05$ ; \*\*  $p < 0.01$ , and ns  $p > 0.05$  compared with pPSL

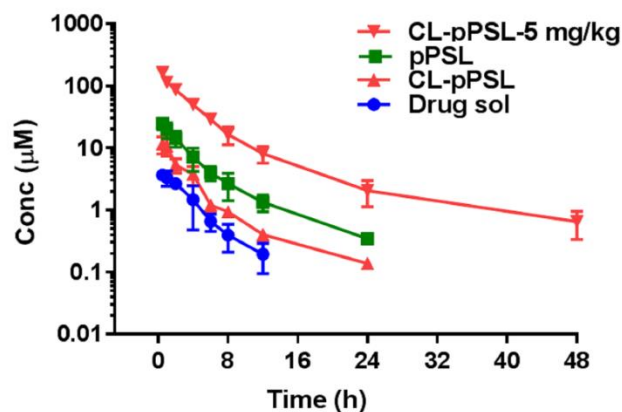


Figure 4-8 A) Pharmacokinetic profiles following *i.v.* injection of gemcitabine solution, pPSL and CL-pPSL ( $n=6$ ) in rats at 1 mg/kg equivalent gemcitabine and dose dependent pharmacokinetic profile of CL-pPSL. Data are mean  $\pm$  SD,  $n = 4$  unless stated otherwise.

## 4.5 Conclusions

This study demonstrated that PEG-detachment using the new polymer PEG<sub>B</sub>-HZ-CHEMS containing acid labile hydrazone and hydrazide bonds facilitated cellular uptake, and particularly endosomal escape. Quantification of the extent of surface PEGylation indicated that that polymer adopted a mushroom conformation on the surface of liposomes, which later correlated with their plasma circulation half-lives. The gemcitabine-loaded CL-pPSL demonstrated rapid pH-triggered drug release, and enhanced cellular uptake and cytotoxicity, compared to the classic pPSL. The pharmacokinetics study suggested that the stealth abilities of CL-pPSL were compromised to some extent, but it was likely due to the lower PEGylation degree, rather than PEG-detachment in the blood stream. In addition, this study also highlights the importance of quantifying the PEGylation degree of liposomes as the insertion efficiency of some polymers, such as PEG<sub>B</sub>-HZ-CHEMS, may be low.

## 4.6 Acknowledgements

This work was supported by the Marsden Fund by the Royal Society of New Zealand (grant number UOA1201) and a Performance Based Research Fund from the School of Pharmacy, University of Auckland. The authors declare that there are no conflicts of interest to disclose.

## **5. Dual pH-sensitive liposomes with low pH triggered sheddable-PEG for tumor targeted drug delivery**

---

## 5.1 Abstract

pH-responsive liposomes (pSL) have emerged as promising nanocarriers for antitumor drugs due to their abilities of faster release and action in the low acidic microenvironment of tumor cells. However, compromised cellular uptake, endosomal escape and lower intracellular drug release has shown to be a serious obstacle because of the steric hindrance of their poly(ethyleneglycol) (PEG) coating. To overcome this PEG dilemma, we designed a new acid labile PEG polymer, PEG<sub>B</sub>-Hz-DPPE. PEG<sub>B</sub>-Hz-DPPE, which was grafted onto cholesteryl hemisuccinate /1, 2-distearoyl-sn-glycero-3-phosphocholine-based pSL to form PEG-cleavable pH-sensitive liposomes (CL-pPSL). This dual pH-responsive liposome system was characterised with regards to pH-responsiveness, cytotoxicity, and in particular the ability for endosomal escape, pharmacokinetics and tissue biodistribution. Gemcitabine and doxorubicin were used as model drugs, and PEG non-cleavable pSL (pPSL) formed with PEG-DSPE was used as a reference. PEG<sub>B</sub>-Hz-DPPE showed the ability of acid-triggered PEG cleavage with a critical micellar concentration of 14.4  $\mu$ M. The gemcitabine-loaded CL-pPSL showed a faster drug release at pH 5.0 and 6.5 than at pH 7.4, demonstrating a more acid-responsive release compared to that of pPSL. Furthermore, CL-pPSL showed rapid cellular uptake by pancreatic cancer Mia PaCa-2 cells and endo/lysosome escape abilities, in contrast to pPSL, which was further confirmed with live cell imaging. Drug-loaded CL-pPSL showed enhanced cytotoxicity over Mia PaCa-2 and U-87 cells compared to pPSL. Compared with pPSL, CL-pPSL demonstrated a similar extended circulation time of gemcitabine in SD rats, and higher tumor biodistribution in the CD-nude mice xenograft models. In conclusion, the dual pH-responsive CL-pPSL with a PEG-sheddable strategy showed enhanced intracellular trafficking and high biodistribution in tumors without compromising their long circulation.

## Chapter 5

**Key Words:** PEG-cleavable pH-sensitive liposomes, Endosome escape, Biodistribution, Gemcitabine.

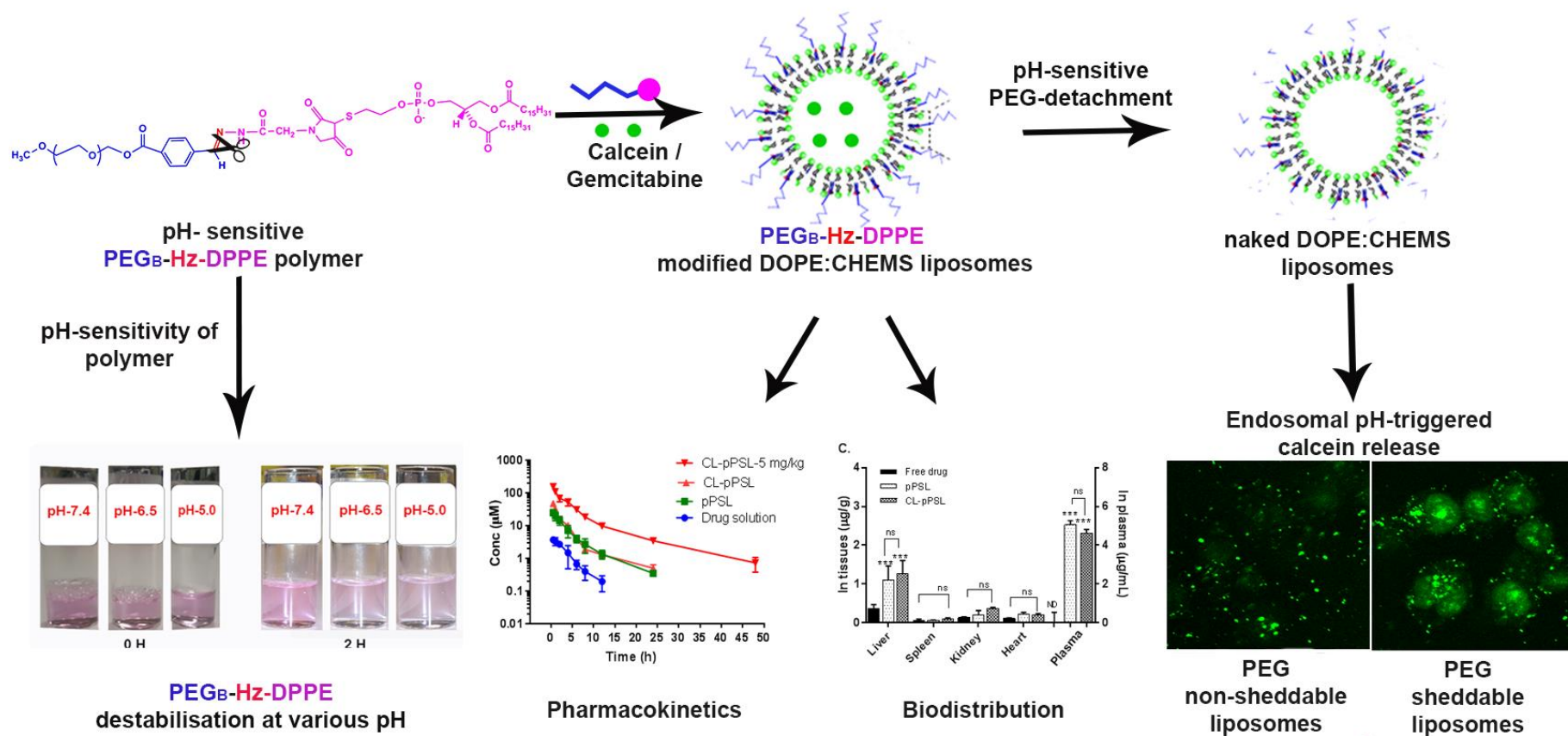


Figure 5-1 Graphical abstract

## 5.2 Introduction

Phosphatidylethanolamine (PE) based, pH-sensitive liposomes (pSL) have been widely investigated for efficient, tumor targeted drug and gene delivery [1-5] due to their fusogenic properties [6, 7]. Along with the poorly-hydrated PE head group, these pSL can be converted to an inverted hexagonal phase on exposure to acidic pH, thus forming destabilised non-lamellar structures, resulting in content release [3, 8, 9]. The most commonly used lipids combination is 1,2-dioleoyl-sn-glycero-3-phosphoethanolamine (DOPE) with cholesteryl hemisuccinate (CHEMS) [10, 11]. DOPE-CHEMS liposomes preferentially release payloads at a threshold low pH by exploiting the tumor extracellular pH 6.8 [5] and/or endosomal pH (5.0-5.5) [12]. To stabilise the liposomes, surface coating with poly(ethylene glycol) (PEG) is essential to prevent their rapid clearance by the reticuloendothelial system (RES) or destabilisation due to *in vivo* interaction with serum proteins, thus prolonging the circulation half-life of liposomes [13]. The primary emphasis so far has been on the development of PEG coated pH-sensitive liposomes, where the PEG layer promotes long circulation by preventing opsonisation and pH-sensitive lipids facilitate release of the content extracellularly at the acidic tumors and mostly to the cytoplasm of the cancer cells via endosomal escape [2, 5, 14, 15].

However, growing evidence shows that hydrophilic PEG coating hinders drug release [16], reduces interaction with target cells [17] and the endosomal escape property [18, 19], and can therefore be an obstacle in the realization of the therapeutic response. This is known as the 'PEG dilemma' [18, 20]. A common approach to achieving tumor-selective cellular uptake is by coating the surfaces of pH-sensitive liposomes with targeting ligands specific to cancer cells [21]. However, these biofunctionalization strategies require gentler chemistries that are not stable in the complex *in vivo* environment [22].

Alternatively, attempts have been made with limited success to design tumor microenvironment-triggered cleavable PEGs, which has the potential to exploit the extracellular low pH of tumor cells [21, 23-26]. However, various challenges involved in the design of PEG-cleavable liposomes for tumor-targeting have been reported to date. Torchilin et al., investigated liposomes coated with aliphatic and aromatic aldehyde-derived hydrazone (Hz)-based acid-sensitive cleavable PEG-1,2-dipalmitoyl-sn-glycero-3-phosphoethanolamine (DPPE) polymers [25]. However, they found that the aliphatic aldehyde-based PEG conjugates more readily destabilized at mildly acidic pH 5.5 with a half-life of 2 min, and were, unfortunately, also unstable at physiologic pH (half-life 2.5 h). In contrast, those derived from aromatic aldehydes were stable enough at pH 7.4 (half-life of 72 h) but less pH-sensitive with a half-life of 48 h at pH 5.5 [24]. More recently, Chen et al., reported on the design of PEG detachable liposomes (non-pH sensitive bilayers) using mPEG-Hz-CHEMS based on ketone-derived hydrazone to achieve enhanced cellular uptake and cytotoxicity [26]. However, a higher accumulation in the liver and spleen was found with the novel liposomes compared with the conventional liposomes due to the poor stability of the polymer at physiological pH. Our previous research [27] showed that the PEG<sub>B</sub>-Hz-CHEMS using amphiphilic lipid anchor CHEMS do have satisfactory stability and pH responsive PEG-detachment. However, they have poor insertion abilities into liposomes, which compromises their stealth abilities [27]. This could be due to the small cholesterol-like hydrophobic head which favours the formation of micelles. Therefore, we inferred that PEG anchored on the head groups of phospholipids may overcome the above challenges.

In this paper, we designed a novel acid labile PEG-cleavable polymer based on DPPE, PEG<sub>B</sub>-Hz-DPPE. We further demonstrated a dual pH-responsive strategy, where a cleavable PEG polymer was coated on a pSL (CL-pPSL). This system takes advantage of both the acid labile sheddable PEG layer (which facilitates the pH-triggered shielding and de-shielding of pH-

sensitive liposomes) and the pH-sensitive lipid bilayer that promotes the rapid intracellular trafficking. These dual pH-sensitive liposomes had not been investigated before, and little was known about their rapid endosome escape abilities. The influence of cleavable PEG on the *in vitro/in vivo* performance of CL-pPSL, including the drug release, intracellular accumulation, rapid endosome escape, higher cytotoxicity in Mia PaCa-2 and U-87 cancer cells and pharmacokinetics and biodistribution, were subsequently investigated with gemcitabine as the model drug in comparison to conventional pH-sensitive PEGylated liposomes (pPSL) with the same degree of PEGylation.

### 5.3 Materials and methods

#### 5.3.1 Materials

Methoxy poly(ethylene glycol) (mPEG,  $M_n = 2000$ ), cholesterol, Sephadex G-25, calcein and Nile Red were acquired from Sigma-Aldrich (St. Louis, MO, USA). Phospholipids such as 1,2-dioleoyl-sn-glycero-3-phosphoethanolamine (DOPE), and 1,2-distearoyl-sn-glycero-3-phosphocholine (DSPC), 1,2-dipalmitoyl-sn-glycero-3-phosphoethanolamine (DPPE) and cholesteryl hemisuccinate (CHEMS) were purchased from Avanti Polar Lipids (Alabaster, USA). Dicyclohexylcarbodiimide (DCC), 4-(dimethylamino)pyridine (DMAP) and N- $\epsilon$ -maleimidocaproic acid hydrazide (EMCH) were purchased from Thermo Fischer Scientific Inc (Auckland, New Zealand). Gemcitabine HCL (99.95 % purity) was obtained from Selleckchem (Houston, USA). Milli Q water (HPLC grade) was obtained from a Millipak filter unit (Millipore, pore size 0.22  $\mu\text{m}$ ). All other reagents were commercially available and used as received.

The Mia PaCa-2 pancreatic cancer cells and glioblastoma U-87 cells were obtained from the American Type Culture Collection (ATCC, Rockville, MD). Gibco™ Dulbecco's Modified

## Chapter 5

Eagle's Medium (DMEM) cell culture medium, foetal bovine serum, Penicillin-Streptomycin-Glutamine (100X) were purchased from Thermo Fisher Scientific (Auckland, New Zealand).

Sprague-Dawley (SD) rats (weighing  $200 \pm 5$  g for pharmacokinetics study) and CD-1 nude mice (weighing  $20 \pm 2$  g for biodistribution study) were obtained from the Vernon Jansen unit, The University of Auckland (Auckland, New Zealand).

All animal studies were carried out under the protocol approved by the Animal Ethics Committee of The University of Auckland (Ethics approval numbers 001593 and 001880).

### 5.3.2 Synthesis of PEG<sub>B</sub>-Hz-DPPE polymer

The synthesis of PEG<sub>B</sub>-Hz-DPPE was carried out with a three-step procedure. Firstly, hydrazide-activated DPPE was synthesized according to our previous method with some modifications [146]. For this, DPPE (22  $\mu$ M) was mixed with 1.5 molar excess of EMCH hydrazide linker in 3 mL of anhydrous methanol. Triethylamine (5 mole excess over lipid) was added to the resulting reaction mixture to achieve a pH of 6.5-7.5, which activates the maleimide moiety of EMCH, and the reaction mixture was stirred at 25 °C overnight. The resulting reaction mixture was purified on a silica gel column by eluting with chloroform:methanol solvent mixtures (v/v). The phosphate containing turbid fractions was pooled, concentrated under reduced pressure, and the structure was confirmed by <sup>1</sup>H NMR spectroscopy (yield: 80%). For step 2, PEG<sub>B</sub> was synthesized according to our previous method [222]. For step 3, PEG<sub>B</sub> (0.06 mmol) was mixed with DPPE-hydrazide (0.09 mmol) in 2 mL of chloroform at 25 °C. After overnight stirring, the resulting reaction mixture was evaporated to dryness and the obtained residue was purified by passing it through a Sephadex G-25 column using purified water, pH 7.4. The fractions containing the compound were pooled, freeze dried and confirmed by <sup>1</sup>H NMR spectroscopy (yield: 84.1%).

### 5.3.3 Characterization of PEG<sub>B</sub>-Hz-DPPE polymer

To determine the pH dependent bond cleavage properties of the polymer, the shift in the particle size of the polymeric micelles was monitored following their incubation at various pH, such as 7.4, 6.5 and 5.0 at 37 °C, using dynamic light scattering (DLS) [257]. Briefly, the polymer (at a concentration of 2.0 mg/mL) was incubated in a phosphate buffer (0.01 M, pH 7.4, 6.5 and 5.0) at 37 °C, with shaking at a speed of 120 rpm for 2 h. Post incubation, the size of the polymeric micelles was measured using DLS. Furthermore, the physical stability of micelles in PBS (0.01 M, pH 7.4) was determined by measuring their size and morphology using DLS and Cryo-Transmission electron microscopy (Cryo-TEM).

In addition, the pH-responsive destabilization behaviour of PEG<sub>B</sub>-Hz-DPPE micelles was further confirmed by a Nile Red assay [258]. Briefly, 100 µL of Nile Red-loaded micelle solutions (2 mg mL<sup>-1</sup>) was incubated in 900 mL of 0.01 M phosphate buffer solutions, at pH 7.4, 6.5 and 5.0 for 1, 2 and 24 h respectively, and the change in colour was monitored over time as a function of pH.

The critical micellar concentration (CMC) of polymer micelles was determined by fluorescence spectroscopy using Nile Red as a fluorescent probe [243]. Nile Red incorporated polymeric micelles were prepared and diluted to a polymer concentration ranging from  $2 \times 10^{-4}$  mM to 0.2 mM. Fluorescence measurement was carried out using a Fluoro Max-4 spectrophotometer at an excitation wavelength of 550 nm and the emission monitored from 580 to 720 nm. The CMC of the polymer was calculated by plotting the fluorescence intensity against log polymer concentration.

### 5.3.4 Preparation of the liposomes

Both CL-pPSL and control formulation pPSL were prepared by thin film hydration-extrusion as described previously [222]. pPSL were prepared by DOPE, DSPC, CHEMS, cholesterol, at

the molar ratio of 4:2:2:2 in addition to 5 mol% of DSPE-PEG<sub>2k</sub> to the total lipids. CL-pPSL were prepared with same composition of lipids, but replacing DSPE-PEG<sub>2k</sub> with PEG<sub>B</sub>-Hz-DPPE. The resulting lipid films were kept under vacuum overnight, followed by hydration with phosphate buffered saline (0.01 M, pH 7.4) at 30 °C. The resulting suspension was subjected to 7 cycles of freeze and thaw and 10 cycles of extrusion via 100 nm membrane with a pressure of ~500 psi and a temperature of 50 °C, close to the T<sub>c</sub> of DSPC. The liposome pellets obtained following ultra-centrifugation of the suspension were then preserved at 4 °C for further studies.

PEGylation of the above non PEGylated liposomes was performed using a post insertion technique [122, 222]. For this, 1 ml of PEG<sub>B</sub>-Hz-DPPE (for CL-pPSL) or DSPE-PEG (for pPSL) micelle suspension (eqv. to 5 mol% to lipids) in PBS 0.01 M, pH 7.4 was used to resuspend the liposome pellet, which was incubated at 37 °C for 2 h with continuous shaking at 350 rpm to form CL-pPSL and pPSL respectively.

### 5.3.5 Characterization of liposomes

To determine the insertion efficiency (IE) of the polymer, Nile Red-loaded polymeric micelles were incubated with the non-PEGylated liposomes for 2 h. The resulting liposome suspension was then ultra-centrifuged to spin down the liposome pellet, and monitored for the colour of the supernatant.

To assess *in vitro* cytotoxicity and *in vivo* long circulation, as well as the targeting abilities of the liposomes, gemcitabine was loaded into the selected preformed empty CL-pPSL and pPSL using a previously reported small volume incubation (SVI) method [249]. Entrapment efficiency (EE) and drug loading (DL) were determined using the following equations respectively.

To assess the cytotoxicity of liposomes on a different cell line as U-87, doxorubicin-loaded liposomes were prepared. For this, lipid films were hydrated with 250 mM ammonium sulfate solution at pH 7.4, at 30 °C, followed by 7 cycles of freeze and thaw and 10 cycles of extrusion using polycarbonate membranes of 0.2 µm and 0.1 µm using a Lipex extruder, Model T001 (Northern Lipids Inc, Vancouver, Canada), which were removed of free ammonium sulfate by dialysis and were subsequently used for drug loading. The pellet was resuspended with 1 mg/mL of doxorubicin solution of pH 7.0 and incubated for 1 h at 37 °C and the non-encapsulated doxorubicin was removed by ultracentrifugation.

$$EE (\%) = \frac{\text{mass of drug in liposomes}}{\text{mass of drug used for loading}} \times 100$$

$$DL (\%) = \frac{\text{mass of drug in liposomes}}{\text{mass of drug loaded in liposomes}} \times 100$$

The mean size and surface charge of drug-loaded pPSL and CL-pPSL were determined using a Malvern Zetasizer (Malvern Instruments, Germany). Particle size and zeta potential for non-PEGylated and PEGylated liposomes were compared to confirm the surface modification of liposomes with PEG. The morphology of the CL-pPSL was observed by a Cryo-Transmission electron microscopy (Cryo-TEM).

### 5.3.6 pH-responsiveness

The pH-responsive drug release of gemcitabine-loaded pPSL and CL-pPSL was determined by a dialysis method. The drug-loaded liposomes were dispersed in 1 mL of PBS (50 mM, pH 7.4) and tightly sealed in cellulose acetate dialysis tubes (MW 12–14 kDa). Then the dialysis tubes were immersed in 50 mL of release medium (PBS 50 mM), pH 7.4, 6.5 (extracellular pH) and 5.0 (endo/lysosomal pH), adjusted with NaCl to 320 mOsm and incubated under 37 °C with shaking of 100 rpm for 48 h. A volume of 100 µL of release media was withdrawn and replaced

with the same volume of fresh release media at various time intervals. The concentration of released gemcitabine was determined by HPLC and the percentage of the drug released was calculated [259].

The *in vitro* drug release-time profiles were compared using the similarity factor ( $f_2$ ) approach [247]. The  $f_2$  value is a logarithmic transformation of the sum-squared error of the differences in % release between two formulations ( $T_j$  and  $R_j$ ) through all the time points. An  $f_2$  value between 50 and 100 indicates the release profiles are similar.

### **5.3.7 *In vitro* cellular uptake and endosomal escape**

For the qualitative study of the cellular uptake and endosome escape properties of CL-pPSL and pPSL, liposomes were dual fluorescent labelled. The lipid bilayer was labelled with fluorescent Nile Red (0.2  $\mu\text{g/ml}$ ) to study the intracellular fate of the liposomes and hydrophilic self-quenched concentration of calcein 80 mM [260], which acts as an indicator of lipid vesicle leakage, which was loaded into their core to study their endosome escape properties [248].  $1 \times 10^5$  cells per well were seeded in 4-well chambered slides and cultured for 24 h. The dual-labelled liposomes were added to the plates with a total lipid concentration of 0.4 mmol/L and incubated at 37 °C for 1 and 2 h respectively. Cells were washed with cold PBS (pH 7.4) and fixed using 4% paraformaldehyde at 4 °C for 10 min. Finally, the nuclei were stained by DAPI for 5 min in the dark. Cells were observed under a confocal laser scanning microscope (CLSM, Olympus Fluroview FV1000, Olympus Corporation, Japan) with an excitation wavelength of 366 nm for DAPI, 488 nm for calcein and 546 nm for Nile Red.

### **5.3.8 Subcellular localisation of CL-pPSL and pPSL with live cell imaging**

To further investigate the intracellular trafficking of the CL-pPSL and pPSL, live cell tracking studies were performed on Mia PaCa-2 cells, using the Olympus Fluroview FV1000 CLSM. Cells were seeded at a density of  $10^3$ /well in a 300  $\mu\text{L}$  medium and allowed to attach overnight

to ibidi 8-well chambered slides. The cells were stained with LysoTracker Deep Red (75  $\mu\text{g}/\text{mL}$ ) at 37 °C for 90 min and Hoescht 33342 (1  $\text{mg}/\text{mL}$ ) at 37 °C for 20 min. A single cell with a clear morphology was chosen in a differential interference contrast (DIC) channel. The cells were then added to Rh-PE labelled CL-pPSL and pPSL at a total lipid concentration of 50  $\mu\text{g}/\text{mL}$  and immediately observed using CLSM with a 60 X oil immersion objective and live cell incubator system. Confocal images were acquired at regular intervals over a 2 h time period.

### **5.3.9 *In vitro* cytotoxicity study**

Cytotoxicity was evaluated with a 3-(4,5-dimethylthiazol-2-Yl)-2,5-diphenyltetrazolium bromide (MTT) assay. Primarily, Mia PaCa-2 cells were seeded into 96-well plates (800 cells/well) and cultured at 37 °C, 5%  $\text{CO}_2$  for 24 h. Then the cells were exposed with a series concentration of blank liposomes, free gemcitabine or gemcitabine-loaded CL-pPSL and pPSL. As gemcitabine is an antimetabolite agent, after 24 h drug exposure, cells were washed and grown for 72 h before an MTT assay was performed. Untreated cells in the culture medium were used as controls (100%).

Furthermore, pPSL and CL-pPSL loaded with doxorubicin, a DNA-damaging anticancer agent, were also tested for their cytotoxic potential in U-87 (glioblastoma) cells. For this, U-87 cells were seeded in 96-well plates (800 cells/well) and exposed with a series concentration of blank liposomes, free doxorubicin or drug-loaded CL-pPSL and pPSL. After 24 h drug exposure, cells were washed and grown for 72 h and evaluated with the MTT assay. The drug concentration causing 50% inhibition of viable cell density with respect to non-treated controls ( $\text{IC}_{50}$ ) with the 95% confident intervals (CI) was calculated using a non-linear fitting model in the GraphPad Prism (GraphPad Software, USA).

### 5.3.10 Pharmacokinetics

Pharmacokinetics were studied in Sprague-Dawley rats (195 - 205 g) using the gemcitabine formulations. For this, animals were randomly divided into three groups, namely CL-pPSL (n=6), pPSL (n = 4) and solution (n=4). Each formulation (0.2 mg/ml) was injected via the tail vein at 1 mg/kg equivalent gemcitabine. Blood samples (100–200  $\mu$ l) were collected from the tail vein at various time intervals. Furthermore, a high dose of 5 mg/kg was injected to study the dose dependent change in the pharmacokinetics of the CL-pPSL. Samples were prepared for analysis as per our previously reported method [222].

### 5.3.11 Biodistribution study

The biodistribution was evaluated in tumor-bearing CD-1 mice.  $5 \times 10^6$  Mia PaCa-2 cells (suspended in 1:1 PBS : Matrigel) were subcutaneously implanted into the hind flank of the mice. When tumors reached  $\sim 300$ - $400$  mm<sup>3</sup>, mice were randomly divided into 3 treatment groups (n=3) and injected with free gemcitabine and gemcitabine-loaded pPSL and CL-pPSL at a dose of 16 mg/kg via the tail vein. After 4 h of dosing, animals were sacrificed, and blood, major organs (liver, kidney, spleen, heart) and tumors were harvested and stored on dry ice before immediate HPLC analysis.

To evaluate the tissue biodistribution after 12 h of dosing, due to the lack of tumor-bearing CD-1 nude mice, normal mice were randomly divided into 3 treatment groups and subsequently treated with the same protocol as described above.

Plasma samples were treated in a similar way to the aforementioned pharmacokinetics study. Organs were added to acetonitrile (0.2 g: 1 mL) and homogenised by a tissue dissociator (gentle MACS Dissociator, Miltenyi Biotech) at  $2,000 \times g$  for 1.5 min, which was programmed to break down the tissues, and samples were then centrifuged at  $10,000 \times g$ . The supernatant was evaporated and the residue re-dissolved in 50  $\mu$ L Milli Q water and gemcitabine concentrations

were determined by the HPLC assay. The limit of detection was 0.05  $\mu\text{g/mL}$  and the extraction recovery was observed as  $>85\%$

### 5.3.12 Data and statistical analysis

The gemcitabine pharmacokinetic profiles were fitted to a non-compartmental model using a Kinetica 5 program and the pharmacokinetic parameters were obtained. Data were analyzed by a one-way analysis of variance (ANOVA) with Tukey's multiple comparisons test using the GraphPad Prism 6.01 (GraphPad Software Inc., La Jolla, U.S.A). The level of significance for all statistical analysis was set at 0.05.

## 5.4 Results

### 5.4.1 Synthesis of PEG<sub>B</sub>-Hz-DPPE polymer

The synthetic routes and the molecular structure of PEG<sub>B</sub>-Hz-DPPE are shown in Figure 5-2A. The chemical structure of the polymer was successfully confirmed by <sup>1</sup>H NMR spectroscopy (Figure 5-2B and C). The detailed peak analysis of the polymer was displayed as chemical shift values  $\delta$  of 0–3 ppm (peak b, the methyl and methylene group of DPPE), 3.09 - 4 (peak a, PEG<sub>B</sub>), and 7.9-8.0 (p-phenyl ring of the benzaldehyde). Furthermore, after the coupling reaction between PEG<sub>B</sub> and DPPE-Hz, the characteristic proton signal of the aldehyde group ( $\delta$  10.5 ppm, peak c) derived from PEG<sub>B</sub> disappeared completely, and the proton signal of the imine group ( $\delta$  8.50 ppm, peak d) appeared in the <sup>1</sup>H NMR spectrum of the conjugate.

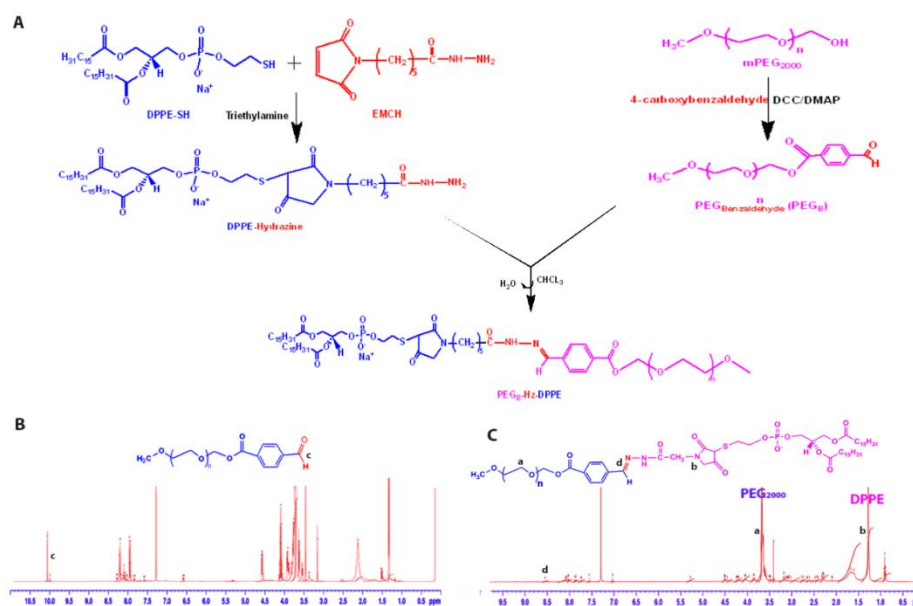


Figure 5-2 A) Scheme of synthesis of PEG<sub>B</sub>-Hz-DPPE; Typical <sup>1</sup>H NMR spectrum of B) PEG<sub>B</sub> and C) PEG<sub>B</sub>-Hz-DPPE.

#### 5.4.2 Characterization of PEG<sub>B</sub>-Hz-DPPE polymer

The synthesized PEG<sub>B</sub>-Hz-DPPE polymer could spontaneously aggregate into polymeric micelles in aqueous media because of the presence of the hydrophilic PEG and hydrophobic DPPE domains. The obtained micelle dispersion in PBS (0.01M, pH 7.4) exhibited an average particle size of 40 nm with a narrow unimodal size distribution at physiological pH (Figure 5-3A). Consistently, Cryo-TEM observations confirmed monodispersed spherical PEG<sub>B</sub>-Hz-DPPE micelles with an average size of 25-35 nm. The CMC of the polymer was determined as 24.2 μM by fluorescence spectrometry (Figure 5-3B).

A rapid increase in the size of the micelles was observed post incubation at pH 5.0 for 2 h, whereas size remained the same after incubation at pH 7.4 for the same period (Figure 5-3A). Confirming the above results, the Nile Red assay also revealed that micelles entrapping Nile Red in their core exhibited strong fluorescence intensity at pH 7.4, which remained the same after 24 h. However, after the incubation of micelles for 2 h at the acidic pH of tumors, such as pH 6.5 (extracellular) and 5.0 (endosome), a sharp reduction in fluorescence intensity was

observed. The colour completely disappeared from the micellar solution after 24 h with a visible amount of Nile Red released to the top of the solution, indicating the ability of micelles to undergo pH triggered destabilization (Figure 5-3C). Additionally, it was found that the colour reduction accelerated with the decrease of pH from 6.5 to 5.0.

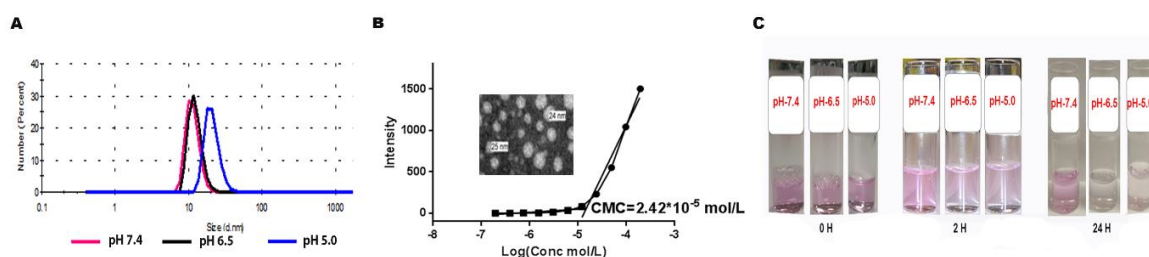


Figure 5-3 A) Measurement of size, and pH-sensitivity of PEG<sub>B</sub>-Hz-DPPE polymer: DLS showing a shift in particle size response after 2 h incubation at various pH, B) morphology and CMC of PEG<sub>B</sub>-Hz-DPPE polymeric micelles, and C) visual observation of changes in colour of micelle solution due to their pH dependent destabilization, which resulted in the precipitation of the dye.

### 5.4.3 Characterization of PEGylated liposomes

Post incubation and ultracentrifugation of the PEG<sub>B</sub>-Hz-DPPE coated liposomes, the supernatant appeared colourless, which indicates that micelles were completely inserted into the liposomes and the IE of the polymer was estimated to be >95% based on visual observation (Figure 5-4A). The average size of the resulting CL-pPSL was  $121 \pm 0.62$  nm (Figure 5-4B) with a round and unilamellar structure (Figure 5-4C). After PEGylation, along with an increase in their size, CL-pPSL exhibited a decrease in the zeta potential (Table 5-1).

The liposomes were then loaded with gemcitabine with an EE of  $37.0 \pm 1\%$ , and a high DL of 4%. The liposomes showed good stability over 2 months when stored at 4 °C as liposome pellets (Table 5-1). Doxorubicin-loaded liposomes showed an EE of  $99.0 \pm 0.5\%$ , and DL of 7% as determined by HPLC.

Table 5-1 Physio-chemical characterization of gemcitabine-loaded liposomes and stability at 4 °C as liposome pellets. Data are mean  $\pm$  SD (n = 3).

Formulation	Time (month)	Size (nm)	PDI	Zeta potential (mv)	Gemcitabine entrapped in lipid pellets (%)
CL-pPSL	0	143 $\pm$ 0.62	0.07 $\pm$ 0.02	-9.5 $\pm$ 1.0	100.0 $\pm$ 0.6
	1	142 $\pm$ 0.36	0.06 $\pm$ 0.01	-9.8 $\pm$ 1.2	98.5 $\pm$ 1.0
	2	146 $\pm$ 0.12	0.09 $\pm$ 0.03	-9.4 $\pm$ 1.5	91.3 $\pm$ 1.0
pPSL	0	142 $\pm$ 0.10	0.04 $\pm$ 0.01	-7.6 $\pm$ 1.4	100.0 $\pm$ 0.2
	1	141 $\pm$ 0.14	0.08 $\pm$ 0.02	-8.2 $\pm$ 1.1	98.2 $\pm$ 0.5
	2	144 $\pm$ 0.11	0.05 $\pm$ 0.02	-8.2 $\pm$ 1.3	92.5 $\pm$ 1.0

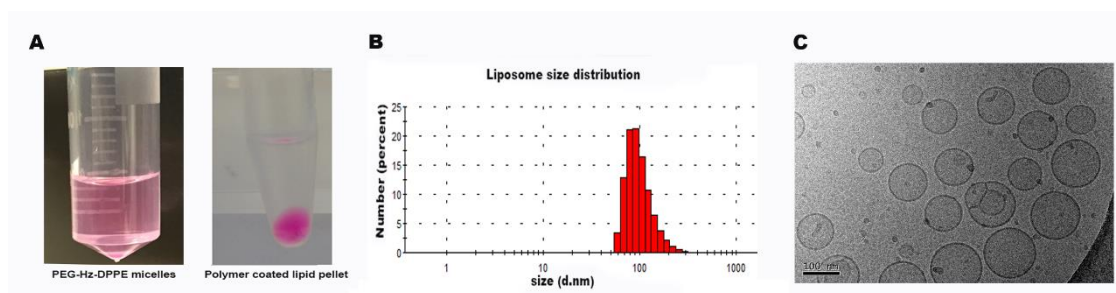


Figure 5-4 Characterization of PEG<sub>B</sub>-Hz-DPPE modified liposomes for A) polymer insertion efficiency: PEG<sub>B</sub>-Hz-DPPE micelles were loaded with Nile Red (left) and incubated with DOPE/CHEMS liposomes (right), showing more Nile Red micelles in the pellet, but less than 5% of free Nile Red micelles were found in the supernatant; B) size distribution and C) morphology of CL-pPSL.

#### 5.4.4 pH-responsive drug release

There was a pH dependence on the drug-release rates from both pPSL (Figure 5-5A) and CL-pPSL (Figure 5-5B). The cumulative release of gemcitabine from pPSL and CL-pPSL was similar (30%) after 10 h at pH 7.4, indicating that cleavable PEGylation did not influence the drug leakage from CL-pPSL at physiological pH. When the pH was reduced to 5.0, approximately 80% of the drug rapidly released from the CL-pPSL, whereas only 55% was released from pPSL.

Between CL-pPSL and pPSL, the overall release profiles of (Figure 5-5) are similar at pH 7.4 and 6.5 with an  $f_2$  factor of 79.1, 75.5 respectively. Whereas, at pH 5.0, an  $f_2$  value of 38.9 indicates that the release profiles from the two liposomes were not similar, with CL-pPSL producing faster release than pPSL. This demonstrates the rapid intracellular drug delivery abilities of CL-pPSL over pPSL.

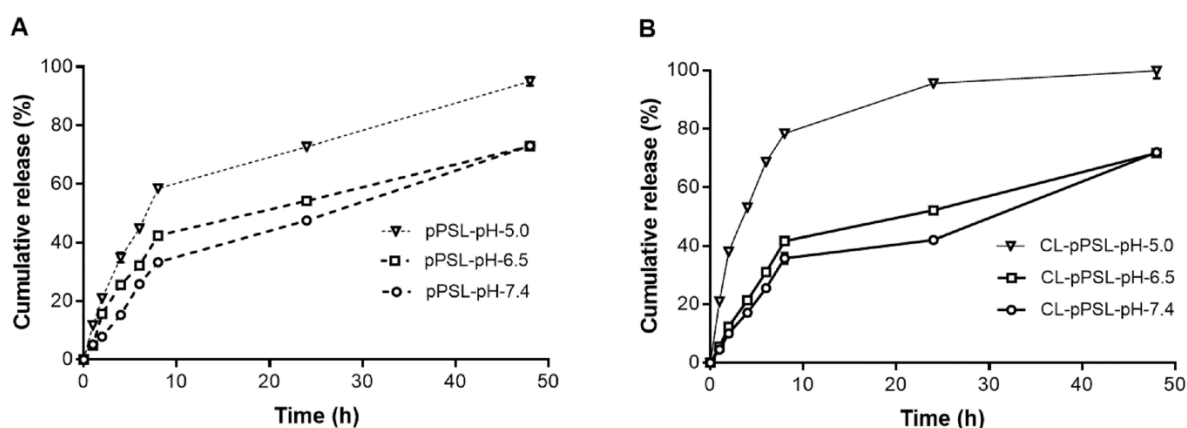


Figure 5-5 pH-responsive gemcitabine release profiles of A) pPSL and B) CL-pPSL (mean  $\pm$  SD,  $n = 3$ ).

#### 5.4.5 *In vitro* cellular uptake and endosome escape studies.

In this study cellular uptake was indicated from the red fluorescence of Nile Red-labelled liposomes, and endosome escape was denoted by the green fluorescence of calcein, which becomes visible only after it is released from the liposomes and is diluted to its de-quenched concentration ( $<10$  mM). It was evident that no difference was observed in the red fluorescence intensity between CL-pPSL and pPSL (Figure 5-6), indicating that both were being taken up to the same extent. The green channel at 30 min clearly demonstrated a rapid endosomal escape of CL-pPSL, which showed the strongest green fluorescence in comparison to the pPSL. Following a 2 h incubation with the cells, CL-pPSL showed a homogenous distribution of calcein around the nucleus, whereas in contrast, pPSL exhibited only a weak punctate distribution of colour.

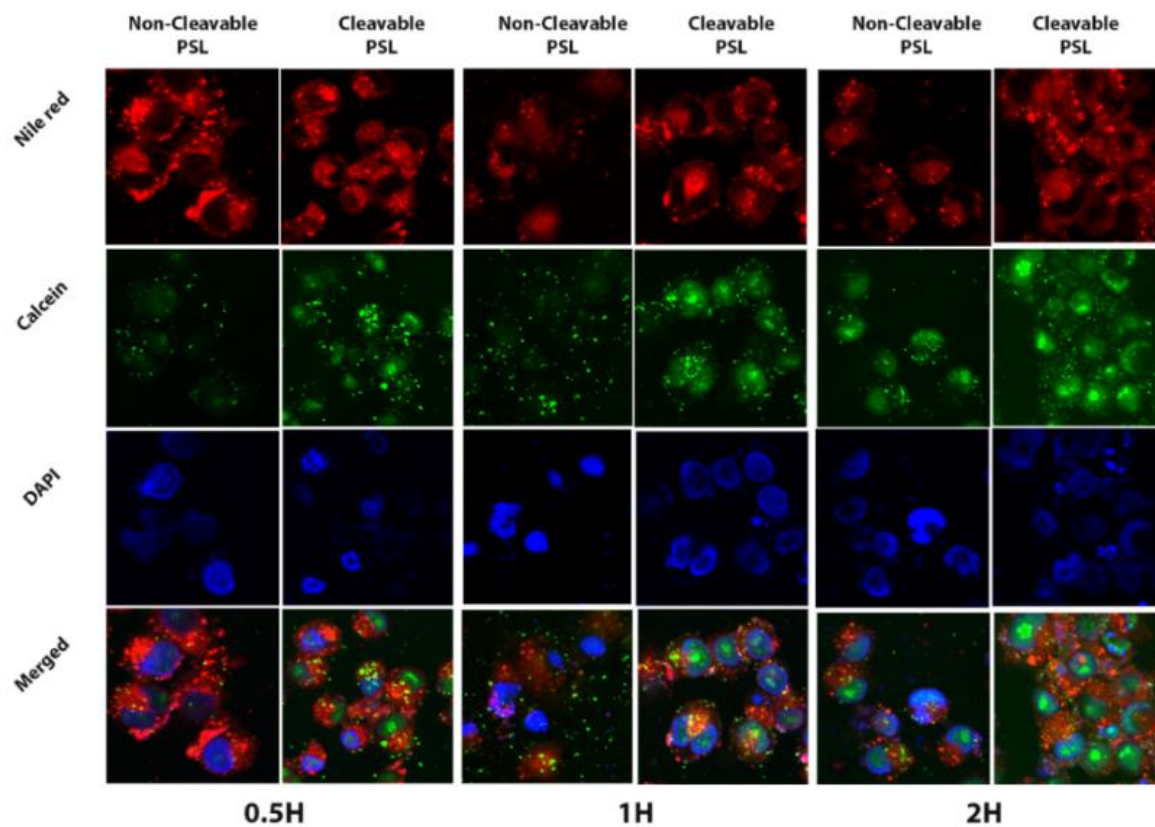


Figure 5-6 CLSM images showing the cell uptake and endosome escape of dual labelled pPSL and CL-pPSL over 2 h. Both liposomes were labelled with 0.2  $\mu\text{g}/\text{mL}$  of Nile Red in the bilayer and 80 mM of calcein in the cores.

#### 5.4.6 Subcellular localisation of CL-pPSL and pPSL by live cell imaging

Interestingly, live cell imaging showed that the LysoTracker Red (green color) labelled vesicles (late endosomes or lysosomes) in Mia PaCa-2 cells were initially concentrated around the centre and distributed around the nucleus, with only a few around the periphery of the cell (Figure 5-7). After 20 min of exposure to liposomes, the Nile Red fluorescence of CL-pPSL (red color) was found to be co-localized in the endo/lysosomal region, which increased over time. By the end of 1 h, bright red fluorescence of liposomes was homogenously distributed around the nucleus, indicating content release into the cytoplasm (Figure 5-7B). In contrast, pPSL showed a very weak red fluorescence signal and by the end of 1 h only the punctate pattern was observed in the endo/lysosomal region (Figure 5-7B). For both CL-pPSL and pPSL, with a progression in time from 5 min to 2 h, the images clearly depicted the trafficking of liposomes in the cell from being taken up into the cells (red fluorescence of liposomes spotted in green stained cells), to fusion with the endo/lysosomal membrane (red merging with green to form yellow), and to release into the cytoplasm around the nucleus (reddish yellow).

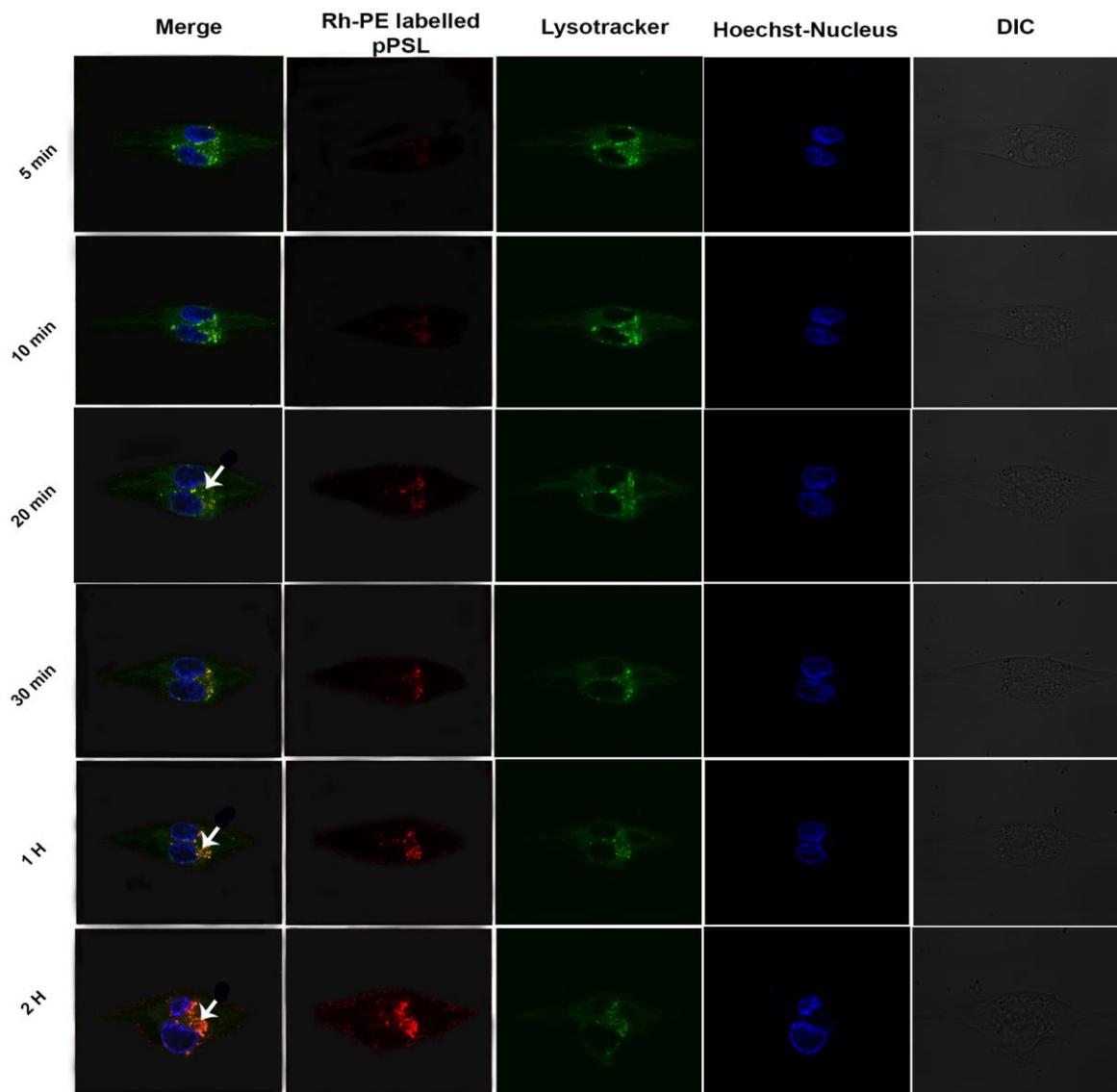


Figure 5-7A Live cell imaging showing the intracellular trafficking of rhodamine-labelled pPSL over a 2 h time period. The lysotracker-labelling (shown here as the green counterstain) was used to label the late endo/lysosomal regions of the cell. Hoechst 33342 (shown here as blue) was used as the nuclear stain. DIC was used to monitor the cell morphology throughout the process. pPSL displayed a weak and fine punctuate colocalization after 20 min of incubation time (see first arrow). However, the pPSL were more evident at the end of 1 h and could be seen to have undergone fusion with the endo/lysosomal membrane (red liposomes merging with green endosomal staining is indicated by the second arrow) and at 2 h the pPSL exhibited a visible leakage from the endosomes into the cytoplasm around the nucleus (bright red dots around the nuclear region is indicated by the third arrow).

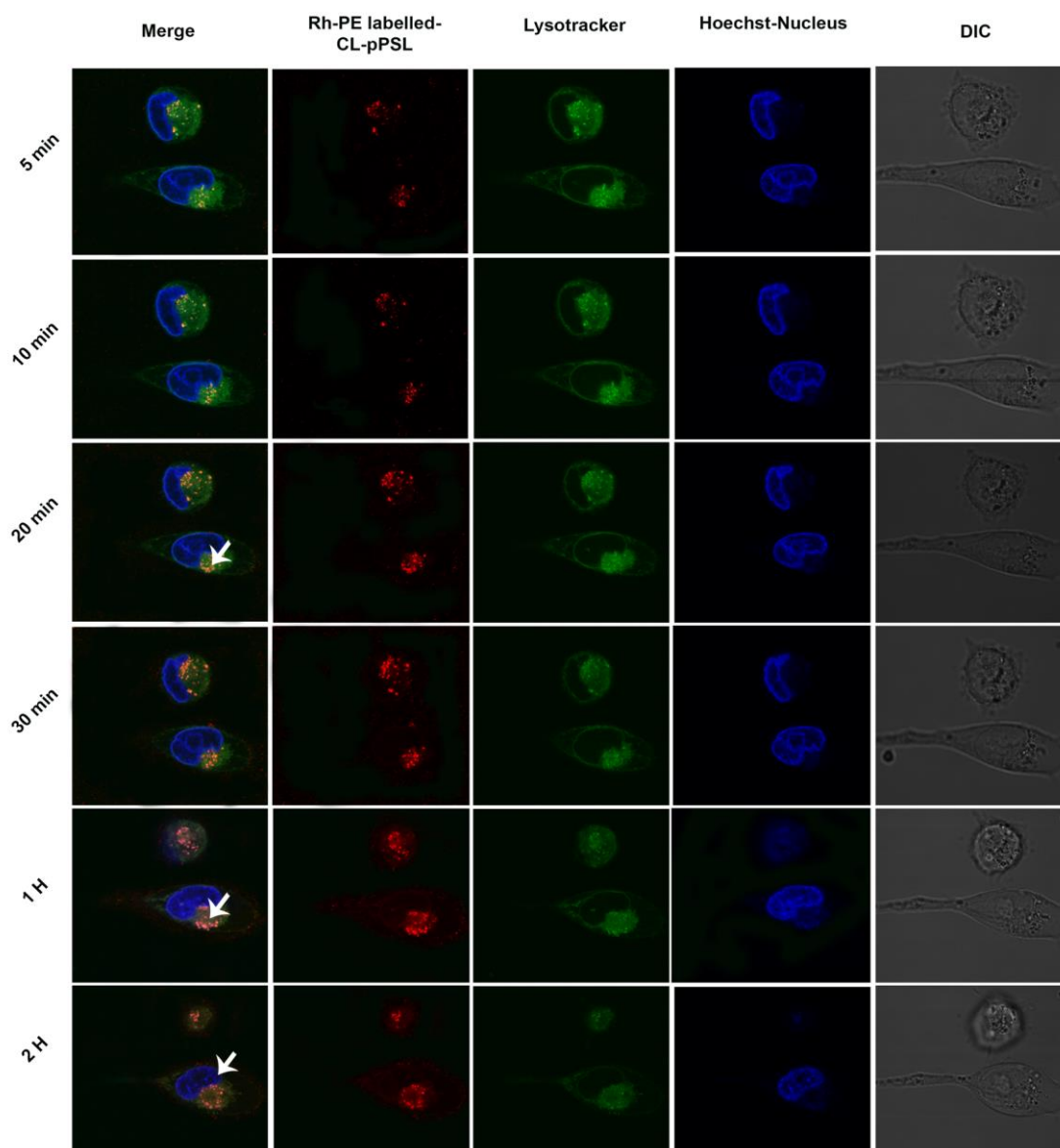


Figure 5-7B Live cell imaging showing the intracellular trafficking of rhodamine-labelled CL-pPSL over a 2 h time period. The lysotracker-labelling (shown here as the green counterstain) was used to label the late endo/lysosomal regions of the cell. Hoechst 33342 (shown here as blue) was used as the nuclear stain. DIC (grey images) was used to monitor the cell morphology throughout the process. The CL-pPSL displayed a clearly evident colocalization after 20 min incubation time indicating their fusion with endo/lysosomal membrane (red liposomes merging with green endosomal staining indicated by the first arrow). After 1 h of incubation, they exhibited rapid leakage from the endosomes into the cytoplasm around nucleus (bright red dots around the nuclear region as indicated by the second arrow and third arrow at 2 h).

### 5.4.7 *In vitro* cytotoxicity study

As shown in Figure 5-8A, gemcitabine formulations showed concentration dependent cytotoxic effects in Mia PaCa-2 pancreatic cancer cells. The CL-pPSL showed a higher cytotoxicity than pPSL ( $P < 0.01$ ) but slightly lower than the free drug solution ( $P < 0.01$ ) with an  $IC_{50}$  of 69 nM, 104 nM and 57 nM, respectively.

However, post exposure of doxorubicin formulations to U-87 cells, CL-pPSL showed significantly higher cytotoxicity than pPSL and free doxorubicin ( $P < 0.01$  in both cases) ( $IC_{50}$  of  $83 \pm 0.5$  nM,  $148 \pm 0.1$  nM and  $209 \pm 0.2$  nM) (Figure 5.8B).

In both the cases, blank liposomes (diluted to lipid concentrations equivalent to the gemcitabine-loaded liposomes) caused negligible toxicity over 24 h exposure periods (about 90% cell viability), indicating good biocompatibility of the liposomes.

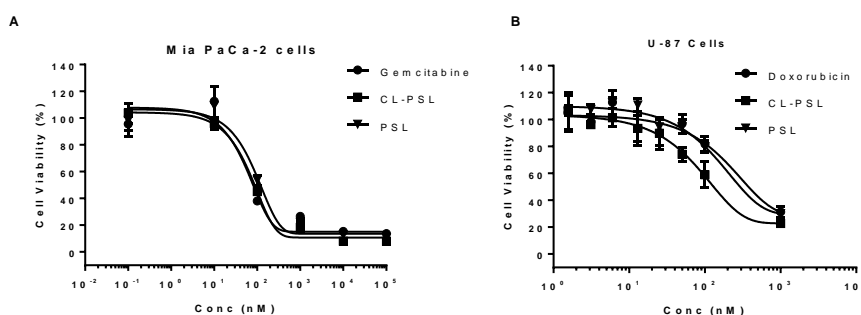


Figure 5-8 Cytotoxicity profiles of A) gemcitabine free drug or drug-loaded pPSL and CL-pPSL over Mia PaCa-2 cells; B) doxorubicin free drug or drug-loaded pPSL and CL-pPSL over U-87 cells. Data are mean  $\pm$  SD,  $n = 3$ .

### 5.4.8 Pharmacokinetics and biodistribution study

The plasma concentration curves as shown in Figure 5-9A show that both liposome formulations increased the retention time of the drug in the blood, whereas free gemcitabine is eliminated quickly during circulation. The pharmacokinetic parameters further confirmed this result (Table 5-2). Compared with the free drug solution, both CL-pPSL and pPSL show significant reductions in gemcitabine plasma clearance (CL), and a 6 to 8-fold increase in the  $AUC_{0-\infty}$  ( $p < 0.001$ ) (Figure 5-9A). In addition, there was an approximate 3-fold increase in the elimination of  $T_{1/2}$  and an approximate 1.5-fold increase in the mean residence time (MRT) for both liposomes compared to the free drug solution ( $p < 0.05$ ). Also, the volume of distribution ( $V_d$ ) and the clearances of both liposomes were significantly reduced compared to the free drug solution. The results clearly indicate that the PEG-detachment from the CL-pPSL did not compromise their stealth abilities. Further study with an increase in the dose of CL-pPSL from 1 to 5 mg/kg resulted in an increase in  $T_{1/2}$  to 9.8 h and MRT to 7.2 h, however the AUC increased proportionally 5-fold.

Table 5-2 Summary of plasma pharmacokinetic parameters after a single i.v. administration drug solution or liposome formulations with a dose of 1 mg/kg to SD rats (unless otherwise stated). Pharmacokinetics of CL-pPSL at a higher dose of 5m/kg (n=4) was further determined. Data are mean  $\pm$  SD, n = 6 for CL-pPSL formulations and n=4 for the rest of them.

Formulation	AUC $\mu\text{g/ml}\cdot\text{h}$	$V_d$ (ml/kg)	Clearance (ml/h/kg)	$T_{1/2}$ (h)	MRT (h)
Free drug	17.0 $\pm$ 1.7	742 $\pm$ 4	202.3 $\pm$ 18.4	3.2 $\pm$ 0.4	3.5 $\pm$ 0.2
pPSL	103.1 $\pm$ 12.8	170 $\pm$ 30	29.3 $\pm$ 4.4	5.8 $\pm$ 0.6	5.0 $\pm$ 0.3
CL-pPSL	142.5 $\pm$ 18.4 <sup>ns</sup>	115 $\pm$ 17 <sup>ns</sup>	25.3 $\pm$ 1.3 <sup>ns</sup>	7.6 $\pm$ 0.9 <sup>ns</sup>	4.9 $\pm$ 0.9 <sup>ns</sup>
CL-pPSL(5 mg/kg)	699.5 $\pm$ 22.4	172 $\pm$ 15	23.9 $\pm$ 1.5	9.8 $\pm$ 0.5	7.2 $\pm$ 0.4

ns = not significant in comparison to the pPSL

Mia PaCa-2 tumor-bearing CD-1 nude mice were used to estimate the tumor distribution of liposomes after 4 h of dosing. Biodistribution results further strengthened the findings from the

## Chapter 5

pharmacokinetics. Data indicate that 4 h after the i.v. injection of CL-pPSL, the concentration of gemcitabine in tumors was 1.5-times higher than for pPSL and 6-times higher than for free drug treated (Figure 5-9B). Furthermore, the drug concentration in the heart following treatment with both liposomes was 3-times lower than free drug treated mice. The level of gemcitabine in the major clearance organ, the liver, was significantly lower for free drug injected mice compared to pPSL and CL-pPSL treated groups, after 4 h post injection, reflecting the faster clearance rates of the free drug [261]. Non-tumor bearing CD-1 nude mice were used to estimate the biodistribution of liposomes after 12 h of dosing. However, at 12 h, CL-pPSL and pPSL treated mice showed similar levels of drug concentrations in the liver and spleen as well as in plasma (Figure 5-9C).

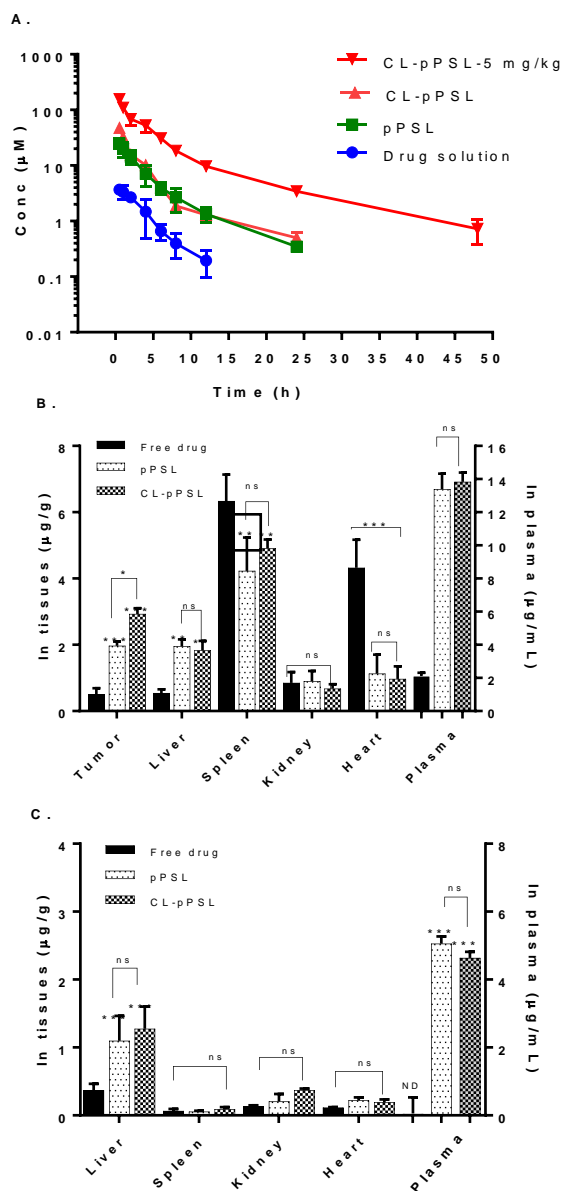


Figure 5-9 A) Plasma pharmacokinetic profiles following i.v. injection of gemcitabine solution ( $n = 4$ ), pPSL ( $n = 4$ ) [222] and CL-pPSL ( $n = 6$ ), in rats at 1 mg/kg equivalent gemcitabine and dose-dependent pharmacokinetic profile of CL-pPSL-5 mg/kg ( $n = 4$  at 5 mg/kg). Concentration of gemcitabine in various tissues at B) 4 h and C) 12 h following a single injection of free gemcitabine, gemcitabine-loaded liposomes as pPSL and CL-pPSL at gemcitabine equivalent dose of 16 mg/kg. ND = not detected. Data are mean  $\pm$  SD from one experiment,  $n = 3$  mice. Data at 12 h are from non-tumor-bearing mice. \*  $p < 0.05$ , \*\*  $p < 0.01$  and \*\*\*  $P < 0.001$

## 5.5 Discussion

pH sensitive liposomes functionalized by fusogenic DOPE and CHEMS have attracted greater interest due to their superior tumor-targeted intracellular drug delivery abilities [237, 238, 255, 262]. The addition of PEG polymers promotes the long circulation and tumor accumulation of pH-sensitive liposomes based on the EPR effect but hinders their cell uptake and acid-sensitive release process. Therefore, it was difficult for PEGylated pH sensitive liposomes to achieve both pH-sensitivity and prolonged circulation simultaneously, which is highly desirable for tumor-targeted drug delivery.

In this study, to overcome the negative effects of PEGylation (i.e. the PEG dilemma), a cleavable long-circulating PEG polymer (PEG<sub>B</sub>-Hz-DPPE) was designed, synthesized and characterised (Figure 5-2). The PEG<sub>B</sub>-Hz-DPPE polymer with a CMC of 25  $\mu$ M (Figure 5-3B) (equal to DSPE-PEG, 20  $\mu$ M [263]) readily self-aggregated above this concentration to form micelles at pH 7.4. The cleavable PEG<sub>B</sub>-Hz-DPPE, which included an acid-labile hydrazone linker, rapidly decomposed under acidic conditions to take off the PEG-coating as evident from a pH-dependent shift in their size (Figure 5.3A) and rapid pH-responsive Nile Red released from the micelles within 2 hours (Figure 5.3C) but remained stable at pH 7.4 for 24 h. In comparison, cleavable PEG polymers synthesized by Torchillin et al., derived from aromatic aldehydes [146], and those developed by Chen et al., were either lacking sufficient pH sensitivity or not stable at pH 7.4 [159]. The PEG<sub>B</sub>-Hz-DPPE synthesized in this study demonstrated an enhanced pH-responsiveness without compromising its stability at physiological pH 7.4. We believe this was due to the presence of unsaturation in PEG<sub>B</sub>, preventing the rapid protonation of the hydrazone bond.

The acid labile PEG<sub>B</sub>-Hz-DPPE polymer was further used to modify DOPE-CHEMS liposomes to form 5 mol% PEGylated CL-pPSL (Figure 5-4A), which was required for optimal stealth

properties [264]. It benefitted the drug-loaded CL-pPSL with an average size around  $141 \pm 0.82$  nm for passive targeting via the EPR effect [265]. CL-pPSL showed a slightly higher negative charge than pPSL (Table 5-1), indicating their increased stability *in vivo*. The high stability and pH-sensitivity of CL-pPSL compared to pPSL was also verified by the pH-sensitive drug release study. The moderate gemcitabine release of the CL-pPSL and pPSL at pH 7.4 implied that the drugs in liposomes could efficiently reach the tumor area even after 48 h (Figure 5.5). Incorporation of DSPC, a high transition lipid, further strengthened the liposomal membrane, which addressed the premature drug leakage issue of gemcitabine-loaded liposomes to some extent. Gemcitabine in the CL-pPSL released quickly compared to pPSL at an endosomal pH, 5.0 as expected (Figure 5-5), which was due to the dual pH responsiveness of PEG<sub>B</sub>-Hz-DPPE and the liposomal membrane.

To characterize endosome escape abilities *in vitro*, 1 and 2 h time periods were selected for the incubation of liposomes with Mia PaCa-2 cells, as the PEG<sub>B</sub>-Hz-DPPE polymer was observed to undergo rapid destabilisation in 2 h at endosomal pH 5.0 (Figure 5-3A, C). After the hydrolysis of PEG<sub>B</sub>-Hz-DPPE polymers, CL-pPSL benefitted from the interaction of the fusogenic DOPE bilayer with endosomal membranes. All the factors listed above lead to the higher endosomal escape of CL-pPSL than pPSL (Figure 5-6), which also prevented the degradation of cargos in the lysosomes [266].

Previous studies reported three pathways for the endosome escape of pPSL [267] as i) rupture of the endosomal membrane; ii) PSL destabilization causing the diffusion of contents; and iii) fusion of PSL with the endosome membranes leading to cytoplasmic delivery [268]. In this study, live cell imaging with the aid of LysoTracker Red further confirmed the rapid endosome escape abilities of CL-pPSL (Figure 5-7B) over the pPSL (Figure 5-7A) and showed that the

rapid intracellular delivery abilities of CL-pPSL in lower pH was probably dependent on fusion pathways following the detachment of PEG.

The higher cytotoxicity of the free drug solution over liposomes was due to the ability of the small molecule to be more quickly uptaken into the cells via the enhanced hCNT1 (a nucleoside transporter) expression in Mia PaCa-2 cells, resulting in enhanced drug influx and accumulation in the cytoplasm (Figure 5-8A). However, during the down regulation of these transporters in clinically gemcitabine-resistant cases [269], formulation would be advantageous. In addition, the enhanced tumor cell cytotoxicity of gemcitabine and doxorubicin-loaded CL-pPSL compared with pPSL illustrated that the PEG<sub>B</sub>-Hz-DPPE modification of liposomes could improve the internalization and intracellular delivery of liposomes into Mia PaCa-2 pancreatic and U-87 glioblastoma cells respectively.

The pharmacokinetics study in rats showed that the PEG<sub>B</sub>-Hz-DPPE based CL-pPSL had similar long circulation abilities to pPSL (Figure 5-9A), indicating the better stability of PEG<sub>B</sub>-Hz-DPPE at physiological pH as shown in the *in vitro* study. Previous work with cleavable polymers showed that the gradual cleavage of the PEG chain from the PEG-CHMC and PEG-CHEMS compromised the circulation half-life of liposomes [270]. Overall the data from this study supported that the PEG-detachment occurred only at lower pH from the CL-pPSL but did not compromise their stealth abilities during blood circulation.

*In vivo* biodistribution in CD-1 nude mice showed that both the liposomes showed significantly lower accumulation in normal tissues indicating their specificity and stealth properties (Figure 5-9B and C). Furthermore, the biodistribution assay in nude mice bearing Mia PaCa-2 xenograft tumors revealed that CL-pPSL increased the accumulation of the drug at the tumor site by 6-times that of the free drug solution, and 1.5 times that of pPSL (Figure 5-9B). In addition gemcitabine accumulation in the heart was 3-times lower for both pPSL and CL-pPSL

compared to free drug treated mice, which relates to the cardiotoxicity side effects of free gemcitabine [271].

All these data indicated that the addition of cleavable PEG<sub>B</sub>-Hz-DPPE allowed the liposomes to have both acid-sensitive release and long circulation performances.

## 5.6 Conclusion

A new acid-sensitive PEG<sub>B</sub>-Hz-DPPE was successfully synthesised and utilised for the preparation of acid-triggered PEG-sheddable pH sensitive liposomes. The CL-pPSL developed with PEG<sub>B</sub>-Hz-DPPE here delivered drugs into tumor cells with higher efficiency compared to conventional pPSL. Furthermore, this is the first study to fully elucidate the endosome escape abilities of dual pH-responsive liposomes facilitated with PEG-detachment. This, in combination with the use of pH-sensitive fusogenic DOPE lipids, overcomes the cellular uptake barrier and facilitates the rapid endosome escape of the contents that are hindered by conventional PEGylation. These dual pH sensitive CL-pPSL are promising in the application of tumor-targeted drug delivery in the future.

## 5.7 Acknowledgements

This work was supported by the Performance Based Research Fund from the School of Pharmacy, University of Auckland. The authors declare that there are no conflicts of interest to disclose.

## **6. General discussion and future prospects**

---

## 6.1 General discussion

Cancer has become one of the most devastating diseases worldwide. Importantly, pancreatic adenocarcinoma (PDAC) is one of the most aggressive and devastating human malignancies with a death-to-incidence ratio of 0.99 [272]. Global demographic characteristics predict an increased cancer incidence in the next decades, with >14 million new cancer cases annually expected by 2030 [273]. Advances in chemotherapy have resulted in the development of many successful cytotoxic drugs such as doxorubicin and paclitaxel. However, the main limitation of chemotherapy is that it annihilates cancer cells but also destroy the normal cells. To overcome this, two recent revolutions in cancer treatment are the emergence of nanomedicine and the targeting of features in the tumor microenvironment. Tumor-targeted drug delivery science using nanotechnology has enabled more effective drug design and the development of multifunctional nanosystems.

Among the various nanosystems, liposomes are well-studied because of their potential to improve tumor specificity and reduce the side effects of cancer chemotherapy. PEGylated pH-sensitive liposomes (pPSL) have attracted interest due to their abilities to remain stable at pH 7.4, but exploit the low pH in solid tumors to undergo rapid destabilisation and release their payload into the cytosol. Subsequently, it was conceived that PEG coating, which is responsible for their long circulation, also causes steric hindrance for the cell uptake or intracellular drug release at the target, often called the 'PEG dilemma'. As a result, only a small proportion of the dose reaches the tumor site after administration. In a review of the literature from the past 10 years, only 0.7% of the administered nanoparticle dose is found to be delivered to a solid tumor [274]. This small proportion of intra-tumoral drug delivery may be a major cause for reducing the clinical significance of pPSL.

To overcome the limitations of pPSL, and the PEG dilemma in particular, this PhD research aimed to design and investigate a combinational strategy, including pH-responsive liposomes (pH-sensitive liposomal system based on the fusogenic DOPE) and PEG detachment (achieving PEG detachment at the target using an acid sensitive hydrazone bond), which exploits the features of solid tumors (low pH and leaky vasculature) to achieve tumor-targeted, enhanced intracellularly drug delivery. Smart PEG-cleavable pH-sensitive liposomes, CL-pPSL, were developed with this combinational strategy.

We hypothesized that CL-pPSL would confer better tumor targeting to the drugs via the desired ‘EPR’ effect (‘passive’ targeting) and thereby reduce toxic side effects. Once in the ‘acidified’ milieu of the tumor microenvironment, these carriers were expected to detach their PEG coating through the hydrolysis of a pH-sensitive hydrazone bond, which could enhance cytoplasmic delivery via both enhanced cellular uptake and endosome escape due to the fusogenic properties of DOPE, and consequently increase the cytotoxicity.

To achieve the aims, we took a systematic approach to the research and development of CL-pPSL, taking into account the importance of understanding polymer design, formulation and biological factors, *in vitro* and *in vivo*. Gemcitabine, a first-line chemotherapeutic for pancreatic cancer, was chosen as the model drug in this study.

### **6.1.1 PEG<sub>B</sub>-Hz-CHEMS polymer design and synthesis**

As outlined in Chapter 3, we designed a PEG-based cleavable polymer, PEG<sub>B</sub>-Hz-CHEMS, by linking a PEG chain of molecular weight 2000 to the acyl (lipids) moiety through a linker. The acyl groups act as anchors embedded in the liposome bilayer, while the PEG chains localize towards the aqueous environment. PEGs of molecular weight 2000 were chosen in this study because of their better stealth abilities (as reported in the literature) [264]. Also, because the choice of linker significantly impacts the pH-sensitivity of the polymer, a hydrazone bond was

chosen among the various available acid labile bonds because of its stability at physiological pH while undergoing rapid hydrolysis at acidic pH. Cholesteryl hemisuccinate (CHEMS) was chosen as the lipid anchor because the presence of excess cholesterol enhances the hydration of the lipid head group [275], stabilizes the membrane, and improves the retention of hydrophilic drugs like gemcitabine. We identified the successful synthesis of PEG<sub>B</sub>-Hz-CHEMS via the reductive amination of Schiff's base between PEG<sub>B</sub> and CHEMS-hydrazide by <sup>1</sup>H NMR and mass spectrometry.

The pH-sensitivity and degradation pathways of the polymer was characterized by a validated stability-indicating HPLC-UV method. Results showed that after 1 h incubation at 37 °C, the PEG detachment was determined as 80%, 50%, and <5% at pH 5.5, pH 6.5, and pH 7.4 respectively (Figure 3-3). The polymer was relatively stable at pH 7.4 with a half-life of 24 h. PEG detachment of the polymer was through the cleavage of either the hydrazide or hydrazone bond depending on pH (Figure 3-4).

One of the major challenges encountered with the design and development of the PEG<sub>B</sub>-Hz-CHEMS was the shorter half-life of the polymer at pH 7.4. Further investigation into pH-dependent polymer degradation revealed that this was due to the rapid hydrolysis of the hydrazide bond of CHEMS. Hydrazone bond hydrolysis was faster at endosomal pH 5.0-5.5, and was therefore assumed to contribute to the rapid endosome escape of the liposomes, which was investigated further in relation to the surface-modification of liposomes (discussed in Chapter 4).

### **6.1.2 Phospholipid composition**

We chose a pH-sensitive liposome (pSL) composed of DOPE/CHEMS as the lipid back bone because of their pH-sensitive and fusogenic potential. Cholesterol was also included as it makes an important contribution in membrane organisation and fluidity by filling in free space formed

by the phospholipids and reducing their rotational freedom [275]. We learned that including DSPC phospholipid with a high phase transition temperature further enhances the strength of the lipid bilayer, preventing drug leakage. However, the ratio of DSPC was limited to 2 mol%, as increasing it could affect the membrane properties, such as thickness and rigidity, which might further affect the insertion efficiency of PEG polymers. We used a lipid composition of 4:2:2:2 because the previous studies carried out in our research group showed that this composition has better pH-sensitivity at acidic pH, without affecting the membrane stability at pH 7.4 [236]. Blank non-PEGylated liposomes were surface modified with the synthesized PEG<sub>B</sub>-Hz-CHEMS polymer to form CL-pPSL<sub>1</sub>. The challenges encountered in the formation of the CL-pPSL<sub>1</sub> and their subsequent characterization is discussed in Chapter 4.

### 6.1.3 Formulation development of CL-pPSL<sub>1</sub>

Overcoming the poor insertion efficiency of this polymer into pH-sensitive liposomes (due to its lower CMC, which facilitated rapid micelle formation) was the major challenge in the formulation process. The thermodynamic barrier to insertion into the liposome bilayers is higher for micellar PEG-lipids compared to monomeric PEG-lipids. Therefore, significant efforts were made to investigate the factors that might affect the insertion efficiency of the polymer, including liposome hydration temperature (30 and 45 °C), PEG polymer concentration (3, 5 and 10 mol%) and incubation time (8 and 24 h). Pre and post insertion techniques for polymer insertion were compared.

We found that the concentration gradient and incubation time had a major influence, which was later used as the determining factor to promote the insertion efficiency of the polymer into our liposomes. A higher concentration of polymer as 5 mol% and a longer incubation time of 24 h achieved a higher PEG density of 1.7 mol% on the surface of the liposomes, close to the minimum PEG coating (0.5 mol%) required for *in vivo* long circulation of the liposomes. In

addition, a further increase in the polymer concentrations, such as 10 mol% on the bilayer surface, showed up the reduction in the size of the liposomes. This could be due to a sharp reduction in the packing parameter of the polymer with an increase in its concentration, favouring the formation of only micelles rather than lipid vesicles.

### **6.1.4 Characterization of CL-pPSL<sub>1</sub>**

Following the optimisation of the formulation and polymer insertion efficiency, our liposomes were loaded with gemcitabine using a small volume incubation technique. Our previous research found that sufficient drug loading (drug to lipid ratio) is a crucial factor for the anti-tumor efficacy of gemcitabine [276]. Therefore, in this method, the concentration gradient was used as driving force to achieve a maximum drug loading of 4%, which is sufficient to achieve the target therapeutic dosage of 16 mg/kg for biodistribution studies. Future studies should look at further enhancing the gemcitabine loading of liposomes by chemical conjugation or active loading techniques.

Due to their nano size of  $144.8 \pm 0.1$  nm, the designed CL-pPSL are more likely to utilise the leaky vasculature of the tumor tissue and accumulate in tumors by passive targeting mechanisms. However, there have been recent debates about the existence and applicability of the EPR effect in tumor targeting. The literature also emphasizes that the EPR effect might differs between tumor xenografts implanted at the same site [277] or it might even be completely absent in human tumors [278]. In addition, animal models don't represent the human situation, which reflects the heterogenous nature of the EPR effect [279]. Therefore, future clinical applications of these liposomal systems need a thorough systematic investigation to confirm the existence of the EPR effect.

We employed a confocal microscopy technique to investigate the mechanisms of cellular uptake and the kinetics of endosome escape, as our previous studies showed that clathrin-mediated

endocytosis is the predominant mechanism of endocytosis for the pH-sensitive liposomes. The cellular uptake of the two liposomes, CL-pPSL and pPSL, in Mia PaCa-2 cells was assessed by quantitatively measuring the intracellular drug concentrations with HPLC under the condition of pH 7.4. CL-pPSL showed a 2.3-times higher intracellular drug concentration compared to those treated with pPSL and a 3-times higher concentration than the free drug solution (Table 4-3). However, because we were unable to develop sensitive quantification methods, the metabolites of gemcitabine were not measured. The cytotoxicity of gemcitabine-loaded CL-pPSL (52.4 nM) on Mia PaCa-2 cells were found to be 1.5-times higher than pPSL (79.5 nM) (Table 4-4). The likely mechanisms for the increase in cell uptake and cytotoxicity of CL-pPSL compared to pPSL, was their PEG-cleavable ability and the fusogenic properties of DOPE, which promote endocytosis at extracellular low pH and endosome escape respectively [72, 280]. Confocal microscopy further supported these results, showing that PEG<sub>B</sub>-Hz-CHEMS substantially improved the endosome escape abilities (Figure 4-7) compared to pPSL.

Despite their enhanced cell uptake, endosome escape and cytotoxicity potentials, the major limitation for the PEG<sub>B</sub>-Hz-CHEMS was their shorter circulation half-life and rapid clearance rates. Pharmacokinetics results showed a 2-times lower AUC and shorter  $T_{1/2}$  (Figure 4-8), and the biodistribution data showed a higher accumulation in the liver after 12h for PEG<sub>B</sub>-Hz-CHEMS compared to pPSL (Appendix 6). We speculated that this rapid clearance of PEG<sub>B</sub>-Hz-CHEMS could be due to two reasons. The first is the short half-life of the polymer due to hydrazide bond hydrolysis at physiological pH, and the second is its lower insertion efficiency into liposomes resulting in lower PEG coverage. Lower insertion efficiency was found to be due to the amphiphilic nature of the polymer, which reduced its CMC. Furthermore, we speculated that the conformational flexibility of PEG will also reduce due to the deeper location of the cholesterol anchor in the liposome membrane. This deeper presence of the PEG chain

further causes the polymer to perturb the lipid bilayer, resulting in relatively rapid release of entrapped drugs leading to lower AUC.

### **6.1.5 Design and development of PEG<sub>B</sub>-Hz-DPPE modified liposomes, CL-pPSL<sub>2</sub>**

As pointed out in 6.1.4, the major limitation with the PEG<sub>B</sub>-Hz-CHEMS polymer is its poor *in vivo* pharmacokinetics and rapid clearance. To overcome this limitation, which is assumed to be due to its lipid anchor CHEMS, a second polymer, PEG<sub>B</sub>-Hz-DPPE, was designed by replacing the lipid anchor to the phospholipid group (DPPE). A hydrocarbon chain EMCH was also used to activate the phospholipid, which further helped to extend PEG to the outside of the liposome surface. The synthesis and characterization of these liposomes are discussed fully in Chapter 5 above.

The polymer was successfully synthesized and characterized by <sup>1</sup>HNMR. However, another limitation for this polymer is the unavailability of proper quantification methods for their characterization. Therefore, the kinetics of the pH sensitive PEG detachment and polymer insertion efficiency into liposomes was monitored using DLS and fluorescence techniques instead. PEG<sub>B</sub>-Hz-DPPE polymeric micelles showed a rapid shift in their size at endosomal pH 5.0, while remaining stable at pH 7.4 (Figure 5-3A). Based on these findings we speculated that the stability of PEG<sub>B</sub>-Hz-DPPE at pH 7.4, was higher than the PEG<sub>B</sub>-Hz-CHEMS. This is much better compared to the previous studies by Torchillin et al, where synthesized cleavable polymers, derived from aromatic aldehydes, were found to be stabilized at acidic pH 5.5 (a half-life of 48 h) [146], and the cleavable polymer-coated liposomes developed by Chen et al., which showed a higher accumulation in the liver and spleen compared to the conventional liposomes [159]. The balance between acid lability and stability at physiological pH was therefore found to be better for this PEG<sub>B</sub>-Hz-DPPE polymer in our study.

## Chapter 6

Among all the systems developed in this thesis, PEG<sub>B</sub>-Hz-DPPE modified liposomes were the most desirable formulation to enhance the cell uptake and endosome escape abilities of pPSL without compromising their long circulation. We employed confocal microscopy and live cell imaging to illustrate the mechanisms of cellular processing, including cell membrane binding, internalisation and endosome escape. Both confocal microscopy and live cell imaging showed the PEG<sub>B</sub>-Hz-DPPE coated CL-pPSL had substantially improved the cellular uptake and endosome escape compared to pPSL (Figure 5-6). Indeed, we observed that pPSL may be entrapped in the endosomes, limiting the drug cytotoxicity due to its subsequent degradation in lysosomes.

This is perhaps the first study to determine the pathways of endocytosis for both pPSL and CL-pPSL [267]. Live cell imaging showed the transition of the liposomes as they were entrapped in the lysosomes (green fluorescence), to fusion with lysosomal membrane (yellow fluorescence), to content release (red fluorescence), supporting the hypothesis that it was achieved by the fusion mechanism [268] and that the CL-pPSL rapidly escaped from the endosome-lysosome compared to the conventional pPSL (Figure 5-9). Our findings correlated with previous studies, which demonstrated that dioleoylphosphatidylethanolamine (DOPE) readily fuses with the endocytic vesicles and rapidly releases its contents into cytoplasm due to its fusogenic potential [281]. Cytotoxicity studies further confirmed all these results with confocal imaging, by showing that gemcitabine-loaded CL-pPSL has a 2-times better cytotoxic potential than pPSL.

These new PEG<sub>B</sub>-Hz-DPPE coated liposomes showed similar long circulation half-life, clearance and volume of distribution as pPSL, indicating that its cleavable PEGylation property does not compromise its *in vivo* stealth abilities (Figure 5-8). We attribute this to three potential improvements in this polymer compared to PEG<sub>B</sub>-Hz-CHEMS: i) the superior abilities

of the PEG<sub>B</sub>-Hz-DPPE to insert into the liposomes, ii) the higher PEG density on the liposomes leading to the formation of a brush configuration and iii) the polymer's superior stability at pH 7.4. Biodistribution studies showed that after 4 h of injection of dosing, the gemcitabine concentration was higher in the CL-pPSL injected group compared to pPSL and the free drug solutions. In addition, accumulation in the heart was much lower for both liposomes compared to the free drug solution, indicating their superior tumor targeting abilities.

The PEG<sub>B</sub>-Hz-DPPE coated liposomes developed with PEG detachment and fusogenic abilities in this study achieved rapid cell uptake, endosome escape and drug-delivery into tumor cells with a higher efficiency compared to the conventional pPSL.

### **6.1.6 Conclusion**

This PhD work emphasizes the usefulness of dual pH-responsive PEG-cleavable strategies for the selective enhanced cytoplasmic delivery of drugs, addressing the major limitation of pPSL: the PEG dilemma. In addition, we believe this is the first time a study has shown the long circulation and pH-responsive tumor targeting abilities of a dual pH-responsive strategy.

Two novel acid-cleavable PEG polymers, developed with the abilities of pH-sensitive PEG liposomes detachment, successfully overcame the limitations of PEG dilemma. However, PEG<sub>B</sub>-Hz-CHEMS showed good pH-sensitivity but a short half-life. By changing the polymer design, the second polymer PEG<sub>B</sub>-Hz-DPPE displayed both a long half-life and pH-sensitivity. The synthesized PEG<sub>B</sub>-Hz-DPPE polymer was also successfully used to modify pH-sensitive DOPE:CHEMS liposomes into dual pH-responsive liposomes, CL-pPSL<sub>2</sub>.

This PhD research demonstrates that: 1) CL-pPSL can improve cytoplasmic drug delivery and is capable of tumor-targeted drug delivery, 2) The delivery of CL-pPSL improves cellular uptake and the endosomal escape abilities of pPSL due to the combination effects of PEG detachment and the fusogenic properties of DOPE. Furthermore, this is the first study to fully

elucidate the endosome escape abilities of a dual pH-responsive liposomes facilitated with PEG-detachment. 3) Our *in vivo* studies show that CL-pPSL<sub>2</sub>, compared with pPSL, displayed an increased tumor accumulation with similar stealth properties.

In summary, the CL-pPSL we developed shows tremendous potential to selectively deliver drugs in low pH regions of tumor cells with high efficiency compared to conventional pPSL. However, future anti-tumor studies are still required to confirm if the enhanced tumor targeting abilities of these cleavable liposomes could result in greater therapeutic potential *in vivo*.

## 6.2 Future directions

Cleavable PEGylation is a hot topic in the field of drug delivery systems which favour vehicles with a long blood circulation time and an efficient phagocytosis by tumor cells. However, the complicated materials synthesis, along with the high cost and problematic reproducibility in manufacturing are limiting its successful translation from bench to bedside. Which is an enormous challenge across the whole novel drug delivery system field. In addition, the road to approving nanotechnology products is also long and tortuous. For the last 20 years, on average, 30 new drugs were approved by the U.S. FDA each year, and only a few liposomal drugs can be found on the approved list [282].

For future studies, a number of potential strategies could be used to improve tumor targeting to enhance the overall antitumor effect, the commercial relevance of CL-pPSL, and its applicability to other anti-cancer drugs, some of these strategies include:

### 6.2.1 Improving the insertion efficiency of PEG<sub>B</sub>-Hz-CHEMS into liposomes

PEG<sub>B</sub>-Hz-CHEMS modified liposomes showed a poor circulation half-life and lower AUC *in vivo*, however they showed enhanced pH-sensitivity at mild acidic pH 6.5, due to the presence of the dual bonds, hydrazide and hydrazone. Future studies could improve the insertion

efficiency of the polymer into liposomes by redesigning its structure, adding lipophilic chains in between CHEMS and hydrazine, for example. This would reduce the CMC of the polymer and increase its insertion efficiency into the liposomes.

### **6.2.2 Quantification of the PEG detachment of PEG<sub>B</sub>-Hz-DPPE**

The quantification of the PEG-detachment of PEG<sub>B</sub>-Hz-DPPE polymer was not determined in this study, due to the unavailability of a sensitive quantification method. In addition, the kinetics of PEG detachment from the surface of liposomes were not clearly demonstrated. It would be helpful if future studies could quantify the surface PEGylation of PEG<sub>B</sub>-Hz-DPPE modified liposomes, to explore in more detail how cleavable PEG coated liposomes achieve long circulation. Future studies could also look at developing quantification methods for PEG<sub>B</sub>-Hz-DPPE using HPLC with fluorescence or mass spectrometric detection.

### **6.2.3 Formulation improvement**

The current pPSL and CL-pPSL formulation post-drug loadings are in a size range of 145 - 154 nm. However to exploit the EPR effect, a size of approximately 60 – 100 nm is highly recommended [283]. We believe it is essential to further reduce the size of the liposomal membrane without affecting its drug loading.

The stability of the formulation should be investigated to improve the potential for the commercial application of CL-pPSL. We found that the physicochemical stability of CL-pPSL and pPSL showed no significant increases in particle size, size distribution and drug leakage within 1 month. To increase stability, studies of the formulation of lyophilisation could be done to extend the shelf-life of liposomal formulations, compared to current pellet or suspension forms.

The drug leakage of gemcitabine is also still an issue. Despite using a high transition temperature lipid as the DSPC, our drug release data shows that about 40% of the transported drug leaked out at pH 7.4. Further studies should look at controlling this with techniques such as the chemical conjugation of gemcitabine with lipids, or by using other active loading techniques.

### **6.2.4 Investigation of anti-tumor efficacy**

CL-pPSL are proven to have better pharmacokinetics and biodistribution, therefore further *in vivo* studies in xenograft tumor models would give a better characterization of their therapeutic efficacy and clinical significance. As a part of our project we attempted to determine the anti-tumor efficacy of gemcitabine-loaded CL-pPSL and pPSL. However, despite our efforts, Mia PaCa-2 tumors were not developed at a 100% frequency in CD-1 nude mice. The potential cause might be that the immune system of the CD-1 nude mice is stronger and therefore not favourable to tumor growth. The anti-tumor efficacy for CL-pPSL was not investigated further in this project, due to time and funding restrictions. Because it is not yet clear if the long circulation, and the enhanced tumor accumulation abilities of PEG<sub>B</sub>-Hz-DPPE modified liposomes would result in enhanced anti-tumor efficacy, it will be of great interest to look for further evidence of its anti-tumor efficacy. We envisage future tumor targeting studies where the mice strain from CD-1 is changed to NIH or NOD Scid, which could result in better tumor development. Furthermore, developing orthotopic tumor mouse models could be considered, as they offer tissue site-specific pathology and are generally deemed more clinically relevant, allowing more productive studies of metastasis [284].

### **6.2.5 Surface ligand modification for tumor penetration abilities**

The cellular uptake of CL-pPSL could be further improved by surface modification of the PEG polymer with specific active targeting ligands, such as hyaluronic acids, transferrin and fucose,

## Chapter 6

which have already shown to be successful for active targeting in previous studies. Recent studies have reported that the modification of the surface of PEG polymer with fusogenic peptides may further enhance their ability to being endocytosed into the cells due to their fusogenicity.

## **7. Appendices**

---

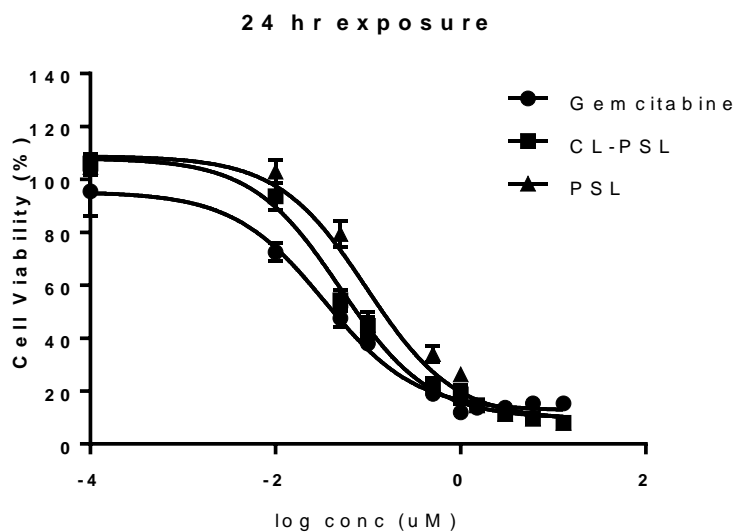
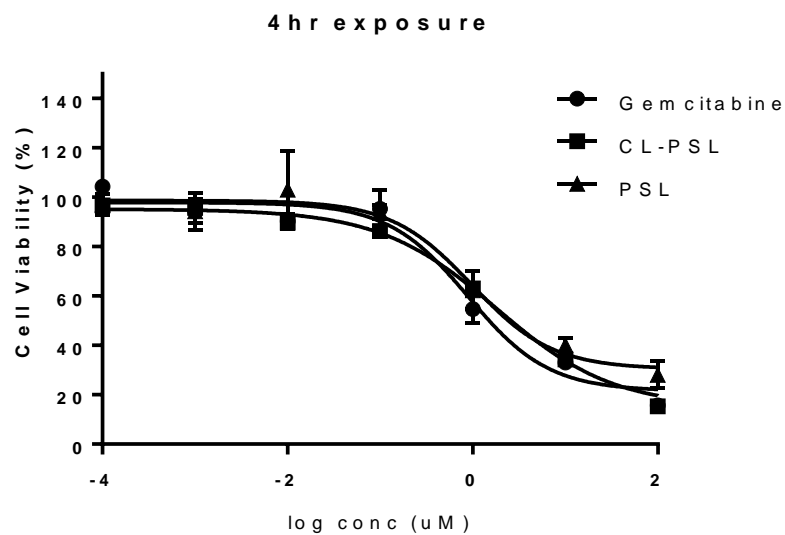
**Appendix 1: Stability-indicating HPLC method development for PEG<sub>B</sub>-HZ-CHEMS**

**A 1.1:** Retentions times of PEG<sub>B</sub>-HZ-CHEMS and PEG<sub>B</sub> with various mobile phases at a flow rate 1 ml/min: predicted values versus experimental data (section 3.4.2).

Water, X <sub>1</sub> (%, v/v)	A/M, X <sub>2</sub> (%, v/v)	Observed R <sub>t</sub> (min)		Predicted R <sub>t</sub> (min)	
		PEG <sub>B</sub> -HZ- CHEMS	PEG <sub>B</sub>	PEG <sub>B</sub> -HZ- CHEMS	PEG <sub>B</sub>
<b>40</b>	3.0	17.00	8.00	16.96	8.02
<b>43</b>	3.1	16.30	7.50	16.29	7.43
<b>45</b>	3.6	15.50	6.80	15.68	6.92
<b>46</b>	5.0	15.00	6.40	14.95	6.36
<b>48</b>	5.5	14.50	5.90	14.35	5.85
<b>49</b>	6.4	13.80	5.40	13.80	5.41
<b>50<sup>a</sup></b>	9.0	11.81	4.93	12.66	4.55

a is the optimum mobile phase subjected for validation in this study.

**Appendix 2:** Cytotoxicity curves of CL-pPSL<sub>1</sub>



A.2.1. Cytotoxicity profiles of Mia PaCa-2 cells treated with free gemcitabine, pPSL and CL-pPSL<sub>1</sub>. Data points are mean  $\pm$  SD, n = 3. Curves are four parameter logistic regressions (section 4.4.7).

**Appendix 3A.** University of Auckland Animal Ethics Committee approval letter for *in vivo* pharmacokinetics study in SD rats.

**UNIVERSITY OF AUCKLAND ANIMAL ETHICS COMMITTEE (AEC)**

08-May-2017

**MEMORANDUM TO:**

Dr Zimei Wu  
Pharmacy

**Application for ethics approval (Our Ref. 001880): Research application approved**

The Committee considered your application for animal ethics approval for your project entitled **Pharmacokinetics of novel liposomal formulations potentially for tumour targeting**. The Committee is pleased to advise you that this application has now been approved for a period of three years.

The approval date is 08-May-2017.

The expiry date is 08-May-2020.

**Conditions of approval**

All deaths which occur prior to the planned end of experiment must be notified to the AEC so that a post mortem may be performed by the Animal Welfare Officer if considered necessary. This includes all animals that are found dead or moribund, or are killed due to abnormalities which make them not fit for purpose.

Please note the requirement of reporting animal use under the Animal Welfare Act 1999. As Responsible Investigator it is your statutory responsibility to provide to this office:

- An annual Animal Usage Return (AUR) for incorporation into the University consolidated return to MPI.
- An End of Approval Report at completion of the project.

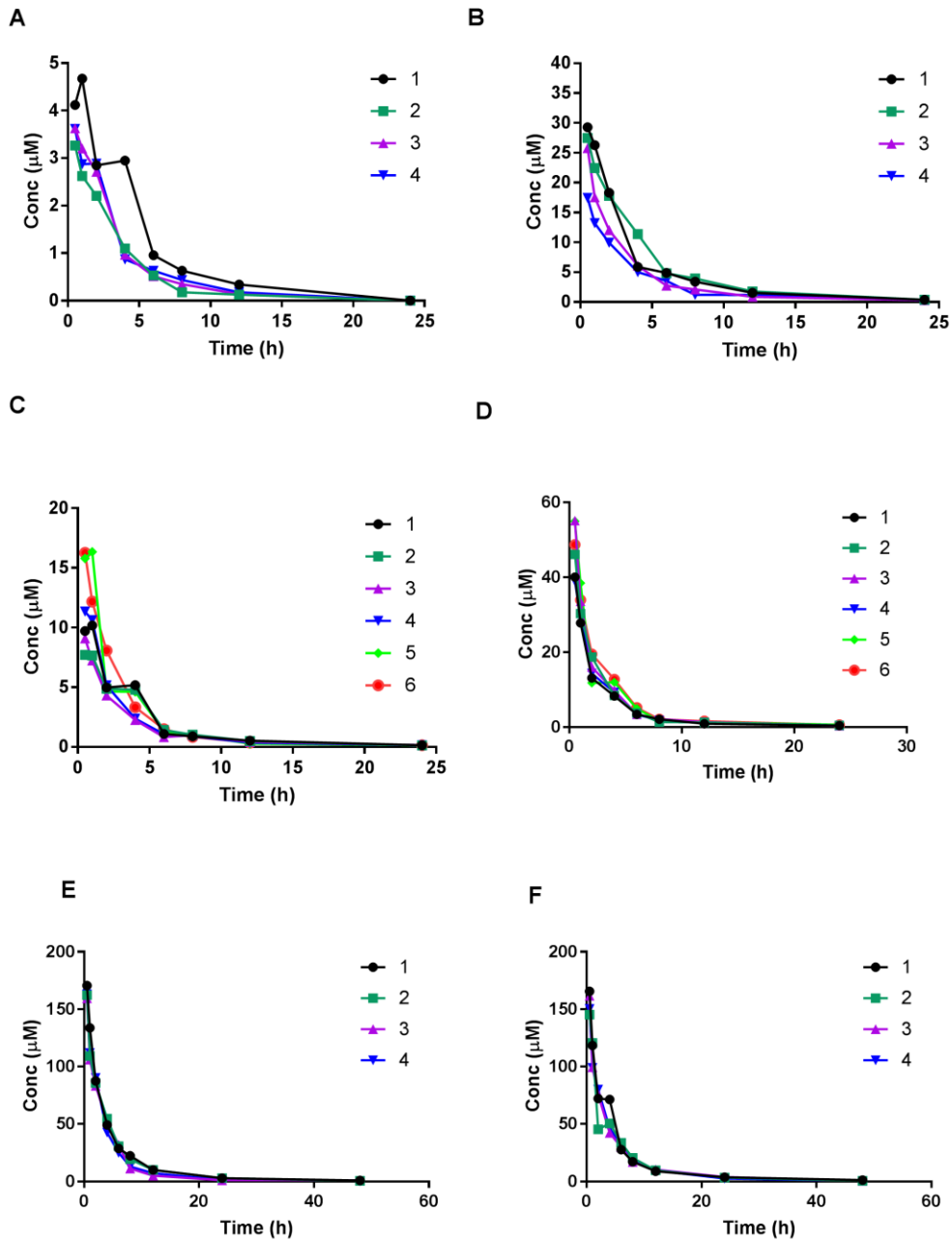
All required forms, general information on the animal ethics procedures, and information on training can be found at [www.auckland.ac.nz/ae](http://www.auckland.ac.nz/ae) or can be provided by the Animal Ethics Administrator on request.

If you have any queries regarding your ethics application or wish to discuss general matters relating to ethics approvals, please contact the Animal Ethics Administrator at [animaethics@auckland.ac.nz](mailto:animaethics@auckland.ac.nz) or +64 9 373 7599 ext 86356.

Please quote reference **001880** for all communication with the AEC regarding this application.

**A.3.1** Letter of approval to undertake *in vivo* pharmacokinetic studies for liposomal formulations of gemcitabine by the University of Auckland Animal Ethics Committee (section 4.4.9 and 5.4.7).

**Appendix 3B.** Individual pharmacokinetic profiles.



**A.3.2** Individual pharmacokinetic profiles of gemcitabine in SD rats following a single i.v. injection of A) free gemcitabine, B) liposomal gemcitabine pPSL, C) CL-pPSL<sub>1</sub> and D) CL-pPSL<sub>2</sub> at a dose of 1 mg/kg and E) CL-pPSL<sub>1</sub> and F) CL-pPSL<sub>2</sub> at a dose of 5 mg/kg (section 4.4.9 and 5.4.7).

**Appendix 4.** University of Auckland Animal Ethics Committee approval letter for *in vivo* tumour targeting study.

**UNIVERSITY OF AUCKLAND ANIMAL ETHICS COMMITTEE**

04-Sep-2015

**MEMORANDUM TO:**

Dr Zimei Wu  
Pharmacy

**Re: Research application approved (Our Ref. 001593)**

The Committee considered your application for animal ethics approval for your project titled **Liposomal delivery systems to improve outcomes of cancer chemotherapy**. The Committee is pleased to advise you that this application has now been approved for a period of three years.

The approval date is 04-Sep-2015.

The expiry date is 04-Sep-2018.

**Conditions of approval**

All deaths which occur prior to the planned end of experiment must be notified to the AEC so that a post mortem may be performed by the Animal Welfare Officer if considered necessary. This includes all animals that are found dead or moribund, or are killed due to abnormalities which make them not fit for purpose.

**Please advise the Animal Welfare Officer, Eddie Dixon, when you are about to start the experiments.**

Please note the requirement regarding the reporting of animal use under the Animal Welfare Act 1999. As Responsible Investigator it is your statutory responsibility to provide to this office:

- Annual Animal Usage figures for incorporation into the University consolidated return to MPI.
- An End of Approval Report along with Final Animal Usage figures for the whole project on completion of the project.

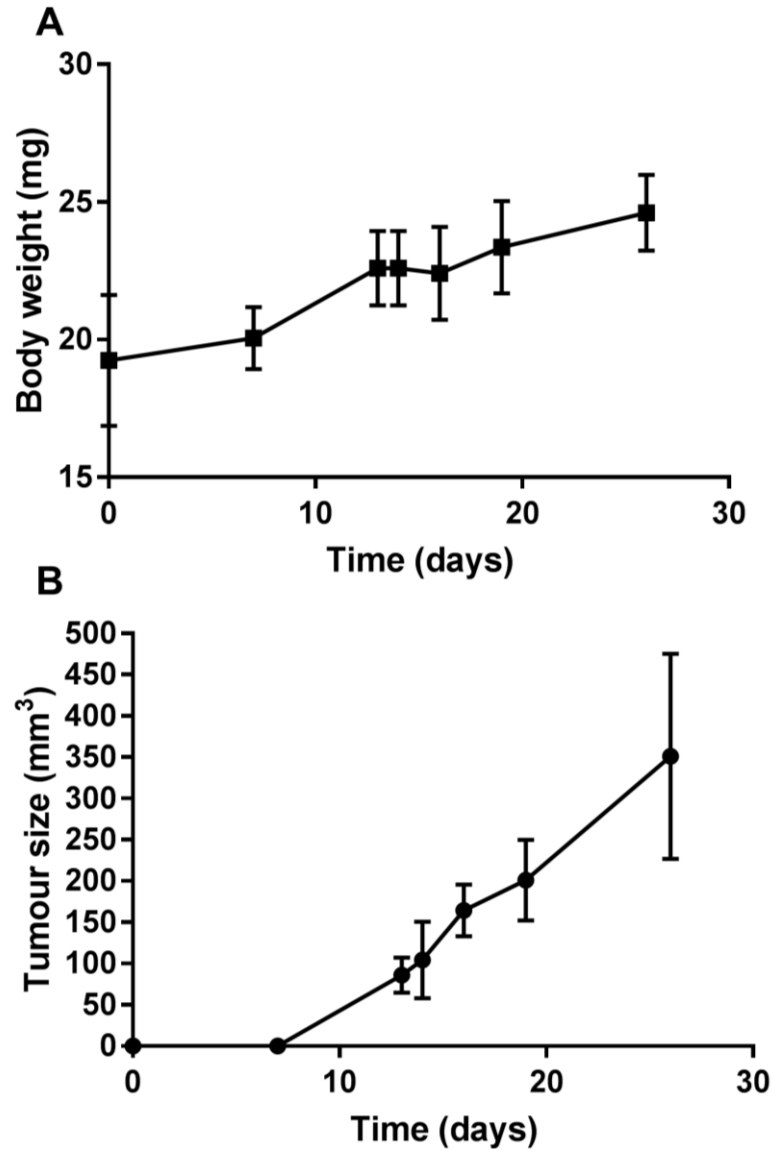
All required forms, general information on the animal ethics procedures, and information on training can be found at [www.auckland.ac.nz/ae](http://www.auckland.ac.nz/ae) or can be provided by the Animal Ethics Administrator on request.

If you have any queries regarding your ethics application or wish to discuss general matters relating to ethics approvals, please contact the Animal Ethics Administrator at [animaethics@auckland.ac.nz](mailto:animaethics@auckland.ac.nz) or +64 9 373 7599 ext 86356.

All communication with the AEC regarding this application should include this reference number: **001593**.

**A4.1** Letter of approval to undertake *in vivo* tumor targeting studies for liposomal formulations of gemcitabine by the University of Auckland Animal Ethics Committee (section 5.4.7).

**Appendix 5.** Pilot tumor growth study in Mia PaCa-2 tumor bearing CD-1 nude mice.



*A5.1.* Data from pilot study showing: A) Body weight and B) Mia PaCa-2 tumour growth in CD-1 nude mice over 25 days (mean  $\pm$  SD, n = 6) (section 5.4.7 and appendix 6).

Appendices

**Appendix 6.** Body weight and tumor growth monitoring of biodistribution studies post tumor inoculation. Tumor bearing mice and non-tumor bearing mice are distributed into 4 treatment groups to study the biodistribution of gemcitabine free drug, pPSL, CL-pPSL<sub>1</sub> and CL-pPSL<sub>2</sub>

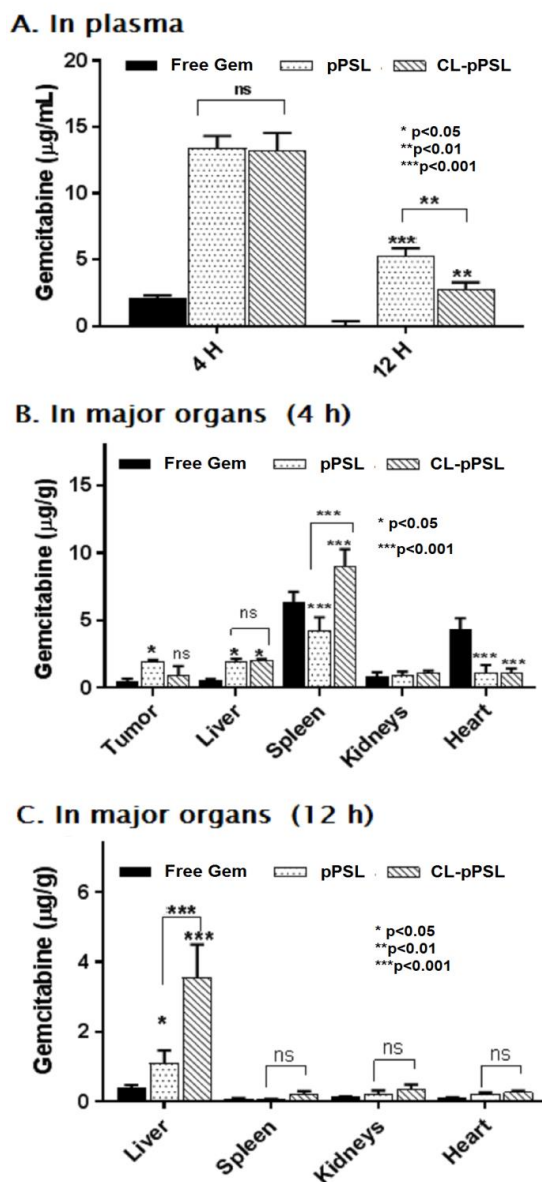
Days after tumor inoculation	0		7		14		21		28		35	
	Body weight (mg)	Tumor volume (mm <sup>3</sup> )	Body weight (mg)	Tumor volume (mm <sup>3</sup> )	Body weight (mg)	Tumor volume (mm <sup>3</sup> )	Body weight (mg)	Tumor volume (mm <sup>3</sup> )	Body weight (mg)	Tumor volume (mm <sup>3</sup> )	Body weight (mg)	Tumor volume (mm <sup>3</sup> )
Cage 1	23.8	-	25.4	-	26.2	150	27.4	180	27.9	234	26.5	284
	22.6	-	23.7	-	24.7	58	25.4	-	26.5	-	27.2	-
	25.0	-	24.6	-	25.2	-	26.5	-	27.2	-	27.5	-
	25.0	-	25.4	-	26.2	-	26.9	-	27.8	-	27.1	-
	20.8	-	22.7	-	22.8	134	23.9	175	25.4	245	24.9	306
	24.1	-	23.1	-	24.1	-	25.7	-	26.5	-	27.4	-
Cage 2	20.9	-	22.4	-	23.8	102	25.1	145	26.5	205	27.3	250
	19.0	-	21.5	-	22.8	-	26.1	-	27.4	-	26.9	-
	21.0	-	22.3	-	21.4	98	24.5	127	25.8	174	27.1	220
	19.8	-	21.4	-	22.7	-	24.5	-	26.1	-	26.9	-
	18.5	-	19.9	-	20.9	-	23.6	-	25.4	-	27.3	-
	19.6	-	21.1	-	23.1	120	25.4	154	26.3	186	27.1	239
Cage 3	22.0	-	22.8	-	23.4	-	24.6	-	25.2	-	27.2	-
	21.9	-	22.5	-	23.9	-	24.5	-	25.6	-	26.5	-
	22.2	-	23.1	-	22.9	109	23.4	156	24.5	210	25.4	234
	21.1	-	22.5	-	23.5	60	25.4	-	26.5	-	27.1	-
	21.3	-	21.9	-	22.4	-	23.6	-	24.9	-	26.2	-
	23.6	-	24.2	-	25.2	120	26.4	180	27.2	234	26.9	271
Cage 4	22.5	-	22.9	-	23.4	-	24.6	-	25.2	-	26.8	-
	22.8	-	23.4	-	23.9	124	24.5	156	26.2	225	27.5	246
	19.7	-	21.6	-	22.6	-	23.2	-	24.8	-	25.9	-
	21.6	-	22.6	-	23.4	79	24.2	-	25.1	-	26.4	-
	19.9	-	21.4	-	22.9	-	23.1	-	24.1	-	25.2	-
	19.6	-	22.6	-	24.9	-	25.8	-	26.8	-	27.5	-

Appendices

**Appendix 7.** Body weight and tumor growth monitoring of biodistribution studies post tumor inoculation. Tumor bearing mice and non-tumor bearing mice are distributed into 4 treatment groups to study the biodistribution of gemcitabine free drug, pPSL, CL-pPSL<sub>1</sub> and CL-pPSL<sub>2</sub>

Days after tumor inoculation	0		7		14		21		28		35	
	Body weight (mg)	Tumor volume (mm <sup>3</sup> )	Body weight (mg)	Tumor volume (mm <sup>3</sup> )	Body weight (mg)	Tumor volume (mm <sup>3</sup> )	Body weight (mg)	Tumor volume (mm <sup>3</sup> )	Body weight (mg)	Tumor volume (mm <sup>3</sup> )	Body weight (mg)	Tumor volume (mm <sup>3</sup> )
Cage 5	22.5	-	22.9	-	23.3	105	24.2	175	26.4	260	27.9	331
	23.3	-	24.2	-	25.6	-	26.8	-	27.2	-	27.9	-
	23.5	-	24.6	-	25.6	-	26.2	-	26.9	-	28.2	-
	21.9	-	23.2	-	24.8	-	25.6	-	26.4	-	27.6	-
	19.9	-	21.6	-	22.4	128	23.6	150	25.4	190	26.8	250
	21.5	-	21.9	-	22.9	-	23.2	-	24.5	-	25.9	-
Cage 6	23.1	-	23.6	-	24.5	-	25.4	-	26.5	-	27.5	-
	21.5	-	22.8	-	23.9	-	24.6	-	25.9	-	26.4	-
	22.7	-	23.5	-	24.2	112	25.3	146	26.4	206	27.2	279
	20.2	-	21.6	-	23.2	-	24.5	-	25.7	-	26.8	-
	21.7	-	22.5	-	23.1	75	24.9	150	26.3	220	27.6	306
	18.8	-	20.8	-	21.9	-	23.2	-	24.5	-	26.2	-
Cage 7	20.8	-	21.9	-	23.1	-	25.3	-	26.5	-	27.0	-
	17.9	-	18.6	-	20.2	-	24.6	-	25.9	-	26.4	-
	21.3	-	22.4	-	24.2	88	25.1	126	26.2	210	27.5	350
	22.1	-	23.5	-	25.1	-	25.4	-	26.8	-	28.1	-
	20.9	-	21.9	-	23.6	-	24.2	-	25.4	-	26.4	-
	--	-	-	-	-	-	-	-	-	-	-	-
Cage 8	21.6	-	22.5	-	23.2	-	24.9	-	26.3	-	27.5	-
	19.9	-	20.5	-	21.6	154	23.6	264	24.8	310	25.9	376
	20.4	-	21.4	-	22.4	-	24.9	-	25.8	-	26.2	-
	21.6	-	22.0	-	23.9	-	25.0	-	26.5	-	27.1	-
	20.9	-	21.6	-	23.5	-	23.5	-	24.7	-	26.2	-
	-	-	-	-	-	-	-	-	-	-	-	-

**Appendix 8.** Biodistribution results of PEG<sub>B</sub>-Hz-CHEMS modified liposomes (CL-pPSL<sub>1</sub> in comparison with pPSL and free drug solution).



**A.8** Biodistribution of gemcitabine in CD-1 nude mice following a single i.v. injection of free gemcitabine, and liposomal gemcitabine (pPSL and CL-pPSL) at a dose of 16 mg/kg, showing concentrations of gemcitabine in plasma (A), and major organs (B and C). Data are mean  $\pm$  SD (n=3). 12 h data is from non-tumor bearing mice. The p values denote comparison with the free drug solution unless specified (Chapter 4).

## References

---

1. Drummond, D.C., M. Zignani, and J. Leroux, *Current status of pH-sensitive liposomes in drug delivery*. Prog Lipid Res, 2000. **39**(5): p. 409-60.
2. Kirpotin, D., K. Hong, N. Mullah, et al., *Liposomes with detachable polymer coating: destabilization and fusion of dioleoylphosphatidylethanolamine vesicles triggered by cleavage of surface-grafted poly(ethylene glycol)*. FEBS Lett, 1996. **388**(2-3): p. 115-8.
3. Sadzuka, Y., *Polyethyleneglycol: a classical but innovative material. Foreword*. Biol Pharm Bull, 2013. **36**(6): p. 877.
4. Fang, Y., J. Xue, S. Gao, et al., *Cleavable PEGylation: a strategy for overcoming the "PEG dilemma" in efficient drug delivery*. Drug Deliv, 2017. **24**(sup1): p. 22-32.
5. Hatakeyama, H., H. Akita, and H. Harashima, *The polyethyleneglycol dilemma: advantage and disadvantage of PEGylation of liposomes for systemic genes and nucleic acids delivery to tumors*. Biol Pharm Bull, 2013. **36**(6): p. 892-9.
6. Sugiyama, T., T. Asai, Y.M. Nedachi, et al., *Enhanced Active Targeting via Cooperative Binding of Ligands on Liposomes to Target Receptors*. PLOS ONE, 2013. **8**(6): p. e67550.
7. Cao, Y., R.A. DePinho, M. Ernst, et al., *Cancer research: past, present and future*. Nat Rev Cancer, 2011. **11**(10): p. 749-754.
8. Rothenberg, M.L., D.P. Carbone, and D.H. Johnson, *Improving the evaluation of new cancer treatments: challenges and opportunities*. Nat Rev Cancer, 2003. **3**(4): p. 303-9.
9. Patel, N.R., B.S. Pattni, A.H. Abouzeid, et al., *Nanopreparations to overcome multidrug resistance in cancer*. Advanced Drug Delivery Reviews, 2013. **65**(13-14): p. 1748-1762.
10. Pathania, D., M. Millard, and N. Neamati, *Opportunities in discovery and delivery of anticancer drugs targeting mitochondria and cancer cell metabolism*. Advanced Drug Delivery Reviews, 2009. **61**(14): p. 1250-1275.

## References

11. Wicki, A., D. Witzigmann, V. Balasubramanian, et al., *Nanomedicine in cancer therapy: challenges, opportunities, and clinical applications*. J Control Release, 2015. **200**: p. 138-57.
12. Jhaveri, A., P. Deshpande, and V. Torchilin, *Stimuli-sensitive nanopreparations for combination cancer therapy*. J Control Release, 2014. **190**: p. 352-70.
13. Kanapathipillai, M., A. Brock, and D.E. Ingber, *Nanoparticle targeting of anti-cancer drugs that alter intracellular signaling or influence the tumor microenvironment*. Adv Drug Deliv Rev, 2014. **79-80**: p. 107-18.
14. Markman, J.L., A. Rekechenetskiy, E. Holler, et al., *Nanomedicine therapeutic approaches to overcome cancer drug resistance*. Advanced Drug Delivery Reviews, 2013. **65**(13-14): p. 1866-1879.
15. Kaasgaard, T. and T. Andresen, *Liposomal cancer therapy: exploiting tumor characteristics*. Expert Opin Drug Deliv., 2010. **7**(2): p. 225-243.
16. Cui, Y., Z. Wu, X. Liu, et al., *Preparation, Safety, Pharmacokinetics and Pharmacodynamics of Liposomes Containing Brucea Javanica Oil*. AAPS PharmSciTech, 2010. **11**(2): p. 878-884.
17. Matsumura, Y. and H. Maeda, *A new concept for macromolecular therapeutics in cancer chemotherapy: Mechanism of tumoritropic accumulation of proteins and the antitumor agent smancs*. Cancer Research, 1986. **46**(12): p. 6387-6392.
18. Fukumura, D., D.G. Duda, L.L. Munn, et al., *Tumor microvasculature and microenvironment: novel insights through intravital imaging in pre-clinical models*. Microcirculation, 2010 **17**(3): p. 206-25.
19. Torchilin, V., *Multifunctional and stimuli-sensitive pharmaceutical nanocarriers*. European Journal of Pharmaceutics & Biopharmaceutics, 2009. **71**(3): p. 431-444.
20. Liu, J., Y. Huang, A. Kumar, et al., *pH-Sensitive nano-systems for drug delivery in cancer therapy*. Biotechnology Advances, 2014. **32**(4): p. 693-710.

## References

21. Torchilin, V., *Nanotechnology for Intracellular Delivery and Targeting*, in *Nanotechnology in Drug Delivery*, M. de Villiers, P. Aramwit, and G. Kwon, Editors. 2009, Springer New York. p. 313-346.
22. Cheng, J., R. Ji, S.-J. Gao, et al., *Facile Synthesis of Acid-Labile Polymers with Pendent Ortho Esters*. *Biomacromolecules*, 2012. **13**(1): p. 173-179.
23. Jiang, T., Y.M. Li, Y. Lv, et al., *Amphiphilic polycarbonate conjugates of doxorubicin with pH-sensitive hydrazone linker for controlled release*. *Colloids Surf B Biointerfaces*, 2013. **111C**: p. 542-548.
24. Moghimi, S.M., A.C. Hunter, and J.C. Murray, *Long-circulating and target-specific nanoparticles: theory to practice*. *Pharmacol Rev*, 2001. **53**(2): p. 283-318.
25. Kierstead, P.H., H. Okochi, V.J. Venditto, et al., *The effect of polymer backbone chemistry on the induction of the accelerated blood clearance in polymer modified liposomes*. *J Control Release*, 2015. **213**: p. 1-9.
26. Zhang, W., G. Wang, E. See, et al., *Post-insertion of poloxamer 188 strengthened liposomal membrane and reduced drug irritancy and in vivo precipitation, superior to PEGylation*. *J Control Release*, 2015. **203**: p. 161-9.
27. Immordino, M.L., F. Dosio, and L. Cattel, *Stealth liposomes: review of the basic science, rationale, and clinical applications, existing and potential*. *Int J Nanomedicine*, 2006. **1**(3): p. 297-315.
28. Felber, A.E., M.-H. Dufresne, and J.-C. Leroux, *pH-sensitive vesicles, polymeric micelles, and nanospheres prepared with polycarboxylates*. *Advanced Drug Delivery Reviews*, 2012. **64**(11): p. 979-992.
29. Fleige, E., M.A. Quadir, and R. Haag, *Stimuli-responsive polymeric nanocarriers for the controlled transport of active compounds: Concepts and applications*. *Advanced Drug Delivery Reviews*, 2012. **64**(9): p. 866-884.
30. Forgac, M., *Vacuolar ATPases: rotary proton pumps in physiology and pathophysiology*. *Nat Rev Mol Cell Biol*, 2007. **8**(11): p. 917-929.

## References

31. Warburg, O., *On respiratory impairment in cancer cells*. Science, 1956. **124**(3215): p. 269-270.
32. Wike-Hooley, J.L., J. Haveman, and H.S. Reinhold, *The relevance of tumour pH to the treatment of malignant disease*. Radiotherapy & Oncology, 1984. **2**(4): p. 343-66.
33. Vaupel, P., F. Kallinowski, and P. Okunieff, *Blood flow, oxygen and nutrient supply, and metabolic microenvironment of human tumors: a review*. Cancer Res, 1989. **49**(23): p. 6449-65.
34. Denny, W.A. and W.R. Wilson, *Considerations for the design of nitrophenyl mustards as agents with selective toxicity for hypoxic tumor cells*. J Med Chem, 1986. **29**(6): p. 879-87.
35. Griffiths, J.R., *Are cancer cells acidic?* Br J Cancer, 1991. **64**(3): p. 425-7.
36. Gillies, R.J., N. Raghunand, G.S. Karczmar, et al., *MRI of the tumor microenvironment*. J Magn Reson Imaging, 2002. **16**(4): p. 430-50.
37. Madshus, I.H., *Regulation of intracellular pH in eukaryotic cells*. Biochem J, 1988. **250**(1): p. 1-8.
38. Cardone, R.A., V. Casavola, and S.J. Reshkin, *The role of disturbed pH dynamics and the Na<sup>+</sup>/H<sup>+</sup> exchanger in metastasis*. Nat Rev Cancer, 2005. **5**(10): p. 786-95.
39. Pouyssegur, J., F. Dayan, and N.M. Mazure, *Hypoxia signalling in cancer and approaches to enforce tumour regression*. Nature, 2006. **441**(7092): p. 437-43.
40. Parks, S.K., J. Chiche, and J. Pouyssegur, *Disrupting proton dynamics and energy metabolism for cancer therapy*. Nat Rev Cancer, 2013. **13**(9): p. 611-23.
41. Helmlinger, G., F. Yuan, M. Dellian, et al., *Interstitial pH and pO<sub>2</sub> gradients in solid tumors in vivo: high-resolution measurements reveal a lack of correlation*. Nat Med, 1997. **3**(2): p. 177-82.
42. Liu, X. and G. Huang, *Formation strategies, mechanism of intracellular delivery and potential clinical applications of pH-sensitive liposomes*. Asian Journal of Pharmaceutical Sciences, 2013. **8**(6): p. 319-328.

## References

43. Danhier, F., O. Feron, and V. Préat, *To exploit the tumor microenvironment: Passive and active tumor targeting of nanocarriers for anti-cancer drug delivery*. Journal of Controlled Release, 2010. **148**(2): p. 135-146.
44. Onaca, O., R. Enea, D.W. Hughes, et al., *Stimuli-responsive polymersomes as nanocarriers for drug and gene delivery*. Macromol Biosci, 2009. **9**(2): p. 129-39.
45. Photos, P.J., L. Bacakova, B. Discher, et al., *Polymer vesicles in vivo: correlations with PEG molecular weight*. Journal of Controlled Release, 2003. **90**(3): p. 323-334.
46. Bellocq, N.C., S.H. Pun, G.S. Jensen, et al., *Transferrin-Containing, Cyclodextrin Polymer-Based Particles for Tumor-Targeted Gene Delivery*. Bioconjugate Chemistry, 2003. **14**(6): p. 1122-1132.
47. Li, Z., L. Qiu, Q. Chen, et al., *pH-sensitive nanoparticles of poly(L-histidine)-poly(lactide-co-glycolide)-tocopheryl polyethylene glycol succinate for anti-tumor drug delivery*. Acta Biomater, 2015. **11**: p. 137-50.
48. Ding, Y., D. Sun, G.L. Wang, et al., *An efficient PEGylated liposomal nanocarrier containing cell-penetrating peptide and pH-sensitive hydrazone bond for enhancing tumor-targeted drug delivery*. Int J Nanomedicine, 2015. **10**: p. 6199-214.
49. Yin, Q., J. Shen, Z. Zhang, et al., *Reversal of multidrug resistance by stimuli-responsive drug delivery systems for therapy of tumor*. Advanced Drug Delivery Reviews, 2013. **65**(13-14): p. 1699-1715.
50. Ganta, S., H. Devalapally, A. Shahiwala, et al., *A review of stimuli-responsive nanocarriers for drug and gene delivery*. Journal of Controlled Release, 2008. **126**(3): p. 187-204.
51. Deng, H., J. Liu, X. Zhao, et al., *PEG-b-PCL copolymer micelles with the ability of pH-controlled negative-to-positive charge reversal for intracellular delivery of doxorubicin*. Biomacromolecules, 2014. **15**(11): p. 4281-92.
52. Zhao, X., P. Liu, Q. Song, et al., *Surface charge-reversible polyelectrolyte complex nanoparticles for hepatoma-targeting delivery of doxorubicin*. Journal of Materials Chemistry B, 2015. **3**(30): p. 6185-6193.

## References

53. Xu, J.X., J.B. Tang, L.H. Zhao, et al., [*Advances in the study of tumor pH-responsive polymeric micelles for cancer drug targeting delivery*]. Yao Xue Xue Bao, 2009. **44**(12): p. 1328-35.
54. Liu, J., Y. Huang, A. Kumar, et al., *pH-sensitive nano-systems for drug delivery in cancer therapy*. Biotechnol Adv, 2014. **32**(4): p. 693-710.
55. Hatakeyama, H., E. Ito, H. Akita, et al., *A pH-sensitive fusogenic peptide facilitates endosomal escape and greatly enhances the gene silencing of siRNA-containing nanoparticles in vitro and in vivo*. Journal of Controlled Release, 2009. **139**(2): p. 127-132.
56. Remaut, K., B. Lucas, K. Braeckmans, et al., *Pegylation of liposomes favours the endosomal degradation of the delivered phosphodiester oligonucleotides*. Journal of Controlled Release, 2007. **117**(2): p. 256-266.
57. Li, Y., R. Liu, J. Yang, et al., *Enhanced retention and anti-tumor efficacy of liposomes by changing their cellular uptake and pharmacokinetics behavior*. Biomaterials, 2015. **41**: p. 1-14.
58. Gao, Z., L. Zhang, and Y. Sun, *Nanotechnology applied to overcome tumor drug resistance*. Journal of Controlled Release, 2012. **162**(1): p. 45-55.
59. Ichihara, M., T. Shimizu, A. Imoto, et al., *Anti-PEG IgM Response against PEGylated Liposomes in Mice and Rats*. Pharmaceutics, 2011. **3**(1): p. 1-11.
60. Yang, Q., Y. Ma, Y. Zhao, et al., *Accelerated drug release and clearance of PEGylated epirubicin liposomes following repeated injections: a new challenge for sequential low-dose chemotherapy*. Int J Nanomedicine, 2013. **8**: p. 1257-68.
61. Ishida, T. and H. Kiwada, *Accelerated blood clearance (ABC) phenomenon upon repeated injection of PEGylated liposomes*. Int J Pharm, 2008. **354**(1-2): p. 56-62.
62. Ma, H., K. Shiraishi, T. Minowa, et al., *Accelerated Blood Clearance Was Not Induced for a Gadolinium-Containing PEG-poly(L-lysine)-Based Polymeric Micelle in Mice*. Pharmaceutical Research, 2010. **27**(2): p. 296-302.

## References

63. van den Hoven, J.M., R. Nemes, J.M. Metselaar, et al., *Complement activation by PEGylated liposomes containing prednisolone*. Eur J Pharm Sci, 2013. **49**(2): p. 265-71.
64. Moein Moghimi, S., I. Hamad, R. Bunger, et al., *Activation of the human complement system by cholesterol-rich and PEGylated liposomes-modulation of cholesterol-rich liposome-mediated complement activation by elevated serum LDL and HDL levels*. J Liposome Res, 2006. **16**(3): p. 167-74.
65. Moghimi, S.M. and J. Szebeni, *Stealth liposomes and long circulating nanoparticles: critical issues in pharmacokinetics, opsonization and protein-binding properties*. Prog Lipid Res, 2003. **42**(6): p. 463-78.
66. Moghimi, S.M., *Chemical camouflage of nanospheres with a poorly reactive surface: towards development of stealth and target-specific nanocarriers*. Biochimica et Biophysica Acta (BBA) - Molecular Cell Research, 2002. **1590**(1-3): p. 131-139.
67. Hamad, I., O. Al-Hanbali, A.C. Hunter, et al., *Distinct Polymer Architecture Mediates Switching of Complement Activation Pathways at the Nanosphere-Serum Interface: Implications for Stealth Nanoparticle Engineering*. ACS Nano, 2010. **4**(11): p. 6629-6638.
68. Moghimi, S.M., A.J. Andersen, D. Ahmadvand, et al., *Material properties in complement activation*. Advanced Drug Delivery Reviews, 2011. **63**(12): p. 1000-1007.
69. Jager, E., A. Jager, T. Etrych, et al., *Self-assembly of biodegradable copolyester and reactive HPMA-based polymers into nanoparticles as an alternative stealth drug delivery system*. Soft Matter, 2012. **8**(37): p. 9563-9575.
70. Grainger, S.J. and M.E. El-Sayed, *Stimuli-sensitive particles for drug delivery*. Biologically-Responsive Hybrid Biomaterials, 2010: p. 171-190.
71. Reyes-Ortega, F., *3 - pH-responsive polymers: properties, synthesis and applications*, in *Smart Polymers and their Applications*, M.R. Aguilar and J.S. Román, Editors. 2014, Woodhead Publishing. p. 45-92.

## References

72. Simões, S., V. Slepishkin, N. Düzgünes, et al., *On the mechanisms of internalization and intracellular delivery mediated by pH-sensitive liposomes*. *Biochimica et Biophysica Acta (BBA) - Biomembranes*, 2001. **1515**(1): p. 23-37.
73. Wang, L., G. Liu, X. Wang, et al., *Acid-Disintegratable Polymersomes of pH-Responsive Amphiphilic Diblock Copolymers for Intracellular Drug Delivery*. *Macromolecules*, 2015. **48**(19): p. 7262-7272.
74. Etrych, T., M. Jelinkova, B. Rihova, et al., *New HPMA copolymers containing doxorubicin bound via pH-sensitive linkage: synthesis and preliminary in vitro and in vivo biological properties*. *J Control Release*, 2001. **73**(1): p. 89-102.
75. Fei, L., L.-P. Yap, P.S. Conti, et al., *Tumor targeting of a cell penetrating peptide by fusing with a pH-sensitive histidine-glutamate co-oligopeptide*. *Biomaterials*, 2014. **35**(13): p. 4082-4087.
76. Kang, X.-J., Y.-L. Dai, P.-A. Ma, et al., *Poly(acrylic acid)-Modified Fe<sub>3</sub>O<sub>4</sub> Microspheres for Magnetic-Targeted and pH-Triggered Anticancer Drug Delivery*. *Chemistry – A European Journal*, 2012. **18**(49): p. 15676-15682.
77. Ding, D., J. Wang, Z. Zhu, et al., *Tumor Accumulation, Penetration, and Antitumor Response of Cisplatin-Loaded Gelatin/Poly(acrylic acid) Nanoparticles*. *ACS Applied Materials & Interfaces*, 2012. **4**(3): p. 1838-1846.
78. Yan, X. and R.A. Gemeinhart, *Cisplatin delivery from poly(acrylic acid-co-methyl methacrylate) microparticles*. *Journal of Controlled Release*, 2005. **106**(1–2): p. 198-208.
79. Bersani, S., M. Vila-Caballer, C. Brazzale, et al., *pH-sensitive stearyl-PEG-poly(methacryloyl sulfadimethoxine) decorated liposomes for the delivery of gemcitabine to cancer cells*. *European Journal of Pharmaceutics & Biopharmaceutics*, 2014. **88**(3): p. 670-682.
80. Schmaljohann, D., *Thermo- and pH-responsive polymers in drug delivery*. *Advanced Drug Delivery Reviews*, 2006. **58**(15): p. 1655-1670.

## References

81. Shalviri, A., G. Raval, P. Prasad, et al., *pH-Dependent doxorubicin release from terpolymer of starch, polymethacrylic acid and polysorbate 80 nanoparticles for overcoming multi-drug resistance in human breast cancer cells*. European Journal of Pharmaceutics & Biopharmaceutics, 2012. **82**(3): p. 587-97.
82. Hamaguchi, T., Y. Matsumura, M. Suzuki, et al., *NK105, a paclitaxel-incorporating micellar nanoparticle formulation, can extend in vivo antitumour activity and reduce the neurotoxicity of paclitaxel*. Br J Cancer, 2005. **92**(7): p. 1240-6.
83. Kato, K., K. Chin, T. Yoshikawa, et al., *Phase II study of NK105, a paclitaxel-incorporating micellar nanoparticle, for previously treated advanced or recurrent gastric cancer*. Invest New Drugs, 2012. **30**(4): p. 1621-7.
84. Matsumura, Y., *The drug discovery by nanomedicine and its clinical experience*. Jpn J Clin Oncol, 2014. **44**(6): p. 515-25.
85. Park, S.Y. and Y.H. Bae, *Novel pH-sensitive polymers containing sulfonamide groups*. Macromolecular Rapid Communications, 1999. **20**(5): p. 269-273.
86. Sethuraman, V.A., M.C. Lee, and Y.H. Bae, *A biodegradable pH-sensitive micelle system for targeting acidic solid tumors*. Pharm Res, 2008. **25**(3): p. 657-66.
87. Ravazzolo, E., S. Salmaso, F. Mastrotto, et al., *pH-responsive lipid core micelles for tumour targeting*. European Journal of Pharmaceutics & Biopharmaceutics, 2013. **83**(3): p. 346-357.
88. Taghizadeh, B., S. Taranejoo, S.A. Monemian, et al., *Classification of stimuli-responsive polymers as anticancer drug delivery systems*. Drug Delivery, 2014: p. 1-11.
89. Verbaan, F.J., P.K. Klouwenberg, J.H.v. Steenis, et al., *Application of poly(2-(dimethylamino)ethyl methacrylate)-based polyplexes for gene transfer into human ovarian carcinoma cells*. International Journal of Pharmaceutics, 2005. **304**(1-2): p. 185-192.
90. Chang, G., C. Li, W. Lu, et al., *N-Boc-histidine-capped PLGA-PEG-PLGA as a smart polymer for drug delivery sensitive to tumor extracellular pH*. Macromol Biosci, 2010. **10**(10): p. 1248-56.

## References

91. Na, K., E.S. Lee, and Y.H. Bae, *Self-Organized Nanogels Responding to Tumor Extracellular pH: pH-Dependent Drug Release and in Vitro Cytotoxicity against MCF-7 Cells*. *Bioconjugate Chemistry*, 2007. **18**(5): p. 1568-1574.
92. Johnson, R.P., Y.I. Jeong, J.V. John, et al., *Dual Stimuli-Responsive Poly(*N*-isopropylacrylamide)-*b*-poly(*l*-histidine) Chimeric Materials for the Controlled Delivery of Doxorubicin into Liver Carcinoma*. *Biomacromolecules*, 2013. **14**(5): p. 1434-1443.
93. Hong, W., D. Chen, L. Jia, et al., *Thermo- and pH-responsive copolymers based on PLGA-PEG-PLGA and poly(*L*-histidine): synthesis and in vitro characterization of copolymer micelles*. *Acta Biomater*, 2014. **10**(3): p. 1259-71.
94. Lee, E.S., H.J. Shin, K. Na, et al., *Poly(*L*-histidine)-PEG block copolymer micelles and pH-induced destabilization*. *Journal of Controlled Release*, 2003. **90**(3): p. 363-374.
95. Wang, C.Y. and L. Huang, *Polyhistidine mediates an acid-dependent fusion of negatively charged liposomes*. *Biochemistry*, 1984. **23**(19): p. 4409-16.
96. Yang, S.R., H.J. Lee, and J.-D. Kim, *Histidine-conjugated poly(amino acid) derivatives for the novel endosomolytic delivery carrier of doxorubicin*. *Journal of Controlled Release*, 2006. **114**(1): p. 60-68.
97. Hu, J., S. Miura, K. Na, et al., *pH-responsive and charge shielded cationic micelle of poly(*l*-histidine)-block-short branched PEI for acidic cancer treatment*. *Journal of Controlled Release*, 2013. **172**(1): p. 69-76.
98. Yin, H., E.S. Lee, D. Kim, et al., *Physicochemical characteristics of pH-sensitive poly(*l*-Histidine)-*b*-poly(ethylene glycol)/poly(*l*-Lactide)-*b*-poly(ethylene glycol) mixed micelles*. *Journal of Controlled Release*, 2008. **126**(2): p. 130-138.
99. Bechinger, B., *Towards membrane protein design: pH-sensitive topology of histidine-containing polypeptides*. *J Mol Biol*, 1996. **263**(5): p. 768-75.
100. Chiang, Y.-T., Y.-T. Cheng, C.-Y. Lu, et al., *Polymer-Liposome Complexes with a Functional Hydrogen-Bond Cross-Linker for Preventing Protein Adsorption and Improving Tumor Accumulation*. *Chemistry of Materials*, 2013. **25**(21): p. 4364-4372.

## References

101. Chiang, Y.T. and C.L. Lo, *pH-Responsive polymer-liposomes for intracellular drug delivery and tumor extracellular matrix switched-on targeted cancer therapy*. Biomaterials, 2014.
102. Shenoy, D., S. Little, R. Langer, et al., *Poly(ethylene oxide)-Modified Poly( $\beta$ -amino ester) Nanoparticles as a pH-Sensitive System for Tumor-Targeted Delivery of Hydrophobic Drugs. I. In Vitro Evaluations*. Molecular Pharmaceutics, 2005. **2**(5): p. 357-366.
103. Min, K.H., J.H. Kim, S.M. Bae, et al., *Tumoral acidic pH-responsive MPEG-poly(beta-amino ester) polymeric micelles for cancer targeting therapy*. J Control Release, 2010. **144**(2): p. 259-66.
104. Kim, J., Y. Oh, K. Lee, et al., *Development of a pH-sensitive polymer using poly(aspartic acid-graft-imidazole)-block-poly(ethylene glycol) for acidic pH targeting systems*. Macromolecular Research, 2011. **19**(5): p. 453-460.
105. Liu, H., M. Liu, L. Ma, et al., *Thermo- and pH-sensitive comb-type grafted poly(N,N-diethylacrylamide-co-acrylic acid) hydrogels with rapid response behaviors*. European Polymer Journal, 2009. **45**(7): p. 2060-2067.
106. Lin, Y.-L., G. Jiang, L.K. Birrell, et al., *Degradable, pH-sensitive, membrane-destabilizing, comb-like polymers for intracellular delivery of nucleic acids*. Biomaterials, 2010. **31**(27): p. 7150-7166.
107. Xu, Q., W. Huang, L. Jiang, et al., *KGM and PMAA based pH-sensitive interpenetrating polymer network hydrogel for controlled drug release*. Carbohydrate Polymers, 2013. **97**(2): p. 565-570.
108. Yuba, E., A. Harada, Y. Sakanishi, et al., *A liposome-based antigen delivery system using pH-sensitive fusogenic polymers for cancer immunotherapy*. Biomaterials, 2013. **34**(12): p. 3042-3052.
109. Sakaguchi, N., C. Kojima, A. Harada, et al., *Preparation of pH-Sensitive Poly(glycidol) Derivatives with Varying Hydrophobicities: Their Ability to Sensitize Stable Liposomes to pH*. Bioconjugate Chemistry, 2008. **19**(5): p. 1040-1048.

## References

110. Kim, M.S., S.J. Hwang, J.K. Han, et al., *pH-Responsive PEG-Poly( $\beta$ -amino ester) Block Copolymer Micelles with a Sharp Transition*. *Macromolecular Rapid Communications*, 2006. **27**(6): p. 447-451.
111. Kim, E.J., S.H. Cho, and S.H. Yuk, *Polymeric microspheres composed of pH/temperature-sensitive polymer complex*. *Biomaterials*, 2001. **22**(18): p. 2495-2499.
112. Hu, Y., J. Wang, H. Zhang, et al., *Synthesis and characterization of monodispersed P(St-co-DMAEMA) nanoparticles as pH-sensitive drug delivery system*. *Materials Science and Engineering: C*, 2014. **45**(0): p. 1-7.
113. Wu, W., J. Liu, S. Cao, et al., *Drug release behaviors of a pH sensitive semi-interpenetrating polymer network hydrogel composed of poly(vinyl alcohol) and star poly[2-(dimethylamino)ethyl methacrylate]*. *International Journal of Pharmaceutics*, 2011. **416**(1): p. 104-109.
114. Paliwal, S.R., R. Paliwal, and S.P. Vyas, *A review of mechanistic insight and application of pH-sensitive liposomes in drug delivery*. *Drug Deliv*, 2015. **22**(3): p. 231-42.
115. Hong, M.S., S.J. Lim, Y.K. Oh, et al., *pH-sensitive, serum-stable and long-circulating liposomes as a new drug delivery system*. *Journal of Pharmacy & Pharmacology*, 2002. **54**(1): p. 51-8.
116. Cullis, P.R. and B. de Kruijff, *Lipid polymorphism and the functional roles of lipids in biological membranes*. *Biochim Biophys Acta*, 1979. **559**(4): p. 399-420.
117. Seddon, J.M., G. Cevc, and D. Marsh, *Calorimetric studies of the gel-fluid (L beta-L alpha) and lamellar-inverted hexagonal (L alpha-HII) phase transitions in dialkyl- and diacylphosphatidylethanolamines*. *Biochemistry*, 1983. **22**(5): p. 1280-9.
118. Rostovtseva, T.K., P.A. Gurnev, M.Y. Chen, et al., *Membrane lipid composition regulates tubulin interaction with mitochondrial voltage-dependent anion channel*. *J Biol Chem*, 2012. **287**(35): p. 29589-98.
119. Duzgunes, N., R.M. Straubinger, P.A. Baldwin, et al., *Proton-induced fusion of oleic acid-phosphatidylethanolamine liposomes*. *Biochemistry*, 1985. **24**(13): p. 3091-8.

## References

120. Lai, M.Z., N. Duzgunes, and F.C. Szoka, *Effects of replacement of the hydroxyl group of cholesterol and tocopherol on the thermotropic behavior of phospholipid membranes*. *Biochemistry*, 1985. **24**(7): p. 1646-53.
121. Lasic, D.D., *Novel applications of liposomes*. *Trends Biotechnol*, 1998. **16**(7): p. 307-21.
122. Xu, H., J.W. Paxton, and Z. Wu, *Enhanced pH-Responsiveness, Cellular Trafficking, Cytotoxicity and Long-circulation of PEGylated Liposomes with Post-insertion Technique Using Gemcitabine as a Model Drug*. *Pharm Res*, 2015. **32**(7): p. 2428-38.
123. Leite, E.A., C.M. Souza, A.D. Carvalho-Junior, et al., *Encapsulation of cisplatin in long-circulating and pH-sensitive liposomes improves its antitumor effect and reduces acute toxicity*. *Int J Nanomedicine*, 2012. **7**: p. 5259-69.
124. Zhang, C., W. Wang, T. Liu, et al., *Doxorubicin-loaded glycyrrhetic acid-modified alginate nanoparticles for liver tumor chemotherapy*. *Biomaterials*, 2012. **33**(7): p. 2187-2196.
125. Lv, Y., H. Huang, B. Yang, et al., *A robust pH-sensitive drug carrier: aqueous micelles mineralized by calcium phosphate based on chitosan*. *Carbohydr Polym*, 2014. **111**: p. 101-7.
126. Zhou, Y.Y., Y.Z. Du, L. Wang, et al., *Preparation and pharmacodynamics of stearic acid and poly (lactic-co-glycolic acid) grafted chitosan oligosaccharide micelles for 10-hydroxycamptothecin*. *International journal of pharmaceutics*, 2010. **393**(1-2): p. 143-151.
127. Liu, J., H. Li, D. Chen, et al., *In vivo evaluation of novel chitosan graft polymeric micelles for delivery of paclitaxel*. *Drug Delivery*, 2011. **18**(3): p. 181-189.
128. Wang, M., H. Hu, Y. Sun, et al., *A pH-sensitive gene delivery system based on folic acid-PEG-chitosan – PAMAM-plasmid DNA complexes for cancer cell targeting*. *Biomaterials*, 2013. **34**(38): p. 10120-10132.
129. Yan, L., S.H. Crayton, J.P. Thawani, et al., *A pH-Responsive Drug-Delivery Platform Based on Glycol Chitosan-Coated Liposomes*. *Small*, 2015. **11**(37): p. 4870-4874.

## References

130. Saravanakumar, G., J.H. Park, K. Kim, et al., *Polysaccharide-Based Drug Conjugates for Tumor Targeting*, in *Drug Delivery in Oncology*. 2011, Wiley-VCH Verlag GmbH & Co. KGaA. p. 701-746.
131. Jiang, T., Z. Zhang, Y. Zhang, et al., *Dual-functional liposomes based on pH-responsive cell-penetrating peptide and hyaluronic acid for tumor-targeted anticancer drug delivery*. *Biomaterials*, 2012. **33**(36): p. 9246-9258.
132. Ouahab, A., N. Cheraga, V. Onoja, et al., *Novel pH-sensitive charge-reversal cell penetrating peptide conjugated PEG-PLA micelles for docetaxel delivery: In vitro study*. *Int J Pharm*, 2014. **466**(1-2): p. 233-245.
133. Subbarao, N.K., R.A. Parente, F.C. Szoka, et al., *The pH-dependent bilayer destabilization by an amphipathic peptide*. *Biochemistry*, 1987. **26**(11): p. 2964-2972.
134. Wyman, T.B., F. Nicol, O. Zelphati, et al., *Design, synthesis, and characterization of a cationic peptide that binds to nucleic acids and permeabilizes bilayers*. *Biochemistry*, 1997. **36**(10): p. 3008-3017.
135. Guo, X.D., N. Wiradharma, S.Q. Liu, et al., *Oligomerized alpha-helical KALA peptides with pendant arms bearing cell-adhesion, DNA-binding and endosome-buffering domains as efficient gene transfection vectors*. *Biomaterials*, 2012. **33**(26): p. 6284-6291.
136. Vogel, K., S. Wang, R.J. Lee, et al., *Peptide-mediated release of folate-targeted liposome contents from endosomal compartments*. *Journal of the American Chemical Society*, 1996. **118**(7): p. 1581-1586.
137. Nakamura, K., K. Yamashita, Y. Itoh, et al., *Comparative studies of polyethylene glycol-modified liposomes prepared using different PEG-modification methods*. *Biochimica et Biophysica Acta (BBA) - Biomembranes*, 2012. **1818**(11): p. 2801-2807.
138. Sakurai, Y., H. Hatakeyama, Y. Sato, et al., *Endosomal escape and the knockdown efficiency of liposomal-siRNA by the fusogenic peptide shGALA*. *Biomaterials*, 2011. **32**(24): p. 5733-5742.

## References

139. Mahato, R., W. Tai, and K. Cheng, *Prodrugs for improving tumor targetability and efficiency*. *Advanced Drug Delivery Reviews*, 2011. **63**(8): p. 659-670.
140. Tang, R., W. Ji, D. Panus, et al., *Block copolymer micelles with acid-labile ortho ester side-chains: Synthesis, characterization, and enhanced drug delivery to human glioma cells*. *Journal of Controlled Release*, 2011. **151**(1): p. 18-27.
141. Sun, T.M., Y.C. Wang, F. Wang, et al., *Cancer stem cell therapy using doxorubicin conjugated to gold nanoparticles via hydrazone bonds*. *Biomaterials*, 2014. **35**(2): p. 836-45.
142. Gillies, E.R. and J.M. Frechet, *pH-Responsive copolymer assemblies for controlled release of doxorubicin*. *Bioconjug Chem*, 2005. **16**(2): p. 361-8.
143. Shin, J., P. Shum, J. Grey, et al., *Acid-Labile mPEG-Vinyl Ether-1,2-Dioleoylglycerol Lipids with Tunable pH Sensitivity: Synthesis and Structural Effects on Hydrolysis Rates, DOPE Liposome Release Performance, and Pharmacokinetics*. *Molecular Pharmaceutics*, 2012. **9**(11): p. 3266-3276.
144. Shin, J., P. Shum, and D.H. Thompson, *Acid-triggered release via dePEGylation of DOPE liposomes containing acid-labile vinyl ether PEG-lipids*. *J Control Release*, 2003. **91**(1-2): p. 187-200.
145. Kim, H.-K., J. Van den Bossche, S.-H. Hyun, et al., *Acid-Triggered Release via dePEGylation of Fusogenic Liposomes Mediated by Heterobifunctional Phenyl-Substituted Vinyl Ethers with Tunable pH-Sensitivity*. *Bioconjugate Chemistry*, 2012. **23**(10): p. 2071-2077.
146. Kale, A.A. and V.P. Torchilin, *Design, synthesis, and characterization of pH-sensitive PEG-PE conjugates for stimuli-sensitive pharmaceutical nanocarriers: the effect of substitutes at the hydrazone linkage on the pH stability of PEG-PE conjugates*. *Bioconjug Chem*, 2007. **18**(2): p. 363-70.
147. Etrych, T., V. Subr, R. Laga, et al., *Polymer conjugates of doxorubicin bound through an amide and hydrazone bond: Impact of the carrier structure onto synergistic action in the treatment of solid tumours*. *Eur J Pharm Sci*, 2014. **58**: p. 1-12.

## References

148. Prabakaran, M., J.J. Grailer, S. Pilla, et al., *Amphiphilic multi-arm-block copolymer conjugated with doxorubicin via pH-sensitive hydrazone bond for tumor-targeted drug delivery*. *Biomaterials*, 2009. **30**(29): p. 5757-66.
149. Shi, J., Y. Liu, L. Wang, et al., *A tumoral acidic pH-responsive drug delivery system based on a novel photosensitizer (fullerene) for in vitro and in vivo chemophotodynamic therapy*. *Acta Biomater*, 2014. **10**(3): p. 1280-91.
150. Nakamura, H., T. Etrych, P. Chytil, et al., *Two step mechanisms of tumor selective delivery of N-(2-hydroxypropyl)methacrylamide copolymer conjugated with pirarubicin via an acid-cleavable linkage*. *J Control Release*, 2014. **174**: p. 81-7.
151. Alani, A.W.G., Y. Bae, D.A. Rao, et al., *Polymeric micelles for the pH-dependent controlled, continuous low dose release of paclitaxel*. *Biomaterials*, 2010. **31**(7): p. 1765-1772.
152. Rodrigues, P.C.A., K. Scheuermann, C. Stockmar, et al., *Synthesis and In vitro efficacy of acid-Sensitive poly(ethylene glycol) paclitaxel conjugates*. *Bioorganic & Medicinal Chemistry Letters*, 2003. **13**(3): p. 355-360.
153. Sawant, R.R. and V.P. Torchilin, *Enhanced cytotoxicity of TATp-bearing paclitaxel-loaded micelles in vitro and in vivo*. *International Journal of Pharmaceutics*, 2009. **374**(1-2): p. 114-118.
154. Hami, Z., M. Amini, M. Ghazi-Khansari, et al., *Synthesis and in vitro evaluation of a pH-sensitive PLA-PEG-folate based polymeric micelle for controlled delivery of docetaxel*. *Colloids Surf B Biointerfaces*, 2014. **116**: p. 309-17.
155. Dhar, S., F.X. Gu, R. Langer, et al., *Targeted delivery of cisplatin to prostate cancer cells by aptamer functionalized Pt(IV) prodrug-PLGA - PEG nanoparticles*. *Proceedings of the National Academy of Sciences of the United States of America*, 2008. **105**(45): p. 17356-17361.
156. Howard, M.D., A. Ponta, A. Eckman, et al., *Polymer micelles with hydrazone-ester dual linkers for tunable release of dexamethasone*. *Pharm Res*, 2011. **28**(10): p. 2435-46.

## References

157. Kostková, H., T. Etrych, B. Říhová, et al., *HPMA Copolymer Conjugates of DOX and Mitomycin C for Combination Therapy: Physicochemical Characterization, Cytotoxic Effects, Combination Index Analysis, and Anti-Tumor Efficacy*. *Macromolecular Bioscience*, 2013. **13**(12): p. 1648-1660.
158. Chen, D., K. Sun, H. Mu, et al., *pH and temperature dual-sensitive liposome gel based on novel cleavable mPEG-Hz-CHEMS polymeric vaginal delivery system*. *Int J Nanomedicine*, 2012. **7**: p. 2621-30.
159. Chen, D., W. Liu, Y. Shen, et al., *Effects of a novel pH-sensitive liposome with cleavable esterase-catalyzed and pH-responsive double smart mPEG lipid derivative on ABC phenomenon*. *International Journal of Nanomedicine*, 2011. **6**: p. 2053-2061.
160. Lebrecht, D., A. Geist, U.P. Ketelsen, et al., *The 6-maleimidocaproyl hydrazone derivative of doxorubicin (DOXO-EMCH) is superior to free doxorubicin with respect to cardiotoxicity and mitochondrial damage*. *Int J Cancer*, 2007. **120**(4): p. 927-34.
161. Cobo, I., M. Li, B.S. Sumerlin, et al., *Smart hybrid materials by conjugation of responsive polymers to biomacromolecules*. *Nat Mater*, 2015. **14**(2): p. 143-159.
162. Hoffmann, S., L. Vystrcilova, K. Ulbrich, et al., *Dual fluorescent HPMA copolymers for passive tumor targeting with pH-sensitive drug release: synthesis and characterization of distribution and tumor accumulation in mice by noninvasive multispectral optical imaging*. *Biomacromolecules*, 2012. **13**(3): p. 652-63.
163. Chytil, P., S. Hoffmann, L. Schindler, et al., *Dual fluorescent HPMA copolymers for passive tumor targeting with pH-sensitive drug release II: impact of release rate on biodistribution*. *J Control Release*, 2013. **172**(2): p. 504-12.
164. Zhou, Z., L. Li, Y. Yang, et al., *Tumor targeting by pH-sensitive, biodegradable, cross-linked N-(2-hydroxypropyl) methacrylamide copolymer micelles*. *Biomaterials*, 2014. **35**(24): p. 6622-35.
165. Takahashi, A., Y. Yamamoto, M. Yasunaga, et al., *NC-6300, an epirubicin-incorporating micelle, extends the antitumor effect and reduces the cardiotoxicity of epirubicin*. *Cancer Sci*, 2013. **104**(7): p. 920-5.

## References

166. Harada, M., I. Bobe, H. Saito, et al., *Improved anti-tumor activity of stabilized anthracycline polymeric micelle formulation, NC-6300*. *Cancer Sci*, 2011. **102**(1): p. 192-9.
167. Pu, Y., S. Chang, H. Yuan, et al., *The anti-tumor efficiency of poly(L-glutamic acid) dendrimers with polyhedral oligomeric silsesquioxane cores*. *Biomaterials*, 2013. **34**(14): p. 3658-3666.
168. Ding, C., J. Gu, X. Qu, et al., *Preparation of Multifunctional Drug Carrier for Tumor-Specific Uptake and Enhanced Intracellular Delivery through the Conjugation of Weak Acid Labile Linker*. *Bioconjugate Chemistry*, 2009. **20**(6): p. 1163-1170.
169. Wang, C., G. Wang, Z. Wang, et al., *A pH-Responsive Superamphiphile Based on Dynamic Covalent Bonds*. *Chemistry – A European Journal*, 2011. **17**(12): p. 3322-3325.
170. Jain, N.K., M.S. Tare, V. Mishra, et al., *The development, characterization and in vivo anti-ovarian cancer activity of poly(propylene imine) (PPI)-antibody conjugates containing encapsulated paclitaxel*. *Nanomedicine: Nanotechnology, Biology and Medicine*, 2015. **11**(1): p. 207-218.
171. Szabó, I., M. Manea, E. Orbán, et al., *Development of an Oxime Bond Containing Daunorubicin-Gonadotropin-Releasing Hormone-III Conjugate as a Potential Anticancer Drug*. *Bioconjugate Chemistry*, 2009. **20**(4): p. 656-665.
172. Jin, Y., L. Song, Y. Su, et al., *Oxime linkage: a robust tool for the design of pH-sensitive polymeric drug carriers*. *Biomacromolecules*, 2011. **12**(10): p. 3460-8.
173. Zloh, M., E. Dinand, and S. Brocchini, *Aconityl-derived polymers for biomedical applications. Modeling study of cis–trans isomerisation*. *Theoretical Chemistry Accounts*, 2003. **109**(4): p. 206-212.
174. Shen, W.-C. and H.J.P. Ryser, *Cis-aconityl spacer between daunomycin and macromolecular carriers: A model of pH-sensitive linkage releasing drug from a lysosomotropic conjugate*. *Biochemical & Biophysical Research Communications*, 1981. **102**(3): p. 1048-1054.

## References

175. Dinand, E., M. Zloh, and S. Brocchini, *Competitive Reactions During Amine Addition to *cis*-Aconityl Anhydride*. Australian Journal of Chemistry, 2002. **55**(7): p. 467-474.
176. Chytil, P., T. Etrych, Č. Koňák, et al., *Properties of HPMA copolymer–doxorubicin conjugates with pH-controlled activation: Effect of polymer chain modification*. Journal of Controlled Release, 2006. **115**(1): p. 26-36.
177. Kakinoki, A., Y. Kaneo, Y. Ikeda, et al., *Synthesis of poly(vinyl alcohol)-doxorubicin conjugates containing cis-aconityl acid-cleavable bond and its isomer dependent doxorubicin release*. Biological & Pharmaceutical Bulletin, 2008. **31**(1): p. 103-110.
178. Yoo, H.S., E.A. Lee, and T.G. Park, *Doxorubicin-conjugated biodegradable polymeric micelles having acid-cleavable linkages*. J Control Release, 2002. **82**(1): p. 17-27.
179. Zhu, S., M. Hong, G. Tang, et al., *Partly PEGylated polyamidoamine dendrimer for tumor-selective targeting of doxorubicin: The effects of PEGylation degree and drug conjugation style*. Biomaterials, 2010. **31**(6): p. 1360-1371.
180. Gillies, E.R., A.P. Goodwin, and J.M.J. Fréchet, *Acetals as pH-Sensitive Linkages for Drug Delivery*. Bioconjugate Chemistry, 2004. **15**(6): p. 1254-1263.
181. Carmali, S. and S. Brocchini, *Chapter 13 - Polyacetals*, in *Natural and Synthetic Biomedical Polymers*, S.G. Kumbar, C.T. Laurencin, and M. Deng, Editors. 2014, Elsevier: Oxford. p. 219-233.
182. Kochhar, K.S., B.S. Bal, R.P. Deshpande, et al., *Protecting groups in organic synthesis. Part 8. Conversion of aldehydes into geminal diacetates*. The Journal of Organic Chemistry, 1983. **48**(10): p. 1765-1767.
183. Heller, J., D.W.H. Penhale, and R.F. Helwing, *Preparation of polyacetals by the reaction of divinyl ethers and polyols*. Journal of Polymer Science: Polymer Letters Edition, 1980. **18**(4): p. 293-297.
184. Tomlinson, R., J. Heller, S. Brocchini, et al., *Polyacetal–Doxorubicin Conjugates Designed for pH-Dependent Degradation*. Bioconjugate Chemistry, 2003. **14**(6): p. 1096-1106.

## References

185. Wu, Y., W. Chen, F. Meng, et al., *Core-crosslinked pH-sensitive degradable micelles: A promising approach to resolve the extracellular stability versus intracellular drug release dilemma*. J Control Release, 2012. **164**(3): p. 338-45.
186. Heffernan, M.J. and N. Murthy, *Polyketal nanoparticles: a new pH-sensitive biodegradable drug delivery vehicle*. Bioconjug Chem, 2005. **16**(6): p. 1340-2.
187. Lin, S., F. Du, Y. Wang, et al., *An Acid-Labile Block Copolymer of PDMAEMA and PEG as Potential Carrier for Intelligent Gene Delivery Systems*. Biomacromolecules, 2008. **9**(1): p. 109-115.
188. Chen, D. and H. Wang, *Novel pH-sensitive biodegradable polymeric drug delivery systems based on ketal polymers*. J Nanosci Nanotechnol, 2014. **14**(1): p. 983-9.
189. Boomer, J.A., M.M. Qualls, H.D. Inerowicz, et al., *Cytoplasmic Delivery of Liposomal Contents Mediated by an Acid-Labile Cholesterol-Vinyl Ether-PEG Conjugate*. Bioconjugate Chemistry, 2009. **20**(1): p. 47-59.
190. Kim, H.-K., D.H. Thompson, H.S. Jang, et al., *pH-Responsive Biodegradable Assemblies Containing Tunable Phenyl-Substituted Vinyl Ethers for Use as Efficient Gene Delivery Vehicles*. ACS Applied Materials & Interfaces, 2013. **5**(12): p. 5648-5658.
191. Heller, J., *Poly (ortho esters)*, in *Biopolymers I*, R. Langer and N. Peppas, Editors. 1993, Springer Berlin Heidelberg. p. 41-92.
192. Masson, C., M. Garinot, N. Mignet, et al., *pH-sensitive PEG lipids containing orthoester linkers: new potential tools for nonviral gene delivery*. Journal of Controlled Release, 2004. **99**(3): p. 423-434.
193. Nathalie, M., C. Mamonjy, B. Michel, et al., *Incorporation of Poly(Ethylene Glycol) Lipid into Lipoplexes*, in *Liposome Technology, Volume II*. 2006, Informa Healthcare. p. 273-292.
194. Guo, X. and F.C. Szoka, Jr., *Steric stabilization of fusogenic liposomes by a low-pH sensitive PEG--diortho ester--lipid conjugate*. Bioconjug Chem, 2001. **12**(2): p. 291-300.

## References

195. Huang, Z., X. Guo, W. Li, et al., *Acid-Triggered Transformation of Diortho Ester Phosphocholine Liposome*. Journal of the American Chemical Society, 2006. **128**(1): p. 60-61.
196. Guo, X., J. Andrew MacKay, and F.C. Szoka Jr, *Mechanism of pH-Triggered Collapse of Phosphatidylethanolamine Liposomes Stabilized by an Ortho Ester Polyethyleneglycol Lipid*. Biophysical Journal, 2003. **84**(3): p. 1784-1795.
197. Luo, S., Y. Tao, R. Tang, et al., *Amphiphilic block copolymers bearing six-membered ortho ester ring in side chains as potential drug carriers: synthesis, characterization, and in vivo toxicity evaluation*. J Biomater Sci Polym Ed, 2014. **25**(10): p. 965-84.
198. Thambi, T., V.G. Deepagan, C.K. Yoo, et al., *Synthesis and physicochemical characterization of amphiphilic block copolymers bearing acid-sensitive orthoester linkage as the drug carrier*. Polymer, 2011. **52**(21): p. 4753-4759.
199. Chen, H., H. Zhang, D. Thor, et al., *Novel pH-sensitive cationic lipids with linear ortho ester linkers for gene delivery*. Eur J Med Chem, 2012. **52**: p. 159-72.
200. Deslongchamps, P., Y.L. Dory, and S. Li, *The Relative Rate of Hydrolysis of a Series of Acyclic and Six-Membered Cyclic Acetals, Ketals, Orthoesters, and Orthocarbonates*. Tetrahedron, 2000. **56**(22): p. 3533-3537.
201. Heller, J., J. Barr, S.Y. Ng, et al., *Poly(ortho esters): synthesis, characterization, properties and uses*. Adv Drug Deliv Rev, 2002. **54**(7): p. 1015-39.
202. Heller, J. and J. Barr, *Poly(ortho esters)From Concept to Reality†*. Biomacromolecules, 2004. **5**(5): p. 1625-1632.
203. Sadighian, S., K. Rostamizadeh, H. Hosseini-Monfared, et al., *Doxorubicin-conjugated core-shell magnetite nanoparticles as dual-targeting carriers for anticancer drug delivery*. Colloids Surf B Biointerfaces, 2014. **117**: p. 406-13.
204. Wike-Hooley, J.L., A.P. van den Berg, J. van der Zee, et al., *Human tumour pH and its variation*. European Journal of Cancer & Clinical Oncology, 1985. **21**(7): p. 785-91.
205. Estrella, V., T. Chen, M. Lloyd, et al., *Acidity generated by the tumor microenvironment drives local invasion*. Cancer Res, 2013. **73**(5): p. 1524-35.

## References

206. Martin, N.K., I.F. Robey, E.A. Gaffney, et al., *Predicting the safety and efficacy of buffer therapy to raise tumour pH: an integrative modelling study*. Br J Cancer, 2012. **106**(7): p. 1280-7.
207. Gerweck, L.E., S. Vijayappa, and S. Kozin, *Tumor pH controls the in vivo efficacy of weak acid and base chemotherapeutics*. Mol Cancer Ther, 2006. **5**(5): p. 1275-9.
208. Gabizon, A., H. Shmeeda, and Y. Barenholz, *Pharmacokinetics of Pegylated Liposomal Doxorubicin*. Clinical Pharmacokinetics, 2003. **42**(5): p. 419-436.
209. Gao, W., C.M. Hu, R.H. Fang, et al., *Liposome-like Nanostructures for Drug Delivery*. J Mater Chem B Mater Biol Med, 2013. **1**(48).
210. Kanamala, M., W.R. Wilson, M. Yang, et al., *Mechanisms and biomaterials in pH-responsive tumour targeted drug delivery: A review*. Biomaterials, 2016. **85**: p. 152-67.
211. Hatakeyama, H., H. Akita, K. Kogure, et al., *Development of a novel systemic gene delivery system for cancer therapy with a tumor-specific cleavable PEG-lipid*. Gene Ther, 2006. **14**(1): p. 68-77.
212. Zhang, L., Y. Wang, Y. Yang, et al., *High Tumor Penetration of Paclitaxel Loaded pH Sensitive Cleavable Liposomes by Depletion of Tumor Collagen I in Breast Cancer*. ACS Applied Materials & Interfaces, 2015. **7**(18): p. 9691-9701.
213. Romberg, B., W.E. Hennink, and G. Storm, *Sheddable coatings for long-circulating nanoparticles*. Pharm Res, 2008. **25**(1): p. 55-71.
214. Nag, A., G. Mitra, and P.C. Ghosh, *A Colorimetric Assay for Estimation of Polyethylene Glycol and Polyethylene Glycolated Protein Using Ammonium Ferrothiocyanate*. Analytical Biochemistry, 1996. **237**(2): p. 224-231.
215. Mui, B.L., Y.K. Tam, M. Jayaraman, et al., *Influence of Polyethylene Glycol Lipid Desorption Rates on Pharmacokinetics and Pharmacodynamics of siRNA Lipid Nanoparticles*. Molecular Therapy - Nucleic Acids, 2013. **2**: p. Article e139.
216. Wilson, S.C., J.L. Baryza, A.J. Reynolds, et al., *Real Time Measurement of PEG Shedding from Lipid Nanoparticles in Serum via NMR Spectroscopy*. Molecular Pharmaceutics, 2015. **12**(2): p. 386-392.

## References

217. Kucerova, J., Z. Svobodova, P. Knotek, et al., *PEGylation of magnetic poly(glycidyl methacrylate) microparticles for microfluidic bioassays*. *Materials Science and Engineering: C*, 2014. **40**: p. 308-315.
218. Li, N., D. Ziegemeier, L. Bass, et al., *Quantitation of free polyethylene glycol in PEGylated protein conjugate by size exclusion HPLC with refractive index (RI) detection*. *Journal of Pharmaceutical & Biomedical Analysis*, 2008. **48**(5): p. 1332-1338.
219. Zabaleta, V., M.A. Campanero, and J.M. Irache, *An HPLC with evaporative light scattering detection method for the quantification of PEGs and Gantrez in PEGylated nanoparticles*. *Journal of Pharmaceutical & Biomedical Analysis*, 2007. **44**(5): p. 1072-1078.
220. Gong, J., X. Gu, W.E. Achanzar, et al., *Quantitative Analysis of Polyethylene Glycol (PEG) and PEGylated Proteins in Animal Tissues by LC-MS/MS Coupled with In-Source CID*. *Analytical Chemistry*, 2014. **86**(15): p. 7642-7649.
221. Alvares, R.D.A., A. Hasabnis, R.S. Prosser, et al., *Quantitative Detection of PEGylated Biomacromolecules in Biological Fluids by NMR*. *Analytical Chemistry*, 2016. **88**(7): p. 3730-3738.
222. Kanamala, M., B.D. Palmer, H. Ghandehari, et al., *PEG-Benzaldehyde-Hydrazone-Lipid Based PEG-Sheddable pH-Sensitive Liposomes: Abilities for Endosomal Escape and Long Circulation*. *Pharm Res*, 2018. **35**(8): p. 154.
223. Wu, Z., N.J. Medlicott, M. Razzak, et al., *Development and optimization of a rapid HPLC method for analysis of ricobendazole and albendazole sulfone in sheep plasma*. *Journal of Pharmaceutical & Biomedical Analysis*, 2005. **39**(1): p. 225-232.
224. Barnett, K.L., B. Harrington, and T.W. Graul, *Chapter 22 - Validation of liquid chromatographic methods A2 - Fanali, Salvatore*, in *Liquid Chromatography (Second Edition)*, P.R. Haddad, C.F. Poole, and M.-L. Riekkola, Editors. 2017, Elsevier. p. 533-552.

## References

225. Zhang, W., J.R. Falconer, B.C. Baguley, et al., *Improving drug retention in liposomes by aging with the aid of glucose*. International Journal of Pharmaceutics, 2016. **505**(1): p. 194-203.
226. Hunter, D.G. and B.J. Frisken, *Effect of Extrusion Pressure and Lipid Properties on the Size and Polydispersity of Lipid Vesicles*. Biophysical Journal, 1998. **74**(6): p. 2996-3002.
227. Kou, D., G. Manius, S. Zhan, et al., *Size exclusion chromatography with Corona charged aerosol detector for the analysis of polyethylene glycol polymer*. Journal of Chromatography A, 2009. **1216**(28): p. 5424-5428.
228. Daquan, C., J. Xiaoqun, H. Yanyu, et al., *pH-Sensitive mPEG-Hz-Cholesterol Conjugates as a Liposome Delivery System*. Journal of Bioactive and Compatible Polymers, 2010. **25**(5): p. 527-542.
229. Woodle, M.C. and D.D. Lasic, *Sterically stabilized liposomes*. Biochim Biophys Acta, 1992. **1113**(2): p. 171-99.
230. Pappalardo, M., D. Milardi, D. Grasso, et al., *Phase behaviour of polymer-grafted DPPC membranes for drug delivery systems design*. Journal of Thermal Analysis and Calorimetry, 2005. **80**(2): p. 413-418.
231. Venditto, V.J. and F.C. Szoka, *Cancer Nanomedicines: So Many Papers and So Few Drugs!* Advanced drug delivery reviews, 2013. **65**(1): p. 80-88.
232. Bulbake, U., S. Doppalapudi, N. Kommineni, et al., *Liposomal Formulations in Clinical Use: An Updated Review*. Pharmaceutics, 2017. **9**(2).
233. Song, G., H. Wu, K. Yoshino, et al., *Factors affecting the pharmacokinetics and pharmacodynamics of liposomal drugs*. J Liposome Res, 2012. **22**(3): p. 177-92.
234. Torchilin, V.P., T.S. Levchenko, K.R. Whiteman, et al., *Amphiphilic poly-N-vinylpyrrolidones: synthesis, properties and liposome surface modification*. Biomaterials, 2001. **22**(22): p. 3035-44.
235. Pattni, B.S., V.V. Chupin, and V.P. Torchilin, *New Developments in Liposomal Drug Delivery*. Chemical Reviews, 2015. **115**(19): p. 10938-10966.

## References

236. Yang, M.M., W.R. Wilson, and Z. Wu, *pH-Sensitive PEGylated liposomes for delivery of an acidic dinitrobenzamide mustard prodrug: Pathways of internalization, cellular trafficking and cytotoxicity to cancer cells*. *Int J Pharm*, 2017. **516**(1-2): p. 323-333.
237. Yatvin, M.B., W. Kreutz, B.A. Horwitz, et al., *pH-sensitive liposomes: possible clinical implications*. *Science*, 1980. **210**(4475): p. 1253-1255
238. Torchilin, V.P., F. Zhou, and L. Huang, *pH-Sensitive Liposomes*. *Journal of Liposome Research*, 1993. **3**(2): p. 201-255.
239. Tang, J., H. Fu, Q. Kuang, et al., *Liposomes co-modified with cholesterol anchored cleavable PEG and octaarginines for tumor targeted drug delivery*. *Journal of Drug Targeting*, 2014. **22**(4): p. 313-326.
240. Farrell, J.J., H. Elsaleh, M. Garcia, et al., *Human equilibrative nucleoside transporter 1 levels predict response to gemcitabine in patients with pancreatic cancer*. *Gastroenterology*, 2009. **136**(1): p. 187-95.
241. Andersson, R., U. Aho, B.I. Nilsson, et al., *Gemcitabine chemoresistance in pancreatic cancer: molecular mechanisms and potential solutions*. *Scand J Gastroenterol*, 2009. **44**(7): p. 782-6.
242. Kim, M.P. and G.E. Gallick, *Gemcitabine resistance in pancreatic cancer: picking the key players*. *Clin Cancer Res*, 2008. **14**(5): p. 1284-5.
243. Liu, G.-Y., C.-J. Chen, D.-D. Li, et al., *Near-infrared light-sensitive micelles for enhanced intracellular drug delivery*. *Journal of Materials Chemistry*, 2012. **22**(33): p. 16865-16871.
244. Yang, M.M., W.R. Wilson, and Z. Wu, *pH-Sensitive PEGylated liposomes for delivery of an acidic dinitrobenzamide mustard prodrug: Pathways of internalization, cellular trafficking and cytotoxicity to cancer cells*. *International Journal of Pharmaceutics*, 2017. **516**(1): p. 323-333.
245. Kenworthy, A.K., K. Hristova, D. Needham, et al., *Range and magnitude of the steric pressure between bilayers containing phospholipids with covalently attached poly(ethylene glycol)*. *Biophysical Journal*, 1995. **68**(5): p. 1921-1936.

## References

246. Petrache, H.I., S.W. Dodd, and M.F. Brown, *Area per Lipid and Acyl Length Distributions in Fluid Phosphatidylcholines Determined by <sup>2</sup>H NMR Spectroscopy*. *Biophysical Journal*, 2000. **79**(6): p. 3172-3192.
247. Xu, H., J. Paxton, J. Lim, et al., *Development of high-content gemcitabine PEGylated liposomes and their cytotoxicity on drug-resistant pancreatic tumour cells*. *Pharm Res*, 2014. **31**(10): p. 2583-92.
248. Slepushkin, V.A., S. Simoes, P. Dazin, et al., *Sterically stabilized pH-sensitive liposomes. Intracellular delivery of aqueous contents and prolonged circulation in vivo*. *J Biol Chem*, 1997. **272**(4): p. 2382-8.
249. Xu, H., J.W. Paxton, and Z. Wu, *Development of Long-Circulating pH-Sensitive Liposomes to Circumvent Gemcitabine Resistance in Pancreatic Cancer Cells*. *Pharm Res*, 2016. **33**(7): p. 1628-37.
250. Johnsson, M. and K. Edwards, *Liposomes, Disks, and Spherical Micelles: Aggregate Structure in Mixtures of Gel Phase Phosphatidylcholines and Poly(Ethylene Glycol)-Phospholipids*. *Biophysical Journal*, 2003. **85**(6): p. 3839-3847.
251. Kastantin, M., B. Ananthanarayanan, P. Karmali, et al., *Effect of the lipid chain melting transition on the stability of DSPE-PEG(2000) micelles*. *Langmuir*, 2009. **25**(13): p. 7279-86.
252. de Gennes, P.G., *Conformations of Polymers Attached to an Interface*. *Macromolecules*, 1980. **13**(5): p. 1069-1075.
253. Schroter, C.J., M. Braun, J. Englert, et al., *A rapid method to separate endosomes from lysosomal contents using differential centrifugation and hypotonic lysis of lysosomes*. *J Immunol Methods*, 1999. **227**(1-2): p. 161-8.
254. Hamann, S., J. Kiilgaard, T. Litman, et al., *Measurement of Cell Volume Changes by Fluorescence Self-Quenching*. Vol. 12. 2002. 139-145.
255. Vanic, Z., S. Barnert, R. Suss, et al., *Fusogenic activity of PEGylated pH-sensitive liposomes*. *J Liposome Res*, 2012. **22**(2): p. 148-57.

## References

256. Gabizon, A., D. Tzemach, L. Mak, et al., *Dose dependency of pharmacokinetics and therapeutic efficacy of pegylated liposomal doxorubicin (DOXIL) in murine models*. *J Drug Target*, 2002. **10**(7): p. 539-48.
257. Cui, C., P. Yu, M. Wu, et al., *Reduction-sensitive micelles with sheddable PEG shells self-assembled from a Y-shaped amphiphilic polymer for intracellular doxorubicin release*. *Colloids and Surfaces B: Biointerfaces*, 2015. **129**: p. 137-145.
258. Huang, X., F. Du, J. Cheng, et al., *Acid-Sensitive Polymeric Micelles Based on Thermoresponsive Block Copolymers with Pendant Cyclic Orthoester Groups*. *Macromolecules*, 2009. **42**(3): p. 783-790.
259. Xu, H., J. Paxton, J. Lim, et al., *Development of a gradient high performance liquid chromatography assay for simultaneous analysis of hydrophilic gemcitabine and lipophilic curcumin using a central composite design and its application in liposome development*. *Journal of Pharmaceutical & Biomedical Analysis*, 2014. **98**: p. 371-8.
260. Kanamala, M., B.D. Palmer, W.R. Wilson, et al., *Characterization of a smart pH-cleavable PEG polymer towards the development of dual pH-sensitive liposomes*. *International Journal of Pharmaceutics*, 2018. **548**(1): p. 288-296.
261. Ebrahim, Q., R.Z. Mahfouz, K.P. Ng, et al., *High cytidine deaminase expression in the liver provides sanctuary for cancer cells from decitabine treatment effects*. *Oncotarget*, 2012. **3**(10): p. 1137-45.
262. Karanth, H. and R.S. Murthy, *pH-sensitive liposomes--principle and application in cancer therapy*. *Journal of Pharmacy & Pharmacology*, 2007. **59**(4): p. 469-83.
263. Vuković, L., F.A. Khatib, S.P. Drake, et al., *Structure and Dynamics of Highly PEG-ylated Sterically Stabilized Micelles in Aqueous Media*. *Journal of the American Chemical Society*, 2011. **133**(34): p. 13481-13488.
264. Dos Santos, N., C. Allen, A.-M. Doppen, et al., *Influence of poly(ethylene glycol) grafting density and polymer length on liposomes: Relating plasma circulation lifetimes to protein binding*. *Biochimica et Biophysica Acta (BBA) - Biomembranes*, 2007. **1768**(6): p. 1367-1377.

## References

265. Bae, Y.H. and K. Park, *Targeted drug delivery to tumors: Myths, reality and possibility*. Journal of Controlled Release, 2011. **153**(3): p. 198-205.
266. Bucci, C. and M. Stasi, *Endosome to Lysosome Transport*, in *Encyclopedia of Cell Biology*. 2016, Academic Press: Waltham. p. 408-417.
267. Varkouhi, A.K., M. Scholte, G. Storm, et al., *Endosomal escape pathways for delivery of biologicals*. Journal of Controlled Release, 2011. **151**(3): p. 220-228.
268. Luzio, J.P., T. Kuwana, and B.M. Mullock. *Signals for Transport from Endosomes to Lysosomes*. in *Molecular Mechanisms of Membrane Traffic*. 1993. Berlin, Heidelberg: Springer Berlin Heidelberg.
269. Bhutia, Y.D., S.W. Hung, B. Patel, et al., *CNT1 expression influences proliferation and chemosensitivity in drug-resistant pancreatic cancer cells*. Cancer Res, 2011. **71**(5): p. 1825-35.
270. Nag, O.K. and V. Awasthi, *Surface Engineering of Liposomes for Stealth Behavior*. Pharmaceutics, 2013. **5**(4): p. 542-569.
271. Khan, M.F., S. Gottesman, R. Boyella, et al., *Gemcitabine-induced cardiomyopathy: a case report and review of the literature*. J Med Case Rep, 2014. **8**: p. 220.
272. Burris, H.A., 3rd, M.J. Moore, J. Andersen, et al., *Improvements in survival and clinical benefit with gemcitabine as first-line therapy for patients with advanced pancreas cancer: a randomized trial*. J Clin Oncol, 1997. **15**(6): p. 2403-13.
273. Ferlay, J., C.P. Wild, and F. Bray, *The Burden of Cancer Worldwide: Current and Future Perspectives*, in *Holland-Frei Cancer Medicine*. 2016, John Wiley & Sons, Inc.
274. Wilhelm, S., A.J. Tavares, Q. Dai, et al., *Analysis of nanoparticle delivery to tumours*. Nature Reviews Materials, 2016. **1**: p. 16014.
275. de Meyer, F. and B. Smit, *Effect of cholesterol on the structure of a phospholipid bilayer*. Proceedings of the National Academy of Sciences, 2009. **106**(10): p. 3654-3658.

## References

276. Xu, H., J. Paxton, J. Lim, et al., *Development of High-Content Gemcitabine PEGylated Liposomes and Their Cytotoxicity on Drug-Resistant Pancreatic Tumour Cells*. *Pharmaceutical Research*, 2014. **31**(10): p. 2583-2592.
277. Jain, R.K., N. Safabakhsh, A. Sckell, et al., *Endothelial cell death, angiogenesis, and microvascular function after castration in an androgen-dependent tumor: role of vascular endothelial growth factor*. *Proc Natl Acad Sci U S A*, 1998. **95**(18): p. 10820-5.
278. Reineke, J., *Terminology matters: There is no targeting, but retention*. *Journal of Controlled Release*, 2018. **273**: p. 180-183.
279. Nichols, J.W. and Y.H. Bae, *EPR: Evidence and fallacy*. *J Control Release*, 2014. **190**: p. 451-64.
280. Simoes, S., J.N. Moreira, C. Fonseca, et al., *On the formulation of pH-sensitive liposomes with long circulation times*. *Adv Drug Deliv Rev*, 2004. **56**(7): p. 947-65.
281. Vidal, M. and D. Hoekstra, *In vitro fusion of reticulocyte endocytic vesicles with liposomes*. *J Biol Chem*, 1995. **270**(30): p. 17823-9.
282. Caracciolo, G., *Clinically approved liposomal nanomedicines: lessons learned from the biomolecular corona*. *Nanoscale*, 2018.
283. Wang, J., W. Mao, L.L. Lock, et al., *The Role of Micelle Size in Tumor Accumulation, Penetration, and Treatment*. *ACS Nano*, 2015. **9**(7): p. 7195-7206.
284. Chi, Y., X. Yin, K. Sun, et al., *Redox-sensitive and hyaluronic acid functionalized liposomes for cytoplasmic drug delivery to osteosarcoma in animal models*. *Journal of Controlled Release*, 2017. **261**: p. 113-125.